HAW HAMBURG

Project

Design of a Hydrogen Near Zero Emission Passenger Aircraft

Author: Kevin Christopher Monroy Melosevich

Supervisor: Prof. Dr.-Ing. Dieter Scholz, MSME
Submitted: 2024-07-01

Faculty of Engineering and Computer Science
Department of Automotive and Aeronautical Engineering

DOI:
https://doi.org/10.15488/xxxxx

URN:
https://nbn-resolving.org/urn:nbn:de:gbv:18302-aero2024-07-01.011
Associated URLs:
https://nbn-resolving.org/html/urn:nbn:de:gbv:18302-aero2024-07-01.011

Any further request may be directed to:
Prof. Dr.-Ing. Dieter Scholz, MSME
E-Mail see: http://www.ProfScholz.de

This work is part of:
Digital Library - Projects & Theses - Prof. Dr. Scholz
http://library.ProfScholz.de

Published by
Aircraft Design and Systems Group (AERO)
Department of Automotive and Aeronautical Engineering
Hamburg University of Applied Science

This report is deposited and archived:

- Deutsche Nationalbiliothek (https://www.dnb.de)
- Repository of Leibniz University Hannover (https://www.repo.uni-hannover.de)
- Internet Archive (https://archive.org)
  Item: https://archive.org/detail/TextMelosevich.pdf

This report has associated published data in Harvard Dataverse.
https://doi.org/10.7910/DVN/SGGLIV

Abstract

Purpose – Seeking sustainable alternatives to traditional fossil fuels, hydrogen emerges as a promising candidate due to its environmental impact.

Methodology – This project reviews the technical challenges and opportunities associated with hydrogen propulsion in aviation. Existing spreadsheets are used (and extended) for the calculation.

Findings – Hydrogen as a propellant in passenger aircraft eliminates CO2 emissions but its altitude dependent non-CO2 repercussions remain. Lowering the cruise altitude reduces greenhouse effects regardless of the fuel used. Based on the equivalent CO2 mass, an LH2 turboprop based on A320 TLAR yields the best-case scenario but has still remaining emissions: 14.6% of the NOx and 1.5% of the Aviation Induced Cloudiness (AIC) effects in terms of equivalent CO2 mass. These impressive results can be achieved with rather conventional technologies. To get started and to learn, already certified aircraft should be converted as prototype. Later a new clean sheet design can follow.

Research Limitations – The results can only be achieved, if assumed secondary effects of water emissions and ice crystal formation on AIC turn out to be true and NOx reduction from lean H2 combustion can be achieved as assumed.

Practical Implications – The findings of this project may be considered by aircraft manufacturers. Students may want to extend calculations based on the extended spreadsheet.

Social Implications – The Open Access distribution of this report allows the public to participate in discussion the results.

DEPARTMENT OF AUTOMOTIVEAND AERONAUTICAL ENGINEERING

Design of a Hydrogen Near Zero Emissions Passenger Aircraft

Task for a Bachelor Project

Background

The European Parliament and the European Commission set the goal for the EU to become climate neutral by 2050. This is also true for the civil aviation industry. The *Refuel EU* aviation legislation is one element to ensure this. A passenger aircraft powered by liquid hydrogen (LH2) is one possibility. The next passenger aircraft to be built will probably be the replacement of the successful Airbus A320. For environmental reasons, it could be an aircraft flying on hydrogen. The environmental evaluation of passenger aircraft can be done with an equation calculating equivalent CO2 mass. Flying low(er) is reducing Aviation Induced Cloudiness (AIC) and its equivalent CO2 drastically. Turboprop aircraft fly slower and as such lower. An LH2 turboprop aircraft could be a good candidate for a new generation A320.

Task

This project should discuss proposals to achieve climate neutrality in aviation. The role of hydrogen as an energy carrier in civil aviation and how close it can get towards the environmental goals. The following subtasks must be considered:

- Review of recent corporate and governmental goals in terms of sustainability and climate change.
- Review data of the Airbus A320. List the Top Level Aircraft Requirements (TLAR).
- Recalculate the A320NEO as reference aircraft.
- Calculate am A320NEO powered by LH2, a kerosene powered turboprop, and a LH2 turboprop with given spreadsheets.
- Calculate the overall environmental impact in equivalent CO2 mass. Consider non-CO2 emissions.
- Optimize the designs for minimum equivalent CO2 mass. Extend an existing spreadsheet (SAS) for this purpose.

The report must be written in English based on German or international standards on report writing.

Table of Contents

List of Figures

List of Tables

List of Symbols

A	Aspect Ratio
b	Wingspan
B_S	Breguet range factor
c	Specific Fuel Consumption, thrust specific (for jets)
c_{root}	Chord at the wing's root
c_{tip}	Chord at the wing's tip
C_D	Drag coefficient
CF	Characterization Factor
C_L	Lift coefficient
CO	Carbon monoxide
CO_2	Carbon dioxide
d	Diameter
E	Lift-to-drag ratio/ Energy
e	Oswald factor
E_d	Energetic density
EI	Emission Index
E_S	Specific energy
F_{NM}	Fuel Consumption per NM
f_{NMref}	Average Fuel Consumption
g	Earth acceleration
h	Altitude
H_2	Hydrogen
LH_2	Liquid hydrogen
m	Mass
M_{CR}	Cruise Mach number
NOx	Nitrogen Oxides
n_{PAX}	Number of passengers
n_E	Number of engines
R	Range
$SGTP$	Sustained Global Temperature Potential
S_{LFL}	Landing field length
S_{TOFL}	Take-off field length
S_W	Wing Surface
T	Thrust
v	Speed
V	Volume

Greek Symbols

γ Climb gradient
λ Taper ratio
ρ Density
σ Relative density

List of Abbreviations

AIC	Aviation Induced Cloudiness
ATC	Air Traffic Control
BPR	Bypass ratio
CFM	Venture: General Electric CF Series + Snecma M Series
Dept.	Department
DLR	Deutsches Zentrum für Luft-und Raumfahrt
DOC	Direct operating costs
EASA	European Union Aviation Safety Agency
EU	European Union
FAA	Federal Aviation Administration
GE	General Electric
HAW	Hamburg University of Applied Sciences
ICAO	International Civil Aviation Organization
MD	McDonnell Douglas
MF	Fuel mass
MLI	Multi-layer insulation
MLW	Maximum Landing Weight
MOE	Operating empty mass
MPL	Maximum Payload Weight
MTOW	Maximum Take-Off Weight
NASA	National Aeronautics and Space Administration
NACA	National Advisory Committee for Aeronautics
OPerA	Optimization in Preliminary Aircraft Design
PW	Pratt & Whitney
RISE	Revolutionary Innovation for Sustainable Engines
SAF	Sustainable Aviation Fuel
SAS	Simple Aircraft Sizing
SFC	Specific Fuel Consumption
SMR	Small Modular (Nuclear) Reactor
TLAR	Top Level Aircraft Requirements
TP	Turboprop
WV	Weight Variant (Airbus intern nomenclature)
WWII	Second World War

List of Definitions

Contrails

"Streamer of cloud sometimes observed behind an airplane flying in clear cold humid air."- (Britannica 2024a)

Cryogenic

"Field of science and engineering that delves into the behavior and utilization of materials at extremely low temperatures."- (Concept Group 2024)

Electrolysis

"Process by which electric current is passed through a substance to effect a chemical change. The chemical change is one in which the substance loses or gains an electron."- (Britannica 2024b)

Radiative Forcing

"Various factors contribute to this change in energy balance, such as concentrations of greenhouse gases and aerosols, and changes in surface albedo and solar irradiance"- (Wikipedia 2024)

Non-CO2 Green House Gases

"Chemical compounds that trap some of the Earth's outgoing energy, thus retaining heat in the atmosphere. This heat trapping causes changes in the radiative balance of the Earth—the balance between energy received from the sun and emitted from Earth—that alter climate and weather patterns at global and regional scales."- (EPA 2023)

1 Introduction

1.1 Motivation

17 November 1903. It was the date in which a man-made machine with a density higher than air took off into the skies. An event that lasted 12 seconds covering a distance of about 36m revolutionized the way we thought about transportation forever. The invention made by the Wright brothers may look too different from what we conceive as any modern aviation technology. Both possess a set of wings attached to a central frame that carries the passenger's body weight, engines that provide thrust by accelerating incoming air and a set of control surfaces which provide stability to the aircraft. Even though these similarities remain unchanged, the pursuit of improvements in terms of efficiency, safety, and economics have been reflected in an overall optimization of the overall performance of modern aircraft.

Modern aircraft's cabins are closed, pressurized, temperature regulated and isolated from external conditions for a more pleasant experience. The streamlined shape helps minimizing air resistance subsequently improving fuel efficiency. Also, turbofan engines have been implemented which are known to have higher reliability than piston engines. Turbine engines are also not limited by the altitude at which they can operate. According to the FAA Piston engines tend to present failures around 3200 flight hours, while turbofans typically fail after about 375.000 flight hours. In comparison, every turbine propulsive system that fails 117 piston propulsion systems fail in the meantime. Cause of this considerable difference in reliability and wear of the components, turbines were rapidly adapted into civilian aircraft.

Even though both methods of propulsive flight have been used in a similar way throughout the years, what is really concerning is that the technology has been used since the end of the Second World War without considerable technological advances besides the implementation of the bypassed flow from turbojet into turbofan.

70 years after the end of the Second World War, many of us have asked ourselves why the promises of science fiction have not been fulfilled yet. When are we going to get electric airplanes? What keeps us from using the same kind of technology that has already proven to be more environmentally friendly in the car industry from developing it into civil aviation?

1.2 Title Terminology

Hydrogen
"The lightest and most abundant element in the universe." (Collins English Dictionary 2023)

Near Zero-Emission
"Technologies that significantly reduce criteria pollutants, toxic air contaminants, greenhouse emissions consistent with meeting mid- and long-term climate goals" (Law Insider 2014)

Passenger
"A traveler in a public or private conveyance" (Merriam-Webster Dictionary 2023a)

Aircraft
"A machine that can travel through air supported either by its own buoyancy or by the air interaction against its surfaces" (Merriam-Webster Dictionary 2023b)

1.3 Objectives

Through this project the benefits and drawbacks of a major change to the existing propulsive technology in aircraft will be analyzed. The first aim is to prove if such a radical change could take us closer to environmental goals set by governments and companies in the industry. Secondly, if the implementation of such systems could be used in terms of Direct Operating Costs for the airlines as well as the production capacity for world demand.

In the aviation industry designing an aircraft from scratch is a task that requires a lot of investment in work and monetary resources besides tangible amount of time spent in the plane's certifications for the design group to make sure that a Type Certificate is properly secured. Revolutionary aviation improvements are also expected to take longer than expected because the safety requirements set by civil aeronautical authorities are mostly based on proven solutions rather than future technological innovations that could potentially lead to even higher safety standards. That is why the biggest challenge for the big players in the industry has been delivering such improvements on time demanded by the clients and investors. The quick path has been sticking with the same means of compliance suggested by EASA or FAA authorities.

Consequently, engineers should not limit themselves to providing a significant improvement in what has already been achieved. Wasting time, effort, and money on designing a radical different passenger aircraft would also make the already available technology obsolete. Pushing world airports to adapt to a dramatic change would potentially risk overwhelming the capacity of operations during the modernization attempts. In this way tying ourselves to stagnant technology or reinventing the airliners as we know are both too risky in the long run.

The right administration resources available is paramount to the development process. Keeping this in mind in regards of energy, materials, construction, and proven technology that has already been certified, the most reasonable thing would be to start by using existing aircraft as a platform for the next generation. Even if it requires a radical change to the propulsion systems, the less challenging the integration of these should not be overlooked.

In this project the same foundation provided by the A320 family of passenger aircraft will be used. The new Hydrogen based propulsive systems being developed by several companies can be put into comparison in regarding energetic efficiency, environmental impact and the overall costs associated with them without having to constantly adjust external factors.

1.4 Corporate and Governmental Goals

One of the main motivations for this research project has been the fact that, an overoptimistic scientific background has served as foundations for the environmental goals for the following two decades. Leaving aside the expected fleet growth of the following years and the possible repercussions of the side effects of taking these measures along the energy supply chain of civil aviation.

In December 2019, the European Commission put forth the Green Deal objectives for decarbonization. As one to their action plans, aims to achieve what they call "climate neutrality" by 2050 (Figure 1.1). To be an economy which net-zero greenhouse emissions. This goal includes all sectors of society, from power generation, mobility, construction, agriculture, and forestry. (European Commission 2019)

Per passenger, the aviation industry has become more carbon efficient over the past three decades with help of higher seat density configurations, operational improvements like higher engine bypass ratios and airframe efficiencies with sharklets have boosted the fuel efficiency per revenue passenger by approximately 50%. (Clean Sky 2, 2020)

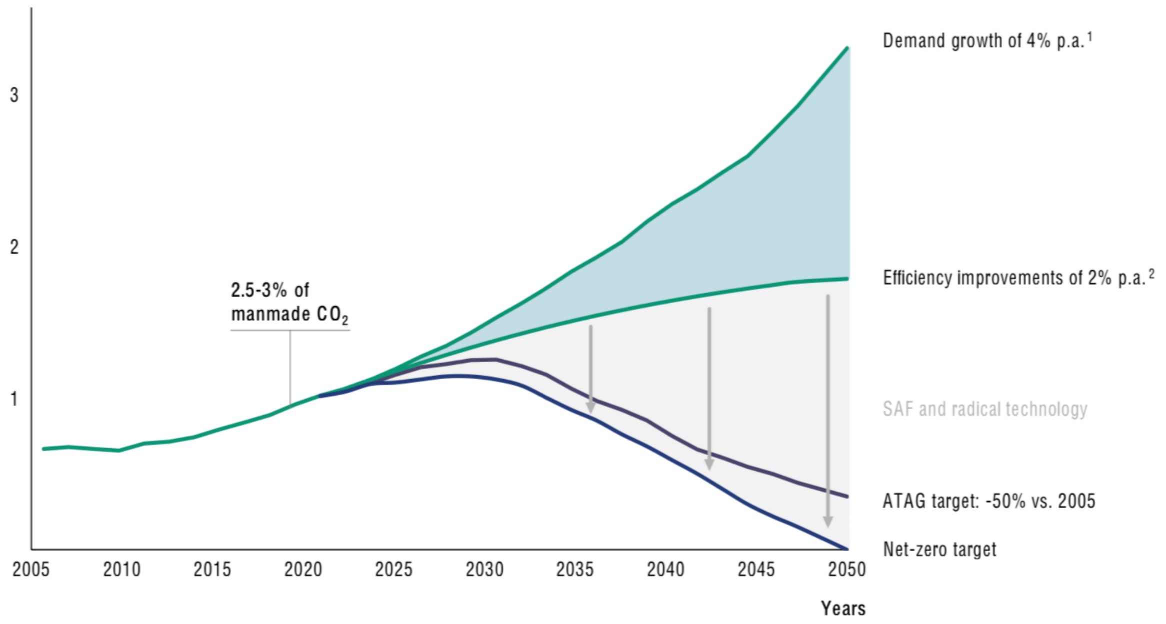

Figure 1.1: Projection CO2 emissions from aviation (Clean Sky 2, 2020)

Nevertheless, the rising demand for air travel has led to a significant increase in direct CO2 emissions from aviation up to 34% over the past five years. Growing population and prosperity will further increase demand with forecasts ranging from 3% to 5% per year. Given the started targets of the EU, further decarbonization measures will be required, even with short-term already applying new fuels such as SAF (Clean Sky 2, 2020)

1.5 Literature Review

The foundations of this project were set on the concrete work of previous investigations. The preliminary sizing process was based on the Aircraft Design Script by Scholz (2015) proceeding from Roskam's *Preliminary Sizing of Airplanes* (1989), Raymer's *Aircraft Design* (1989) and Loftin's *Matching of Size to Performance* (1980) adhered to CS25 from the EASA (2023). Nita (2008), Dib (2015), Seeckt (2010) and Scholz (2021) paved the way for the parameter selection for hydrogen aircraft preliminary sizing. The fuselage extension to integrate the hydrogen tanks as a measure to reduce investment costs was inspired by Scholz (2020 DGLR Presentation). The environmental repercussions of the non-CO2 emissions by Bock (2019), Scholz (2020) and Sethi (2021). The calculations spreadsheet with the fuel selection switch on the GUI was built over the previous SAS-Part25-Jet and SAS-Part25-Prop developed by Heinemann (2012) and Krull (2022). Finally, the calculations on altitude dependent emissions characteristics of kerosene and hydrogen by Scholz (2020c) with the forcing factors by Schwartz (2009) to be automated on the SAS-Part25.

1.6 Structure of the Project

This project was structured in the following way:

Chapter 2	Recalls the development of hydrogen propulsion in aviation up to this day.
Chapter 3	Sets forward the current use of fossil-based fuels in aviation.
Chapter 4	Presents the substitution of kerosene with hydrogen and its environmental implications.
Chapter 5	Tackles the hydrogen production methods and its existing economical limitans.
Chapter 6	Lays on the possibility of making an LH2 propelled aircraft by adapting the current ones describing the main conversion parameters and fuel tanks.
Chapter 7	Explains about the fundamentals of the preliminary sizing.
Chapter 8	Depicts the gathered aircraft requirements to be replaced by the LH2 variant.
Chapter 9	Goes through the implementation of the LH2 variants into the SAS program. Compares the conventional A320NEO aircraft with the LH2 variants.
Chapter 10	Describes the environmental impact of the non-CO2 emissions of the LH2 variants taking as a reference the conventional kerosene passenger aircraft.

The associated Excel spreadsheets are:
- *SAS-Part25_A320NEO.xlsm*
- *SAS-Part25_LH2-A320NEO.xlsm*
- *SAS-Part25_A320NEO_TP.xlsm*
- *SAS-Part25_LH2A320NEO_TP.xlsm*
- *LH2_Fuel_Tanks_Integration.xlsm*

as well as the Fuel Tank's renders are separately available at:
https://doi.org/10.7910/DVN/SGGLIV .

2 State of the Art

Tendencies to find a different way of propulsion in the automotive industry have proven a quick overview in the last years of the adoption process for the end consumers. Companies like Tesla and Toyota have developed ways of making the use of electric motors in their cars a possibility. Slowly but steadily, the aviation industry has also been working on the development of similar solutions. Various manufacturers, universities and startups are working on prototypes of this technology by trying their products on smaller general aviation aircraft which could potentially be scaled up for larger passenger planes. The following companies, still on the test phase, may set a precedent for the aircraft propulsion systems of the future in civil aviation.

2.1 Tupolev-155 Hydrogen Plane

Hydrogen propulsion in an aircraft is not new, since the first experimental hybrid plane powered by hydrogen was flown dates to 1988 in the USSR by the Tupolev Design Bureau. The chief designer was Vladimir Andreev who chose a TU-154 as a base and called it TU-155. It was flown with a NK-88 modified to run on liquid hydrogen while the remaining two engines typically found on the TU-154 on were running on kerosene, (Figure 2.1). Out of its more than hundred flights, only 5 of them were using hydrogen as a fuel. Further tests beyond air shows were not conducted. It was done in a time in which people were concerned about running out of kerosene instead of decreasing the environmental impact of aviation. (Sidelnikov 2023)

Figure 2.1: Tupolev TU-155 on cryogenic fuel (McLachan 2023)

2.2 NACA's Hydrogen Aircraft Project

Also, NACA were able to fly a hydrogen powered plane prior to the soviet Tupolev. In 1955 NACA published a classified research program (Figure 2.2) in which calculations for a proposal of a subsonic/supersonic bomber, subsonic/supersonic reconnaissance aircraft and a supersonic fighter were conducted.

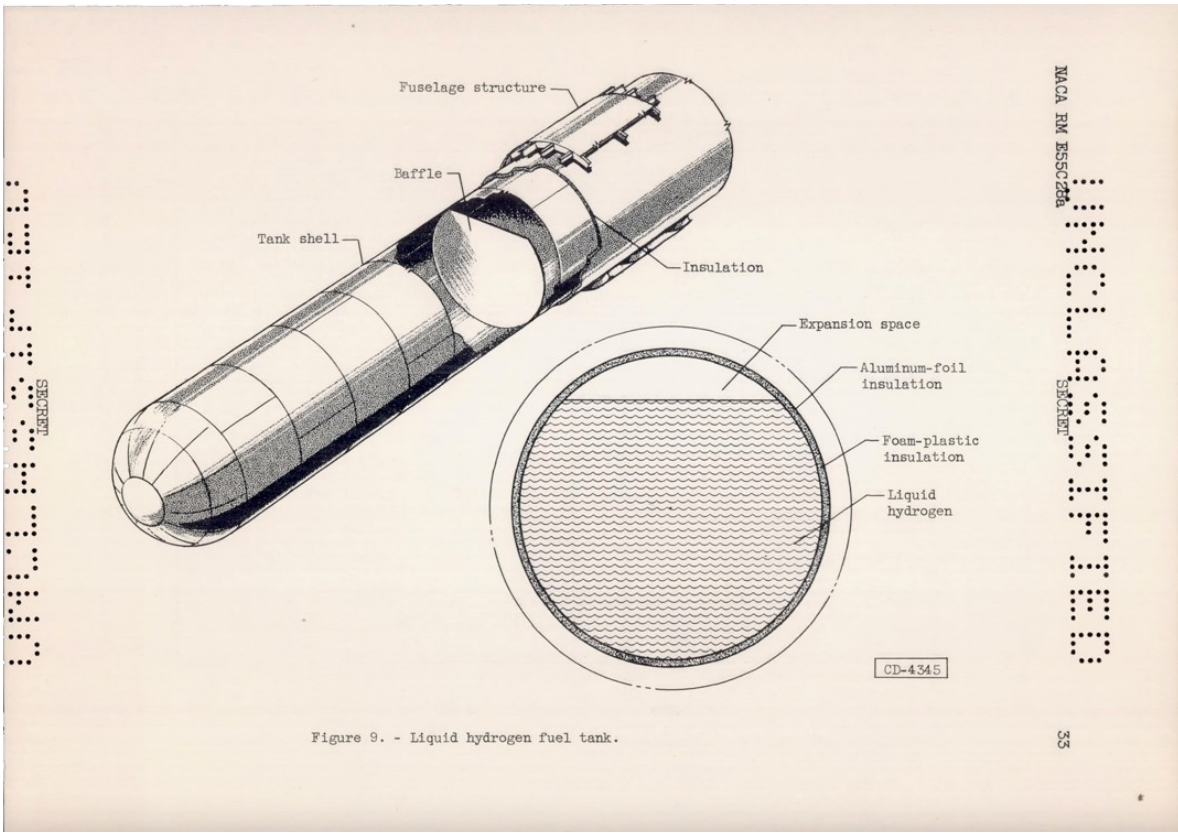

Figure 2.2: NACA's Liquid hydrogen fuel tank illustration (Silverstein 1955)

The conclusions of this report were the future possibilities of using hydrogen in reconnaissance subsonic missions with a range around 5500 NM and supersonic fighter missions up to Mach 2.5 up to 700 NM (Figure 2.3). Many assumptions were made in which substantial development would be required to obtain the described back then. (NACA 1955)

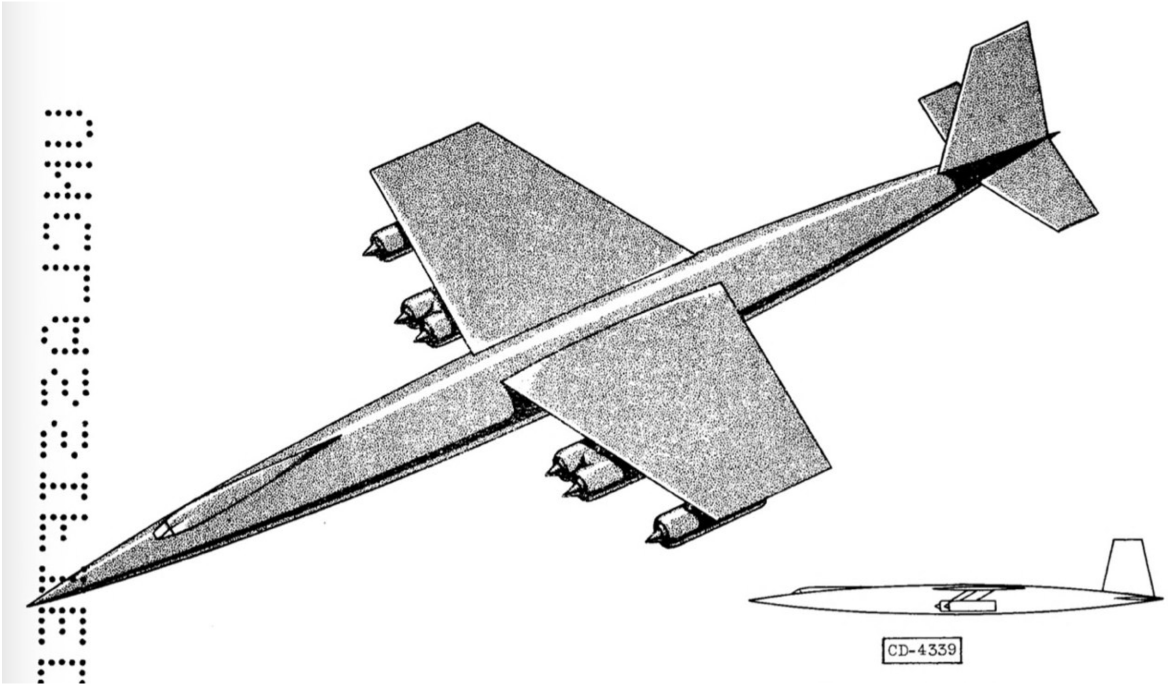

Figure 2.3: Supersonic bomber. Flight Ma 2.0 target FL750 (Silverstein 1955)

2.3 Rolls-Royce Pearl 700 Engine Running on LH2

Rolls-Royce has been conducting tests in conjunction with DLR and Loughborough University in converting a long-range business jet engine from their catalog to run on pure hydrogen (Figure 2.4). This involved overcoming combustion challenges since hydrogen burns at much higher temperatures and at a faster rate than kerosene. The company explained that new fuel spray nozzles especially designed to work with hydrogen were able to control the flame position while progressively mixing the air with hydrogen to maximize its reactivity. The Pearl 700 engine designed to power the shortly introduced G700 form Gulfstream was used as a test platform. (Alcock 2023)

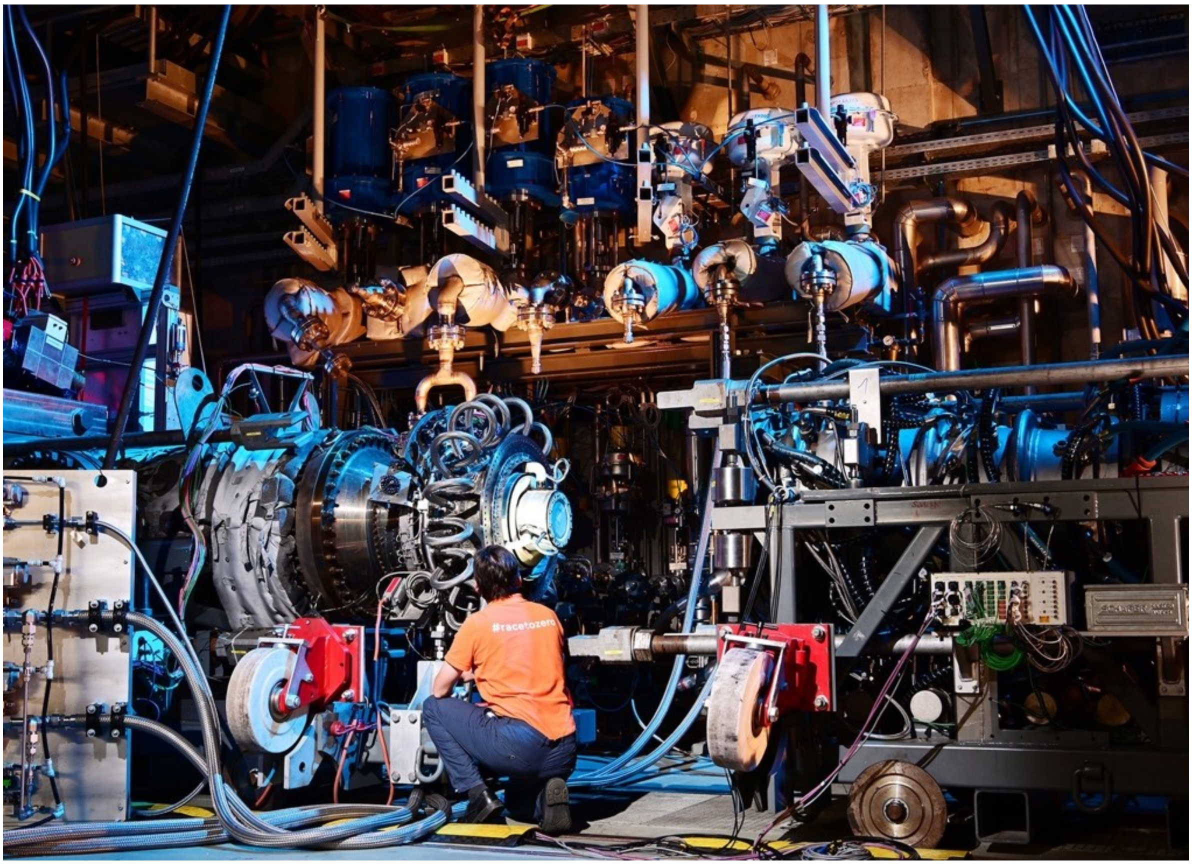

Figure 2.4: Combustor testbed Loughborough University UK (Weigelt 2023)

In 2022 Rolls-Royce developed a larger hydrogen propulsion system working with lo low-cost airline EasyJet. Back then an AE2100 turbofan was used as a platform to run the hydrogen combustion tests. (Rolls-Royce 2022)

2.4 Airbus: ZEROe Concepts and Goals

Airbus as the biggest manufacturer of passenger aircraft aims to bring to market the world's first hydrogen-powered aircraft by 2035. (Airbus 2020a). Presenting in September 2020 the three different ZEROe concepts (Figure 2.5, Figure 2.6 & Figure 2.7) and adding a fourth fully electrical concept by December 2020 (Figure 2.8), Airbus came under the spotlight as a brand in the environmentally friendly aviation of the future.

Figure 2.5: ZEROe turbofan aircraft render (Airbus 2020a).

Figure 2.6: ZEROe turboprop aircraft render (Airbus 2020a)

Figure 2.7: ZEROe blended wing body aircraft render (Airbus 2020a)

Figure 2.8: Airbus ZEROe Fully electric Render (Airbus 2020a)

Even though Airbus has drawn the attention of experts and enthusiasts with the four unconventional aircraft configurations renders, the development of these has not yet be shown to the public in 4 years. Some of the designs do not even comply with the CS 25.807 requirements for evacuation of the passengers in case of an emergency in less than 90s (EASA 2023). The ZEROe name and campaign also misleadingly implies that the aircraft will not have any effect on the environment.

2.5 TECNAM P-Volt Postponed

The Italian aircraft company which has been working intensively on the design of a small regional twin-engine all-electric propeller aircraft called P-Volt suspended its further development in June 2023 after 3 years of research. TECNAM has concluded that the viability of an electric aircraft with today's technology is not possible in terms of operating costs, profitability, and environmental impact. One of the main conclusions was that an aircraft with a battery pack at the end of its life would be worse in terms of Net Present Value. The possible further development of the P-Volt in the future depends on the speculation of uncertain technological developments (Figure 2.9). An important argument against it was the failure in the development of batteries with higher capacity. By having batteries with a maximum charge less than 170 Wh/kg the batteries would have to be replaced after a few hundred flights, in consequence the operating costs increase dramatically due to the replacement of the battery pack units. (TECNAM 2023)

Figure 2.9: Tecnam P-Volt Render (TECNAM 2023)

2.6 EnerVenue: Hydrogen-Based Battery Technologies

Nickel Hydrogen battery technology has already proven to be useful in aerospace applications. Its first application has been in American Intelligence Program satellite NTS-2. Highly energy dense enough to be considered the best energy transport solution in the ISS, Hubble Telescope, Mars Rover Perseverance. These batteries can retain up to 86% of their capacity after 30.000 cycles. With an average of 3 cycles per day it lasts up to almost 30 years without having to service them. These batteries are extremely temperature tolerant, able to keep working on the extreme temperatures of space. The most modern designs provide up to 1500W Nominal Power. The solid construction has been thoroughly tested with ballistic penetration and no explosion, fire or ejection of materials were detected, even if in the case of a hypersonic impact the failure would not end in a catastrophe. (Miller 2017)

As seen on Figure 2.10, the battery systems are encapsulated under high pressure between 34,5 bar and 103,4 bar (500 to 1500 psi). This extreme pressure is necessary chemically and mechanically to facilitate the reaction. It increases the energy density of the battery, which indirectly increases the energy efficiency of a vehicle by allowing more energy to be stored per given volume. Without going deep into chemistry. The electrode is also a porous structure making it easier for the electrolyte to squeeze through to react.

Figure 2.10: Energy Storage Vessel (EnerVenue 2023)

Although the advantage of not needing a heating or cooling system to keep Nickel-Hydrogen batteries running properly, the risk of a thermal runaway is drastically reduced, Ni-H2 batteries have an energetic density of 48 Wh/kg (Table 2.1) while Lithium-Ion batteries get 260 Wh/kg steadily increasing 5% each year on the last decade. But beyond that the most significant advantage is the absence dendrite formation on the anode throughout the lifecycle causing an inevitable short circuit in Li-Ion batteries. (Flux Power 2020)

EnerVenue claims that it only requires 20 components to build each unit. The simplicity of the chemical reaction of non-toxic components and the lack of moving parts in a practical maintenance free energy carrier seems to be a good option for environmentally friendly aviation of the future, thus the energy density still needs to improve for this purpose.

Unfortunately, these great features also come at a high price. Making it the reason why we have not seen this technology on Earth so often, despite the cost savings of maintenance, the commonality of the components. Without mass production and standardization, it would not be possible to reduce the costs. EnerVenue has already invested into the construction of a scale production facility in Shelby County, Kentucky, which is expected to open in 2024 on its first phase with a capacity of 1GWh per year in its assembly line. (EnerVenue 2023c)

Table 2.1: Energy Storage Vessel Spec. Sheet (EnerVenue 2023b)

Type	**Description**	**Specification**
Mechanical	Dimensions (Diameter x Length)	168mm x1800mm
	Format	Tubular
	Type	Large Format Battery
	Weight	62kg/136lb
	Operating Temperature	-10°C to 45°C
	Storage Temperature	-15°C to 60°C
	Cooling Type	Convection, Forced Air
Electrical	Nominal Amp-hour Charge/ Discharge	137 Ah
	Nominal Energy Capacity	3000Wh @ 25°C
	Voltage Range	23-30 Vdc across full range of SOC (0% to 100%) @ 25°C
	Nominal Power	1500 W
	C-Rates	C/2 – C/12
	Peak RTE	>90% @ 25°C
	Expected Capacity Retention	86% after 30,000 cycles
	Chemistry	Ni-H2
	Modes	Constant Current, Constant Power
	BMS	EnerVenue BMS 1000V /1500V

Batteries to be considered as a possible energy carrier on aviation must overcome multiple its energy density by a factor of 6 at least. But even if the required energetic density is not achieved it would still be a good alternative for another aspect of civil aviation as an in-site energy storage at airports for a possible plug-in hybrid solution to meet the European Airports Sustainability electrification of ground support equipment goals. (ACI Europe 2024)

3 Aviation in Terms of Energy

3.1 Energy Options

On the most basic level, to fly a winged aircraft an aerodynamic sense (without any use of buoyancy in the air like hot-air-balloons or gas-filled airships), it's necessary to displace a certain amount of air mass downwards. Condensed into Newton's third law by reaction, the resulting force should produce lift. As expected, energy is required to accelerate air that provides enough thrust and lift for a winged aircraft to travel. Passenger aircraft get this propulsive thrust force out of the engines which constantly accelerate a high volume of air to greater speeds than the intake. Then by increasing the aircraft's relative speed to the air it encounters, wings fulfill its main objective of providing lift by deflecting air downwards in the most efficient way possible. Even aircraft without built in engines, not capable of producing thrust fly by exchanging potential energy for kinetic energy while still trying to keep drag as low as possible. In other words, flying without energy is not possible.

At the end of the day, the means in which the energy is carried into the aircraft is irrelevant. Kerosene, LH2, batteries, nuclear or even other energy sources which have not been discovered yet will not have any impact by themselves other than weight. But what it does is the way the available energy is turned into forces that make flying as efficient as possible and its derived environmental and economic impact.

3.2 Factors Contributing to the Persistent Use of Kerosene

If kerosene is going to be replaced in civil aviation, it is crucial to understand why it has been used in the first place. Kerosene is a low viscosity clear hydrocarbon derived from crude oil. Crude oil consists of a blend of many different hydrocarbons, all with different carbon chain length molecules (Figure 3.1). There are short chain gas molecules ranging from C_1 to C_4 Methane and Butane. Then longer gasoline molecules with chain lengths between C_5 to C_{10}, while kerosene molecules range from around C_{10} to C_{16}. These fuel types can be separated from crude oil thanks to the carbon chain lengths impact on the boiling point of each component, allowing a fractional distillation of crude oil being possible. (US-EERE 2016)

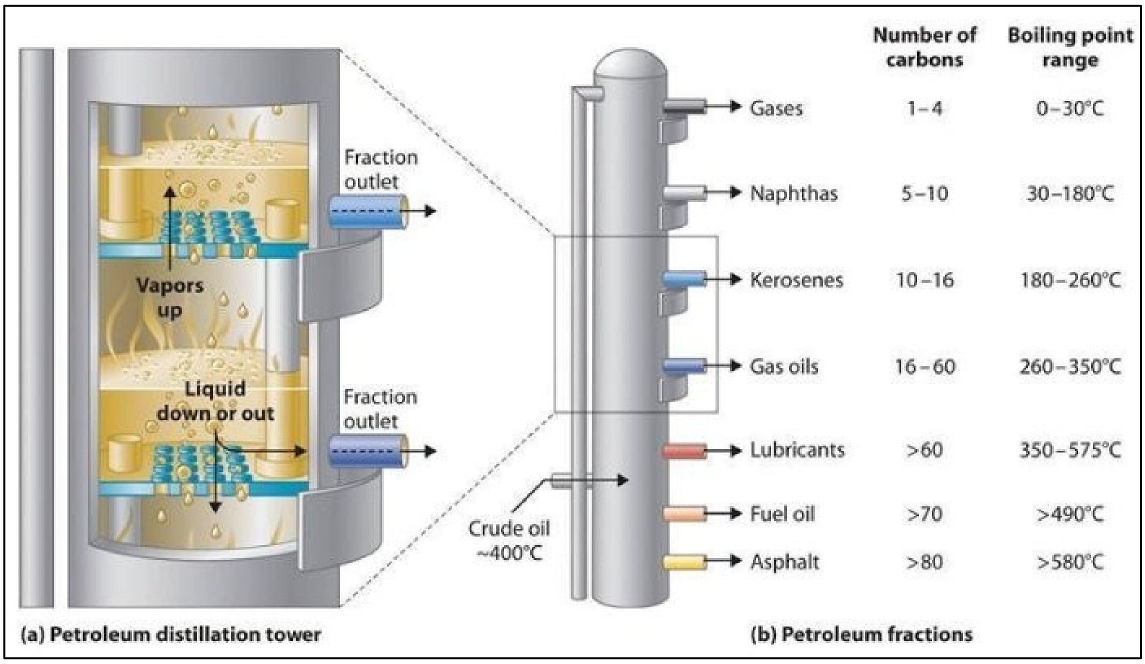

Figure 3.1: Crude oil distillation column (US-EERE 2016)

The longer chain hydrocarbon liquify lower in the distillation tower thanks to their lower boiling point. Shorter chain molecules will remain gaseous and continue rising through the tower. Between 180 °C to 260 °C kerosene carbon chains are extracted from crude oil.

Internal combustion in jet engines is not that demanding related to the fuel used. If the fuel burns hot and can be pumped into a combustion chamber, there is a high chance it can run a gas turbine. (Bevill 2010)

Kerosene, for aviation grade, known as Jet-A has some notorious properties for aviation. One of them being its low freezing point of -40 °C. A lower freezing point is desirable when it comes to routes flying over colder regions at higher altitudes. This is needed to prevent fuel from solidifying into wax. Freezing points and boiling points are generally linked. The level of refinement to achieve this result is done by excluding hydrocarbons with longer carbon chains, therefore excluding lower boiling point molecules from the mix. (Chevron 2007)

Early aircraft engines were powered mostly by gasoline but later replaced by Kerosene. The freezing point issue excluded longer chain molecules like diesel from being considered. Diesel powered vehicles in colder countries cut their fuel with kerosene to prevent it from freezing in winter months. Because of the same reason another type of jet fuel, Jet-B is used in parts of Canada and Alaska. It is a wider cut fuel made from a mix of 30% kerosene and 70% gasoline to achieve an even lower freezing point of -60 °C. (NW Fuel Canada 2017)

Even if Jet-B seems to have an advantage over the most widely used Jet-A, there are some reasons behind. Gasoline, with its shorter carbon chain lengths, is too volatile for general use in aviation since its *flash point* is much lower than kerosene. Flash point is the lowest temperature vapors can form from a liquid to create an ignitable mixture in the air. The lower temperature of vaporization also causes problems in an aircraft's fuel distribution system with vapor locks of bubbles causing blockages in plumbing. At higher altitudes this problem becomes a larger issue for jet engines, as boiling points lower as pressure decreases. So low flash points of a gasoline-based fuel make unintended explosions and fires more likely. This was a constant in American aircraft carriers in WWII with the predominance of gasoline powered piston engines. Kerosene has a flashpoint of 60 °C and (US-NHHC 2021)

The function aviation fuel play is being an energy carrier to power the engines. This is achieved by rising pressure in the combustion chamber when ignited, consequently adding energy to the incoming airflow. To fulfil this task efficiently a high energy density carrier is required. The most obvious reason to use kerosene in aviation has been its energy content at a lower cost.

4 Liquid-Hydrogen as a Propellant

4.1 Hydrogen Basics

Fuels energy content can be expressed by the ratio of energy released out of a given amount of mass under specific conditions. There are two ways of describing energy quantity measurements. *Specific Energy* as energy per unit mass and *Energy Density* as energy per unit volume. (Neutrium 2014)

$$E_s = \frac{E}{m} = \left[\frac{\mathrm{MJ}}{\mathrm{kg}}\right] \tag{4.1}$$

$$E_d = \frac{E}{V} = \left[\frac{\mathrm{MJ}}{\mathrm{l}}\ or\ \frac{\mathrm{MJ}}{\mathrm{m}^3}\right] \tag{4.2}$$

In general, a dense fuel with high volumetric energy is desired in commercial aircraft that only fill their tanks with enough fuel to reach their destination and some extra as reserve in case of emergency. On average fossil fuels are characterized by having a specific energy of around 40MJ/kg. In the case of Jet-A fuel ranges from 43 MJ/kg to 48 MJ/kg. Comparing these values to hydrogen there are several factors that must be addressed. Hydrogen in its liquid state is the densest form in which it can be stored. Taking mass as a reference once again, LH2 has a specific energy between 120 MJ/kg to 141,48 MJ/kg. Setting side by side the density of kerosene being 0,785 kg/l and liquid hydrogen of 0,07085 kg/l at 20 K can be also used to compare both. (Absolut Hydrogen 2021)

As expressed in Table 4.1 the same mass of Kerosene stores only one third of the energy in the same mass of LH2. This seems to be the best argument companies have been considering for using liquid hydrogen as an energy carrier in aviation, but there are some caveats lost in terms of density.

Table 4.1: Volumetric & gravimetric density comparison

Fuel	Energy	Mass	Volume
Kerosene	1 MJ	23,26 g	29,63 ml
LH2	1 MJ	8,33 g	117,62 ml
Difference Factor		2,79 less weight	3,97 more space

Liquid hydrogen occupies almost four times more space to store the same amount of energy available in a given volume of kerosene. This should not be a motive to rule out hydrogen as a fuel. Knowing the efficiency factors throughout the propulsion system, an estimate of the total mass of the fuel required for a given flight can be calculated to detail. Volumetric and Gravimetric densities are both equally important when designing an aircraft. In order words, the amount of energy available per kilogram and liter of our energy carrier are both relevant in the propellant decision.

4.2 Challenges to Hydrogen Combustion

Although hydrogen gas does not have a flash point as a gas at ambient conditions, cryogenic hydrogen will flash at all temperatures above its boiling point of 20 K. This could also lead to bubbles in the fuel pipes and unintended explosions and fires more likely on the aircraft than with fossil fuels. (Jordan 2007)

This added to the range of mixture between fuel and oxidizer in which hydrogen combustion can take place, combined with the Minimum Energy of Ignition of 0,018 mJ can be dangerous if not handled correctly. A weak spark or the electrostatic discharge by a flow of pressurized Hydrogen gas or by a person (10 mJ) would be sufficient for an ignition; this is, however, no different from other burnable gases. The minimum ignition energy is further decreasing with increasing temperature, pressure, or oxygen contents. The hot air jet ignition temperature is lowest for hydrogen compared to all hydrocarbons decreasing further with increasing jet diameter. It is also dependent on jet velocity and mixture composition. (Jordan 2007)

5 Making Liquid Hydrogen Ecological

The fundamental problem with hydrogen comes down to how our universe works. Despite hydrogen being the most abundant element in the universe, it isn't particularly available in its pure form. Commonly hydrogen can be found bonded to other elements like carbon forementioned in the previous chapter. Its extraction out of the bonded elements can be a very energy consuming process that if not taken into the equation could result in even higher emissions into the atmosphere than the ones produced by the kerosene's combustion.

Making a distinction on the several ways hydrogen can be synthesized will help us identify the most practical path of breaking hydrogen out of more complex molecules. Energy consumption and the economics behind these manufacturing processes are also critical factors to make hydrogen an ecological solution to the EU Goals. Several hues of hydrogen are used to describe the processes.

On one hand we have that most of the hydrogen being synthetized up to this day is also highly contaminant. Grey-Hydrogen is an easy way to make hydrogen to them out of fossil fuel by running hot steam over it. This process is called Steam Reformation. (U.S. Dept. of Energy 2023)

Steam methane Reforming Reaction

$$CH_4 + H_2O + \Delta Q \rightarrow CO + 3H_2 \tag{5.1}$$

Water-Gas shift Reaction

$$CO + H_2O \rightarrow CO_2 + H_2 + \Delta Q \tag{5.2}$$

The problem is that it produces CO2 as a by-product, the very same compounds we are trying to avoid from Kerosene combustion. There are ways of capturing the CO2 of fossil fuel in the steam reformation process (Figure 5.1) and if fossil fuels are used to heat the steam, the CO2 of these emissions are harder to capture. Grey-Hydrogen using methane and Black/Brown-Hydrogen using coal already contributes to 2% of the global CO2 emissions just as the whole civil aviation.

Figure 5.1: Steam-methane reforming facility (Hydrogen Newsletter 2022)

The dream idea behind an ecological hydrogen cycle is to use the energy of renewable sources to make its extraction. Wind and solar power generation are not reliable as it depends on the weather conditions but the energy from these sources could be stored into hydrogen via Electrolysis. That way no CO2 is produced, and hydrogen is directly broken out of water.

Green-hydrogen has been the way in which the Spanish company Iberdrola's Green Hydrogen division has been generating hydrogen in a smaller scale in their facility in Puertollano (Figure **5.2**). Solar energy from a near photovoltaic field is used to conduct the electrolytic process on water on 16 cells. The hydrogen goes directly into an adjacent factory to produce ammonia, an ingredient of plant fertilizer. Any excess is stored since it can only run during the day.

Figure 5.2: Green-Hydrogen Facility Puertollano (Iberdrola 2022)

The problem is efficiency because water itself has very poor electric conductivity to begin with and as the oxygen is separated from hydrogen in bubbles the surface area of the cathode and anode plates is reduces as water gets displaced. Electrodes to get a reasonable hydrogen extraction are also made of expensive materials like platinum or iridium. Heating the water can also increase efficiency but heating also requires energy, making the process overall more inefficient. We get a 70% benchmark efficiency in terms of electrical power to hydrogen generation. Likewise trying to ger electricity out of hydrogen we encounter the same problems in reverse in fuel cells. (H2Pro 2023)

Then Pink-Hydrogen involves electrolysis with the electricity generated from nuclear plants instead. On the eyes of activists might be a non-ecological solution, but considering the environmental impact of the so-called renewables might be even greater on the long run.

The harsh truth is, there is not such a thing as clean energy. Solar panels after their lifecycle cannot be fully recycled just as wind turbine blades (Figure 5.3) being cut into thirds and buried by the thousands in Casper landfill in Wyoming. (Paddison 2023)

Figure 5.3: Thousands of Old Wind Turbine Blades (Rosen 2023)

But Green-Hydrogen is not the only CO2-free solution. Other methods like Blue-Hydrogen process also break up fossil fuels but in this case the CO2 emissions are captured and stored to later be used for industrial purposes. This also seems to be a reasonable solution compared to Green-Hydrogen. Besides being the most promising cost-effective solution in the near term, they have been heavily boosted by the fossil fuel industry. Critics are concerned about the risk of a greenhouse gas leakage that wipes out any improvement towards climate neutrality. (Financial Times 2023)

Up to this day the most effective way of extracting Hydrogen has be the recent development made by a company called HiiROC from Ireland. The Thermal Plasma Electrolysis Process (Figure 5.4) is an extraction of the carbon out of methane in a solid inert state. By combining Green-Hydrogen and Blue-Hydrogen calling it *Turquoise-Hydrogen* a series of plasma torches run on in a vacuum to separate hydrogen from carbon. Carbon is a very useful by-product, it can later be sold to the rubber industry to make tires, coatings, steel alloys. More innovatively, carbon is being used into building materials in cement. This process uses less energy per kg of hydrogen produced. It gives us a means of using the worlds reserves of fossil gas without pollutant emissions. (HiiROC 2024)

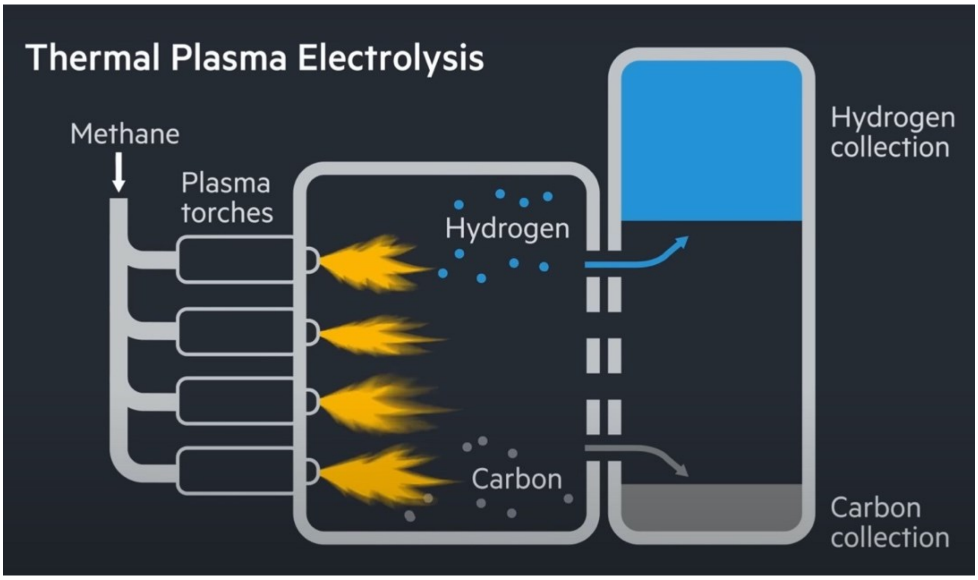

Figure 5.4: HiiROC Thermal Plasma Electrolysis (Financial Times 2023)

Another kind of Turquoise-Hydrogen developed by the company C-Zero separates carbon from hydrogen by running methane through a pyrolysis reactor. A chamber filled with molten salts in which natural gas is passed through in the form of bubbles leaving piles of carbon in its elemental form behind and capturing hydrogen at the top (Figure 5.5). This new technology has proven on their lab tests to be 7.5 times more efficient in producing Hydrogen than regular electrolysis of Green-Hydrogen. (C-Zero 2023)

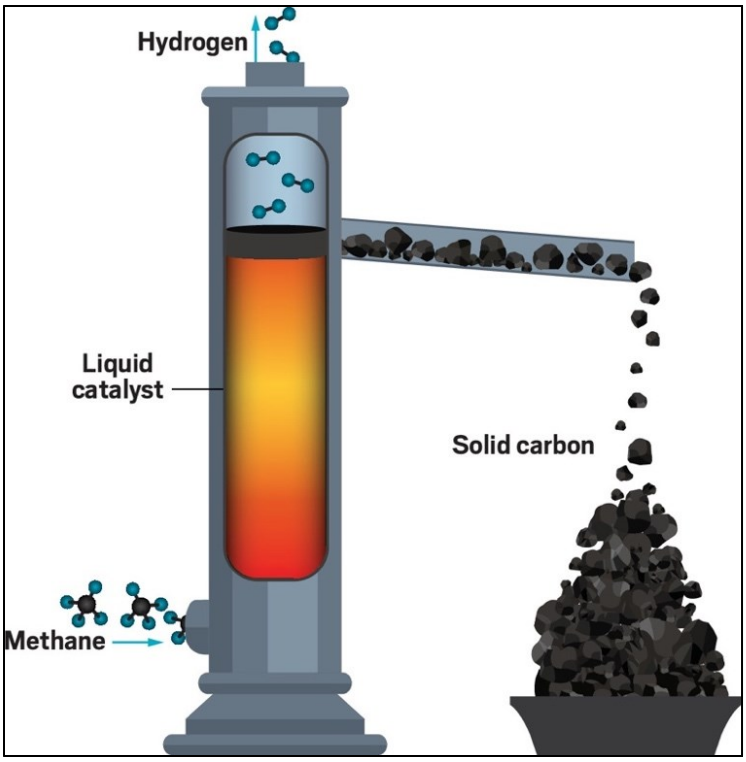

Figure 5.5: C-Zero Methane Pyrolysis (McCoy 2021)

According to Bloomberg analytics, the long-term goal for hydrogen to become a viable fuel must reach a price as low as 1 € or 2 € per kg. Right now, it is nowhere near that price around 4€ to 5€ per kg on Green-Hydrogen. Electrolysis market share of Green-Hydrogen makes only 2% of hydrogen production today. (Bloomberg 2022b)

6 Airbus A320 Conversion to Liquid Hydrogen

As an undisputed leader on the narrow body airliners in the market, the Airbus A320 family still holds a strong potential for the future. From the airport operations perspective, it has proven to fulfil the needs of travelers without needing more investment to terminal infrastructure. Just as small regional airports with high amounts of annual passengers struggled in terms of infrastructure in the past with bigger airliners as the A380 and 747 variants which slowly come to the end of their journey.

6.1 Hydrogen Conversion Parameters for a Passenger Aircraft

Starting from a conventional aircraft preliminary sizing, some adjustments must be made to consider in a general manner the changes required by an LH2 aircraft. These changes comprise the following three aspects.

6.1.1 Specific Fuel Consumption Adjustment

Kerosene and hydrogen have many differences as discussed in Chapter 4 . These differences must have an influence in the way a turbofan handles the energy density of hydrogen. Nonetheless, there is no information available on the propulsive nor thermal efficiency of turbofan engines running on hydrogen can be used to compare.

Considering the same assumptions from Chapter 4.1, in which the hydrogen combustion is stable, the flame propagation velocity is controlled, the temperature in the combustion chamber does not exceed the temperature from Jet-A fuel, the specific fuel consumption of turbofan engine running on LH2 is calculated as an estimate in which the energy supplied must meet the same criteria as a Kerosene engine. (Scholz 2021)

If hydrogen has 2.79 more energy per kg than Kerosene. This means that LH2 can store up the same amount of energy of Jet-A fuel in just 35,84% of mass. The same fuel fraction applies to hydrogen consumption on the different flight segments.

$$SFC_{LH2} = k_{c,LH2} \cdot SFC_{Kerosene} \tag{6.1}$$

$$With\ k_{c,LH2} = 0{,}3584$$

6.1.2 Operating Empty Mass Adjustment

Another aspect to consider in the preliminary sizing further discussed in Chapter 7, the fuel systems of LH2 aircraft vary significantly from the ones in the conventional current generation of kerosene passenger airplanes. The larger tanks of hydrogen being pressurized and not integrated into the wing represents an overall increase of the structural weight of the aircraft. Regardless of the LH2 tank system integration, the ratio between Operating Empty Mass (m_{OE}) and Maximum Take-Off Weight (m_{MTO}) rises. (Scholz 2021)

$$\left(\frac{m_{OE}}{m_{MTO}}\right)_{LH2} = k_{OEM,LH2} \cdot \left(\frac{m_{OE}}{m_{MTO}}\right)_{Kerosene} \tag{6.2}$$

Based on parameters of past LH2 passenger aircraft projects, the factor for the Operating Empty Mass Ratio $k_{OEM,LH2}$ documented by Scholz in 2021 are shown on Table 6.1

Table 6.1: Operating empty mass adjustment factors (Scholz 2021)

Aircraft similar to….	Average $k_{OEM,LH2}$	Source
ATR-72	1.102	Seeckt 2010a
Airbus A320CEO	1.140	Dib 2015
Lockheed C5	1.020	Seeckt 2010b
Average	1.087	

On the calculations included in the preliminary sizing postulated in Chapter 9.2, the value $k_{OEM,LH2}$ = 1.140 from the Airbus A320CEO was considered.

6.1.3 Maximum Glide Ratio Adjustment

By having a greater volume of the fuselage due to LH2 tanks and systems, the surface in contact with the surrounding air increases. This area difference of the wetted area of the aircraft leads to a reduction of the maximum glide ratio E_{max}. (Scholz 2021)

$$E_{max} = K_{E,LH2} \cdot \sqrt{\frac{A}{S_{wet}/S_w}} \tag{6.3}$$

During the preliminary sizing the actual value for the wetted area is still unknown. Despite that, the difference of the wetted area of a LH2 aircraft to a conventional passenger airplane, plenary on its influence on the maxim glide ratio can be included in the factor K_E.

$$K_{E,LH2} = K_{k,E,LH2} \cdot K_{E,K} \tag{6.4}$$

With the factor for the maximum glide ratio adjustment $K_{K,E,LH2}$ extracted from parameters of past LH2 passenger aircraft projects were documented by Scholz in 2021 which are shown on Table 6.2.

Table 6.2: Maximum glide ratio adjustment factors (Scholz 2021)

Aircraft similar to….	Average $k_{K,E,LH2}$	Source
ATR-72	0.982	Seeckt 2010a
Airbus A320CEO	0.968	Dib 2015
Lockheed C5	0.974	Seeckt 2010b
Average	0.975	

Once more, for the calculations included in the preliminary sizing postulated in Chapter 9.2, the value $K_{K,E,LH2} = 0.968$ from the Airbus A320CEO was considered.

6.2 Fossil Fuels Storage in Aviation

On modern aircraft most of the Kerosene fuel tanks are embedded into the wings. One argument could be that it might be the easiest way of making use of the volume inside the wings by filling them with liquid (Figure 6.1), but the main reason is that as a plane flies and Kerosene is burned down by the engines, the center of gravity will not shift considerably as if it was situated further away, besides providing some counterweight on the wing bending moments.

Moreover, if this area inside the wings wouldn't be used the fuselage volume would have to be adjusted accordingly. Having a longer or thicker fuselage would increase the aircraft's drag in consequence and therefore cause a shift on the center of gravity. However, some aircraft may use a smaller fuel tank at the empennage area to shift the center of gravity on demand to increase efficiency. That happens because as the aircraft starts burning fuel the lift force required to stay at the same cruise height would decrease. Accordingly, the required opposite lift made by the horizontal stabilizer also decreases. Even though the angle of attack of the horizontal stabilizer could be changed, they were conceptually optimized to have a certain angle, therefore having the possibility of shifting this weight around is required.

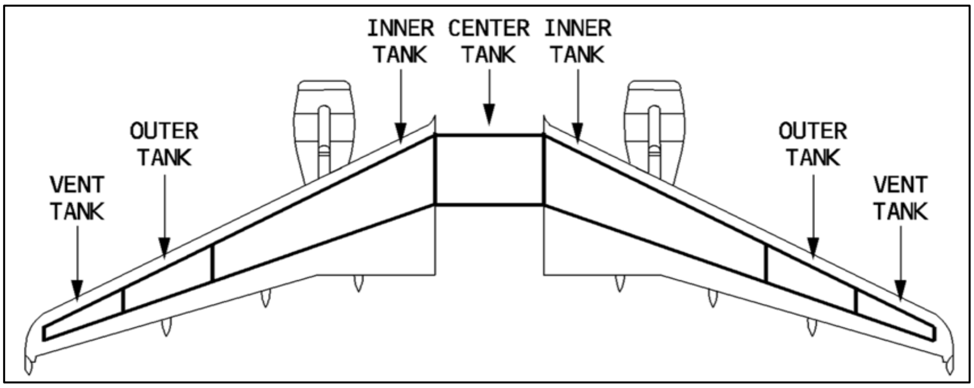

Figure 6.1: A320 Wing fuel storage (Airbus 2020b)

6.3 Liquid Hydrogen Storage Solutions

Assuming both combustive propulsion alternatives capability of converting chemical energy from Kerosene and LH2 to thrust are equal, a comparison of the equivalent space for fuel in an A320NEO is presented in Table 6.3.

Table 6.3: Volumetric comparison setting energy as a reference.

A320NEO-Kerosene		
Tanks Capacity (Inner, Outer and Central)	23.86 liters	(Airbus 2020b)
Maximum Fuel Weight	18729 kg	(Chevron 2007)
Maximum Energy Storage Estimate	805.347 MJ	(Chevron 2007)
LH2-A320NEO		
Equivalent Energy Storage	805.347 MJ	(Absolut Hydrogen 2021)
Equivalent LH2 Weight	6712 kg	(Keen 2020)
Equivalent LH2 Tanks Required	94818 l or 94,04 m^3	

As expressed in Table 6.3, switching from Kerosene to Liquid Hydrogen does not add up weight to the aircraft itself. However, the volume of LH2 required to substitute Kerosene as an energy carrier in the aircraft is substantially higher. Besides that, the storage means in which LH2 needs to be carried safely for the equivalent energy consumption cannot be stored into the wings truss structure as it is done with kerosene. A pressurized and thermal insulated tank is required to do so. To incorporate such systems (Chapter 6.3.4) rather than making the plane lighter would result in additional mass for the aircraft's empty weight in around 14% percent. (Scholz 2021)

The use of lighter composites materials on the fuselage as used on the top section of A380's fuselage could somehow counterbalance this weight increment around 25%. In a similar manner the specific fuel consumption would be altered. (Clean Sky 2, 2020)

The most effective shape of a high-pressure tank that will undergo thousands of cycles of charge and discharge would be spherical or cylindrical. Having several smaller pressurized tanks for wing storage would add up as an inefficient use of this space between them. Any other tanks that could be added to the external structure of the aircraft, such as wingtip tanks, as the ones on the Learjet 35, are also contributing to a drag increase. The military aircraft solution of using external auxiliary fuel tanks might come to mind but the energetic demand remains unfulfilled. (Scholz 2015)

6.3.1 Fuselage Tank Integration

Freeing more than 83m^3 inside the fuselage can be tricky without interfering with its payload capacity. Using the cargo area of the A320 would not be enough since it is only 34,7m^3. Then again cause of the shape of the LH2 containers, only a fraction of the available volume in the cargo compartments could be used. Refitting cryogenic LH2 into the fuselage of existing aircraft requires freeing some space. Removing 10% to 20% of a passenger aircraft is a tough ask for airlines, especially low-cost whose profit is around 2,7% being generous. This could be reflected on a Cost per Available Seat Mile if other factors on the direct operating costs (DOC) do not decrease with the integration of hydrogen propulsion. (Bloomberg 2022a)

Following the low-cost carrier market trend of keeping discounted tickets to compensate charging extra fees for checked baggage in the cargo compartment, short and medium range flights below 3000 NM tend to be flown with passengers taking their belongings as carry-on luggage to reduce spendings and waiting at the baggage belt upon arrival. According to the Time Magazine, with lost luggage becoming more common and staff shortages, delays, and cancelations. Out of a poll from 2022 in the USA only roughly 55% of travelers checked their luggage while flying in 2022. (Time Magazine 2022).

Starting from here, the use of the cargo compartment in the fuselage of single aisle aircraft has the possibility of being fitted to accommodate the LH2 Tanks and cryogenic systems.

6.3.2 Fuselage Sizing

Keeping the lowest modifications possible from the base A320NEO ensures that undergoing the long and expensive process of airworthiness of regulatory authorities such as the FAA and

EASA is minimized. Planning on requesting a supplemental type certificate for the fuselage approval based on the already in use of variants in which the addition or subtraction of frames constitute an aircraft family. On the conventional A320NEO the cargo compartments are located and divided as shown in Figure 6.2.

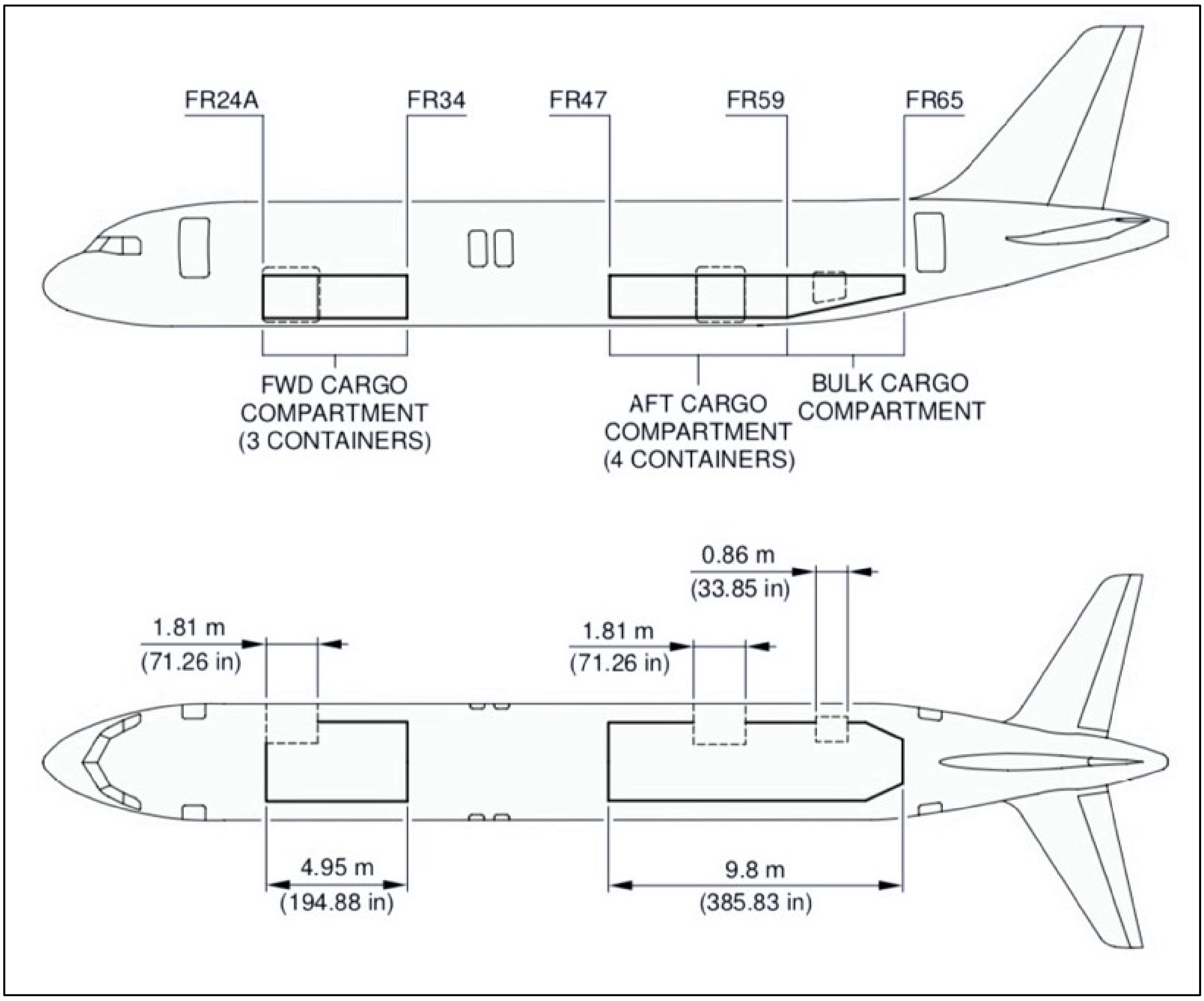

Figure 6.2: A320NEO Cargo compartments dimensions (Airbus 2020b)

The total volume of the cargo compartments according to the Aircraft Characteristics and Maintenance Planning is expressed in Table 6.4. Although the totality of this volume could not be used as a direct equivalent of the hydrogen tanks capacity, it will help as a reference to determine how much longer the fuselage must be to accommodate the required volume.

Table 6.4: Conventional A320NEO cargo compartments volume (Airbus 2020b)

	Capacity
Usable volume, forward cargo compartment	13.28 m^3
Usable volume, aft cargo compartment	15.56 m^3
Usable volume, bulk cargo compartment	5.88 m^3
Total usable volume	34,72 m^3

6.3.3 Cross-Sectional Useable Area

Taking as a reference the LD3-45 cargo containers (Figure 6.3) designed for the A320 Family, two LH2 containers with the outer diameter of 1,0922 m (∅ 43 in) could easily be fitted into the forward and aft cargo compartments. (Delta Cargo 2024)

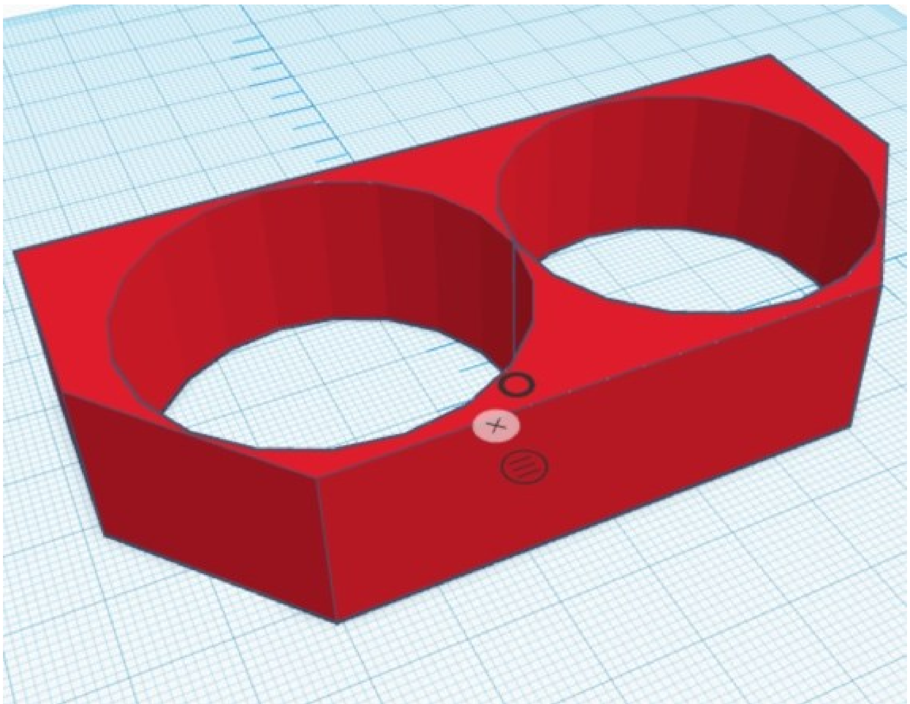

Figure 6.3: LH2 tanks projected over a LD3-45 container

The cargo area could be divided into a front and a back section taking the approach of the Fokker 50 and Boeing 747 Combi shown in Figure 6.4 for an even weight distribution without blocking the access of the cockpit through the cabin.

Figure 6.4: KLM’s Boeing 747-400M (Boeing-747.com 2017)

To fulfill the fuel capacity of 112,68 m^3 of required by the LH2 variant of the A320NEO, the fuselage extension should be minimized to still fit in the A320 Family of aircraft. To do so the LH2 Tanks are fitted into 3 different categories. One Aft Tank, two Front Tanks and two Back Tanks as shown in Figure 6.5 and Figure 6.6. The overall length of the front and back tanks can be adjusted in such a way that the position of the aircraft's center of gravity is not affected. The length of the single Aft Tank is chosen also in a way that the length of the other four tanks is not too long as well.

Figure 6.5: LH2-A320 Fuel Tanks in the Fuselage

Figure 6.6: LH2-A320 Cross section concept with tanks installed

6.3.4 Wall Thickness: LH2 Tanks Integrity

On the structure of the tanks, Hydrogen molecules are small enough to get through the metallic crystal grid of steel and corrode it from the inside causing an embrittlement of a container (Figure 6.7) if not properly isolated by an inner lining (Liu 2021). The same might occur with some engine components and ducts inducing a premature failure of components after a long exposure to hydrogen. However, aluminum-, copper- and beryllium-based alloys are less susceptible to hydrogen induced embrittlement along with other non-steel-based alloys. (Gao 2017)

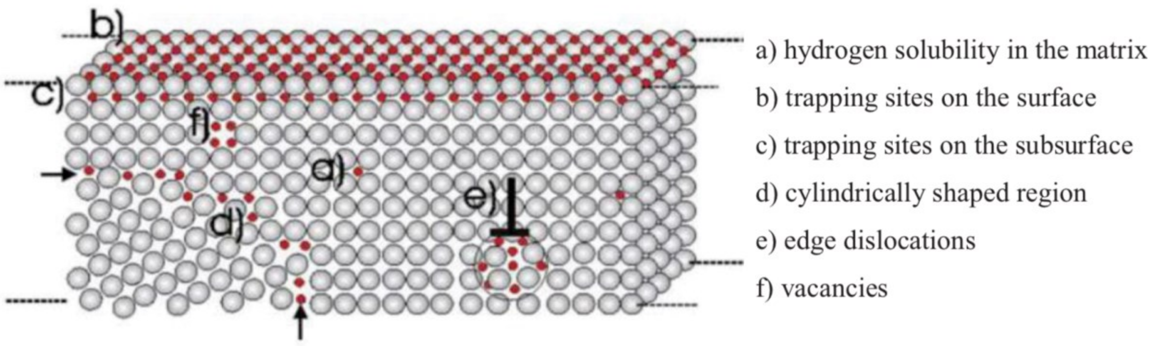

Figure 6.7: Reaction of hydrogen on steel structures (Gao 2017)

The wall thickness of the LH2 tanks on the aircraft lights a series of doubts on the weight increase, the volumetric capacity of the inner vessel, the insulation, safety and the life cycle of the fuel systems. By using a *Multi-Layer Insulation* (MLI) (Figure 6.8) a method developed by NASA the heat radiation inleaks of the environment to the LH2 vessels are minimized (Wikipedia 2024b). The MLI is used where great temperature differences exist. The recommended 40 Layers of Insulation for temperatures up to -260 °C would only be 16mm thick. (Frankoterm 2024)

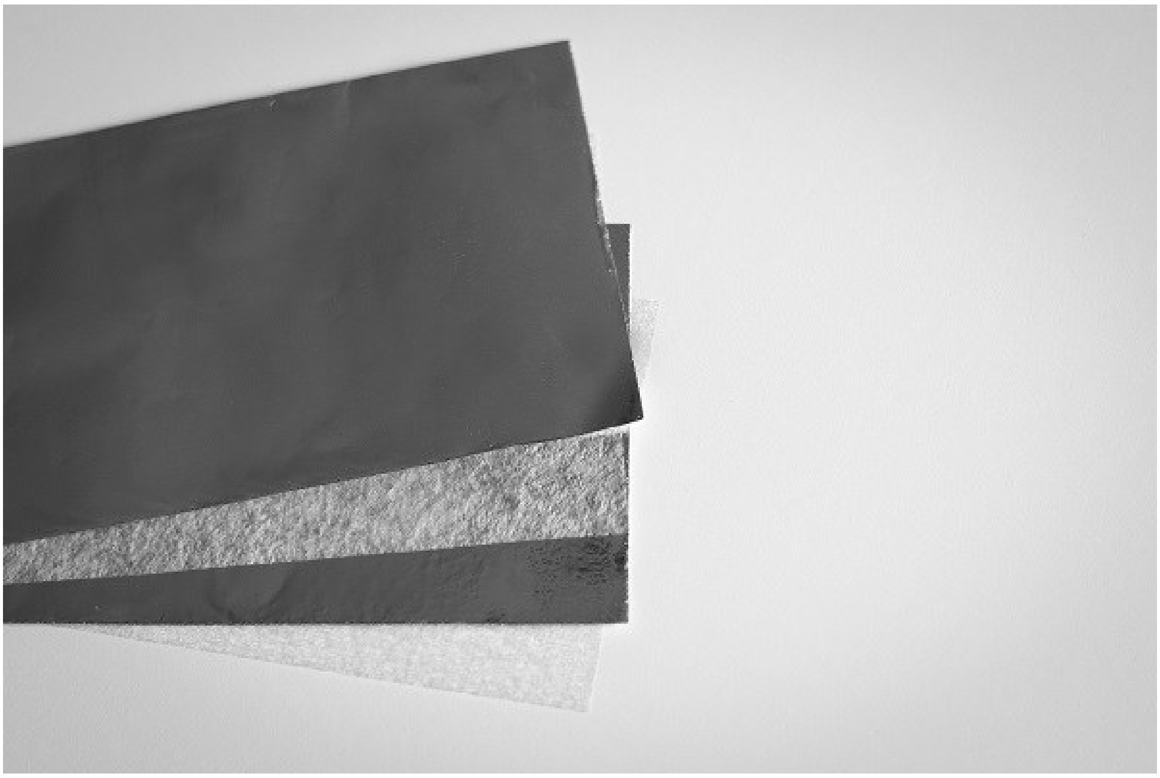

Figure 6.8: Aluminum and Spacer Multi-Layer-Insulation (Frankoterm 2024)

To comply with the EASA Requirements for the A321XLR, the fuselage integrated tank's structure must ensure adequate protection of occupants against the hazards of external fire and burn, ignition of fuel vapor and explosion of the fuel tank, as well as to ensure the shock resistance of this fuel tank, so that no fuel is released in quantities sufficient to start a serious fire in an otherwise survivable collision event. (Beresnevicius 2023)

On the structural integrity of the LH2 Tanks, the worst-case scenario of a weapon impact should also be considered. Relying on the tests of *Kural 2018*, the minimum wall thickness of an AL6061 T6 hydrogen tank should be 42 mm. On Figure 6.9 stresses, shock waves on tank caused by the penetration of 7.62 mm projectiles into various thicknesses hydrogen tanks (a) 10 mm, (b) 20 mm, (c) 30 mm, (d) 40, and (f) 42 m. (Kural 2018.)

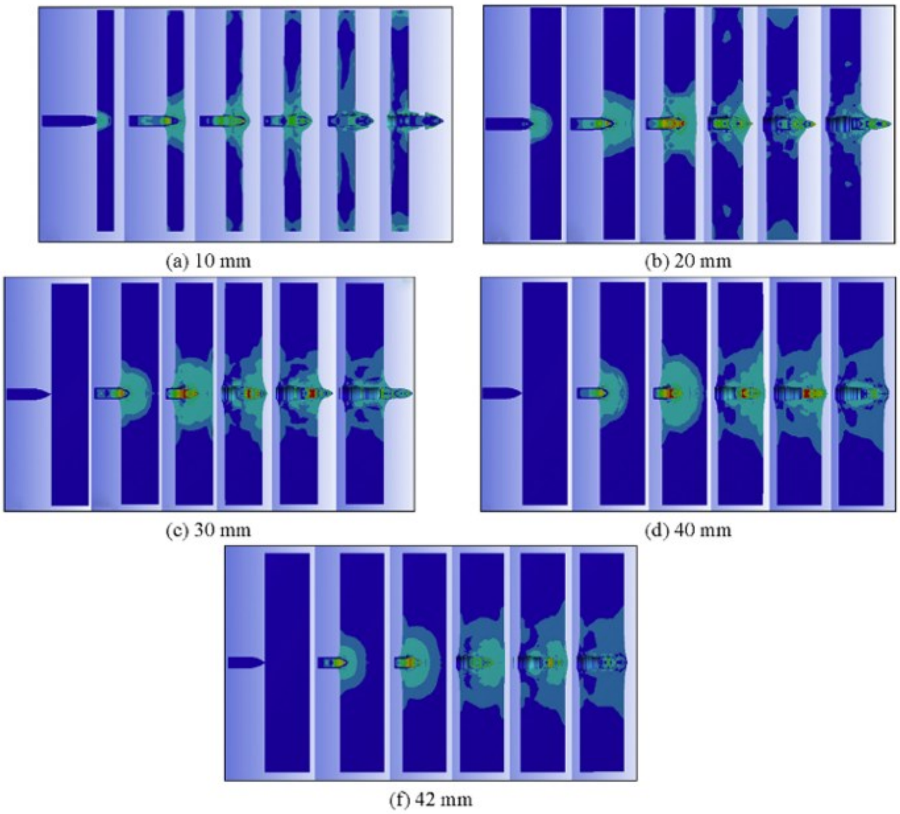

Figure 6.9: Stresses by projectiles' penetration in aluminum (Kural 2018)

During the LH2 fuel tanks sizing, the wall thickness was set at 65mm considering a more MLI than necessary and an increase of the Aluminum thickness of the outer vessel for an increased safety factor. The hydrogen tanks dimensions are summarized on Table 6.5 and the detailed formulas are available in the Excel File *"LH2_Fuel_Tanks_Integration.xlsx"* or Figure 6.10 as a preview of the approach taken. (Torenbeek 1982)

	A	B	C	D	E	F	G	H
1		Liquid Hydrogen A320 Fuel Tanks Integration						
2		Radius	Units	Quantity	Sphere Volume[m^3]	Cylinder Section Volume [m^3]	Fuel Percentage	Mass [kg]
3	Wall Thickness	0.065	Multi Layer Insulation					
4	Front Tanks	0.48	m	2	0.466438811	11.99788046	22.12%	1766.19
5	Back Tanks	0.48	m	2	0.466438811	2.181432812	4.70%	375.20
6	Aft Tank	1.91	m	1	29.18694979	53.29292534	73.18%	5843.70
7								
8	Total LH2 Volume Required	112.68	Cubic meters					7985.10
9								
10	Front Tanks Length	16.5	m					
11	Back Tank Length	3.0	m	Total Volume	112.7042569	Cubic meters		
12	Aft Tank Length	4.65	m					
13	Overall Tanks Length in the Fuselage	30.28	m					
14								
15	M Cargo Front	309.00	Kg					
16	M Cargo Back	617.66	Kg					
17	M Fuel	7985.10	Kg					
18								
19	Mass balance	144.41	Kg*m					
20	CG Variation	0.02	m					
21								
22	Fitnesse Ratio	12.12	OPTIMAL is 8. Extended Aircraft Reach up to 14	ROSKAM III	Length of the fuselage divided by Fuselage diameter			
23								
24	Seat Pitch	30.00	In (RAYMER 89) —>	0.762	m			
25	nPAX	180.00						
26	nSA	6.04						

Figure 6.10: Preview of the LH2 Fuel Tanks Sizing in Excel

Table 6.5: LH2 Tanks Integration Preview

	Units	Diameter[m]	Length [m]	Volume [m^3]	Mass [kg]	Percentage
Front Tanks	2	0.48	16.5	24.93	857.28	22.12%
Back Tanks	2	0.48	3	5.30	187.75	4.70%
Aft Tank	1	1.91	4,65	82.48	5546.84	73.18%
Total Fuel				112,71	7985.10	
Cargo Front					309	33,33%
Cargo Back					617,66	66,66%
Estimate Fuselage length (Scholz 2015)			50.31			
Finesse Ratio				12,12		
Number of Frames added (Airbus 2020b)	24 (8+5 from A321NEO and 11 from LH2 Variant)					
CG Variation			0,02 m			

Regardless of providing negligible CG variation in this solution, the proposal made by Airbus on the ZEROe designs Figure 6.11 taking the same approach of the TU-155 seems to be the most efficient way of LH2 storage in a fuselage. Having a reduced tank surface area by condensing the volume in one section of the aircraft without compromising the cargo area.

Figure 6.11: ZEROe liquid hydrogen tank integration proposal (Airbus 2020a)

A more detailed solution to the tank integration and systems (Figure 6.12) will be required for further development of LH2 aircraft. Primarily depending on the volumetric capacity required in a manner that does not interfere drastically with the payload capacity.

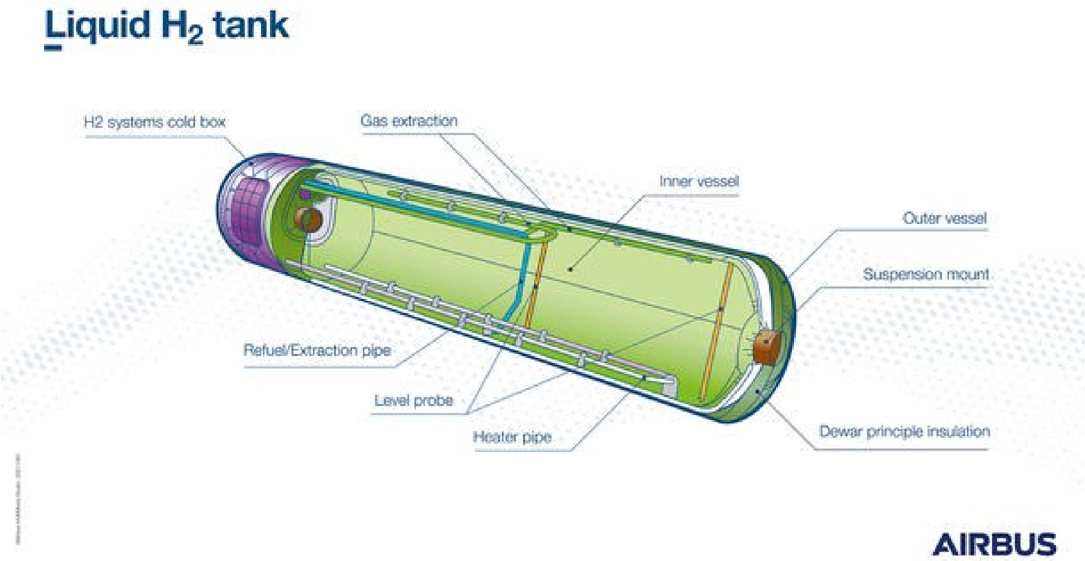

Figure 6.12: Airbus ZEROe LH2 Tank proposal (Airbus 2021)

6.4 Turboprop Engines Airframe Integration on a A320NEO

Besides determining the wing aspect ratio and wingspan, the turboprop engines have to be integrated. Based on the PW-Allison 578-DX (Figure 6.13) and GE36-UDF initially tested on the Boeing 7J7 (Figure 6.14) in 1986 and later the MD-80 on the Farnborough Airshow in 1988, the most advanced turboprop development of the recent years has been the CFM-RISE (Figure **6.16**). Following the past development of Safran-GE venture, the open fan architecture promises 20% propulsive efficiency improvement. Tests with LH2 have already been conducted. (CFM RISE 2021)

Figure 6.13: PW Allison 578-DX (Wikipedia 2024a)

Figure 6.14: GE36-UDF Flight Test (CFM RISE 2021)

Aside from these benefits, the technology could also facilitate the integration of the turboprop engines under the wing of the conventional A320NEO reducing the required propeller diameter and the concerns of blade tip inefficiency by approaching the speed of sound. (Figure 6.15). The fuselage sections alongside the propellers must also be reinforced as known from the ATR family to stop any fragments in the event of a blade-out scenario.

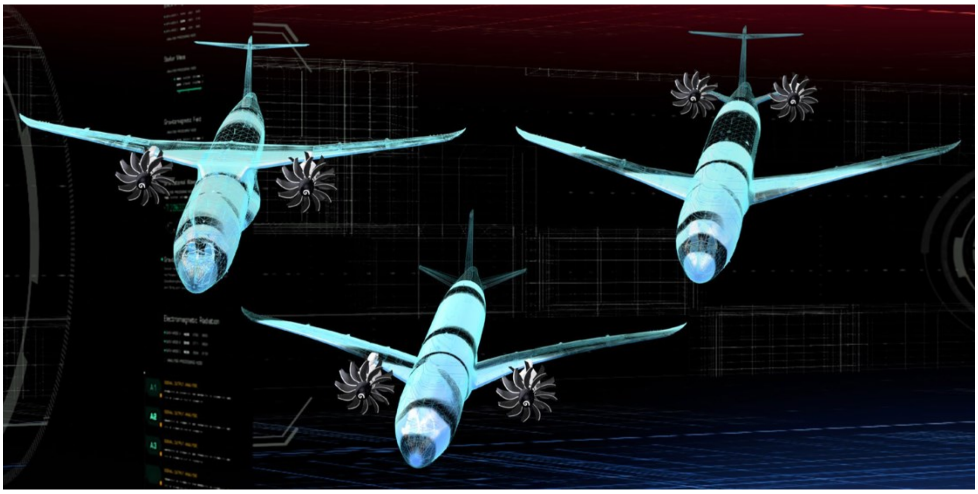

Figure 6.15: CFM concept rendering of the integration proposals (CFM RISE 2021)

The main difference from the canceled projects from the 80's has been instead of compromising the reliability of the geared contra-rotating blades the approach to reduce energy loss of the flow on swirl was modified. The second set of blades does not spin. Acting as an adaptable stator, the fans have a variable pitch to optimize the direction of the airflow. With advanced computing and fluid dynamics models, the challenge of excessive noise from the previous open fan technologies has been overcome, easily complying with the current and near future noise level regulations as those applicable to the latest LEAP models.

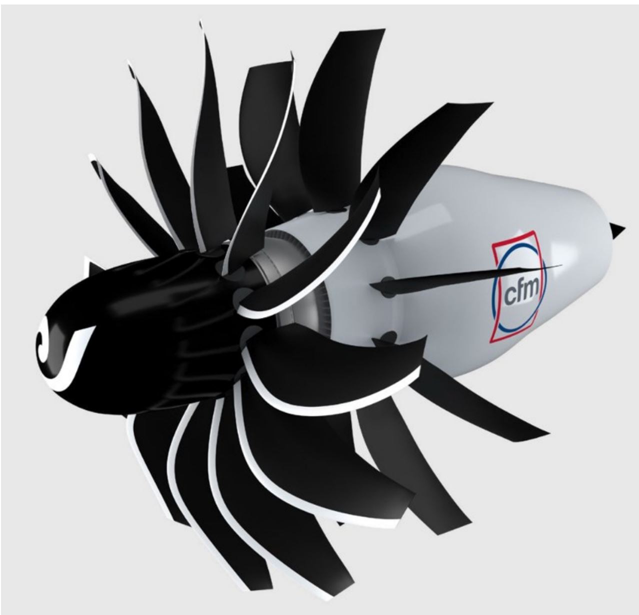

Figure 6.16: CFM RISE Engine Render (CFM RISE 2021)

7 Preliminary Sizing of an Aircraft

Based on the work of Loftin (1980), the preliminary sizing project phase is crucial while designing a new aircraft. In this stage the overall mass of the aircraft is reduced to a point mass. Without having a full grasp of the final geometry of the aircraft, the synergic adjustment of discrete and continuous design parameters provides an analysis of the aircraft's performance on different flight phases: Take-off, 2nd segment climb, cruise, landing and missed approach.

7.1 Landing

The landing distance safety requirements are defined in CS25.125. An aircraft's landing is allowed if the runway's length is bigger than the aircraft's landing distance divided by the safety factor. The safety factor is defined as 60% for jet aircraft and 70% for propeller aircraft within the runway's length. This means the runway's minimum length is equal to 1.667 times the landing distance for jets and 1.429 for propeller aircraft. The aircraft design needs to adjust to existing runways to still meet the CS criteria.

The approach speed of an aircraft is related to the landing distance but not directly mentioned on the CS25.125 regulations to the landing distance. The approach speed relation to the landing field length is defined as

$$V_{App} = K_{app} \cdot \sqrt{S_{LFL}} \tag{7.1}$$

With K_{app} =1.70 $\sqrt{m/s^2}$ keeping in mind that the approach speed with a CAS may not be less than $1.3V_S$

The wing loading at maximum landing weight m_{ML}/S_w is calculated by considering the air's density ρ at the airfield and the maximum lift coefficient with the high lift systems on landing configuration $C_{L,max,L}$.

$$\frac{m_{ML}}{S_w} = K_L \cdot S_{LFL} \cdot C_{L,max,L} \tag{7.2}$$

With the K_L adjustment factor set at 0,107 kg/m^3. Then the actual wing loading at maximum take-off weight m_{MTOW} is calculated

$$\frac{m_{MTO}}{S_w} = \frac{m_{ML}/S_w}{m_{ML}/m_{MTO}} \tag{7.3}$$

The ratio of m_{ML}/m_{MTO} is statistically set based on the range and type of aircraft to be around 0.89 in the case of passenger jets. (Roskam 1989).The wing loading calculation sets the position of the vertical line before which the landing phase is later represented in the matching chart.

7.2 Take-Off

The take-off distance safety requirements are defined in CS25.111. The take-off field length must be 15% longer than the distance the aircraft needs to leave the ground and overfly the take-off surface at a height of 35ft. The aircraft must be accelerated on the ground to a speed VEF, at which one engine remains inoperative for the rest of the take-off. With one engine less, the aircraft must be accelerated to V2 such that if the engine failure occurs before V1, the take-off procedure must be aborted. With engine failures after the V1 speed is reached, the take-off must continue with the remaining engines since there is no longer enough runway left to come to a full stop safely. The landing gear retraction may only begin when the aircraft is airborne. From the take-off phase, a thrust-to-weight ratio proportional to the wing loading follows. Depending on the take-off field length, atmospheric density ratio to the one at sea level, lift coefficient with flaps in take-off configuration and the factor $k_{TO} = 2.43\,\frac{\mathrm{m^3}}{\mathrm{kg}}$

$$\frac{T_{TO} \cdot (m_{MTO} \cdot g)}{m_{MTO}/S_W} = \frac{k_{TO}}{S_{TOFL} \cdot \sigma \cdot C_{L,max,TO}} \tag{7.4}$$

The maximum lift coefficient in take-off configuration follows from the lift coefficient in landing configuration. It can also be taken from aircraft statistics (Roskam 1989). The set of values determines the slope of the straight line representing the take-off phase in the matching chart.

7.3 Climb Rate during Second Segment

The second segment safety requirements are defined on the CS25.121. Following the take-off requirement of being able to climb with an inoperative engine, the flight path with the landing gear retracted must not be less than 2.4% for two-engine aircraft at V_2 speed. The remaining engines continue at the available maximum thrust. The weight remains as the one at the end of the take-off path. The thrust-to-weight ratio of all engines must be larger than during the situation when an engine failed.

$$\frac{T_{TO}}{m_{MTO} \cdot g} = \left(\frac{n_E}{n_E - 1}\right) \cdot \left(\frac{1}{E_{TO}} + \sin\gamma\right) \tag{7.5}$$

Due to the small climb rate percentage required on the CS regulations, the angle can be simplified by the conversion by its decimal equivalent. For example, $\gamma = 0.024$ by 2.4% minimum climb rate. The lift to drag ratio E_{TO} is calculated by an approximation following the assumptions described by Loftin 1980 considering the high-lift systems and retracted landing gear influence.

$$E_{TO} = \frac{C_L}{C_D} = \frac{C_L}{C_{D,p} + \frac{{C_L}^2}{\pi \cdot A \cdot e}} \tag{7.6}$$

The drag of the profile is composed of the profile's drag and induced drag component. The induced drag depends on the Oswald's efficiency factor, which is set to $e = 0.7$ due to the extended high-lift systems, the aspect ratio of the wing A and the lift coefficient.

$$C_{D,p} = C_{D,0} + \Delta C_{D,flap} + \Delta C_{D,slat} + \Delta C_{D,Gear} \tag{7.7}$$

The profile drag is formed by the zero-lift drag, the increase by the influence of the extended flaps $\Delta C_{D,flap}$ proportional to the lift coefficient for $C_L \geq 1.1$.

$$\Delta C_{D,flap} = 0.05 \cdot C_L - 0.055 \tag{7.8}$$

The influence of the slats is neglected, and the effect of the landing gear is zero since it is already retracted during this flight phase. The obtained thrust-to-weight ratio determines the position of the horizontal line over which the second segment is later represented in the matching chart. (Scholz 2015)

7.4 Climb Rate during Missed Approach

The missed approach safety requirements are defined in CS25.121. During this phase the landing procedure is aborted. The aircraft is still in landing configuration but climbs with considerable drag to make a new landing approach. Following the take-off requirement of being able to climb with an inoperative engine, the flight path climb must not be less than 2.1% for two-engine aircraft. The remaining engines continue at the available maximum thrust.

The approach speed may not be less than $1.3 V_S$ as predefined in the landing procedure, with extended landing gear (only by FAR Part25 but excluded on CS25.121) and flaps in landing configuration.

$$\frac{T_{TO}}{m_{MTO} \cdot g} = \left(\frac{n_E}{n_E - 1}\right) \cdot \left(\frac{1}{E_{TO}} + \sin\gamma\right) \cdot \frac{m_{ML}}{m_{MTO}} \tag{7.9}$$

Although being pretty similar to the method used for the second segment flight phase, the maximum landing weight during the procedure must be converted to its maximum take of weight equivalent only to fit proportionally to the thrust-to-weight ratio in the other calculations. The obtained thrust-to-weight ratio determines the position of the horizontal line over which the missed approach is later represented in the matching chart.

7.5 Cruise

During this flight phase it is assumed that the plane travels at a constant speed at a given altitude. The total lift produced equals the weight and the overall drag is balanced out by the thrust. The thrust-to-weight ratio is calculated using Equation 7.10.

$$\frac{T_{TO}}{m_{MTO} \cdot g} = \frac{1}{\left(\frac{T_{CR}}{T_{TO}}\right) \cdot E} \tag{7.10}$$

The maximum glide ratio is determined by a similar equation previously mentioned on Chapter 6.1.3 .The K_E factor equals 15.8. The relative wetted area S_{wet}/S_w ranges from 6.1 and 6.2 among passenger aircraft. (Scholz 2015)

$$E_{max} = K_E \cdot \sqrt{\frac{A}{S_{wet}/S_w}} \tag{7.11}$$

The thrust during the cruise flight phase can be calculated based on the cruise altitude and the by-pass ratio μ.

$$\frac{T_{CR}}{T_{TO}} = (3.962 \cdot 10^{-7} \cdot \mu - 1.210 \cdot 10^{-5}) \frac{1}{ft} h_{CR} - 0.0248\mu + 0.7125 \tag{7.12}$$

The wing loading following the lift and weight equivalence can be determined with the lift coefficient C_L, the standard atmospheric pressure *p(h)*, isentropic exponent $\gamma = 1.4$ and cruise Mach number.

$$\frac{m_{MTO}}{S_W} = \frac{C_L \cdot M^2}{g} \cdot \frac{\gamma}{2} \cdot p(h) \tag{7.13}$$

The set of values for wing loading and thrust-to-weight ratio for different altitudes are entered into a table. These values define the cruise curve on the matching chart.

7.6 Matching Chart

The matching chart provides a graphical representation of a two-dimensional optimization problem. By considering and regulating these flight stages synchronously in a matching chart, the preliminary sizing optimization of the aircraft is condensed into two variables. (Scholz 2015)

- Thrust to weight ratio $T_{TO}/(m_{MTO} \cdot g)$ (as low as possible: 1st priority)
- Wing loading m_{MTO}/S_W (as high without surpassing *landing* and *take-off*)

A design point is assigned to the set of values that optimally fulfills these criteria. In Figure 7.1 a hypothetical matching chart is shown as an example.

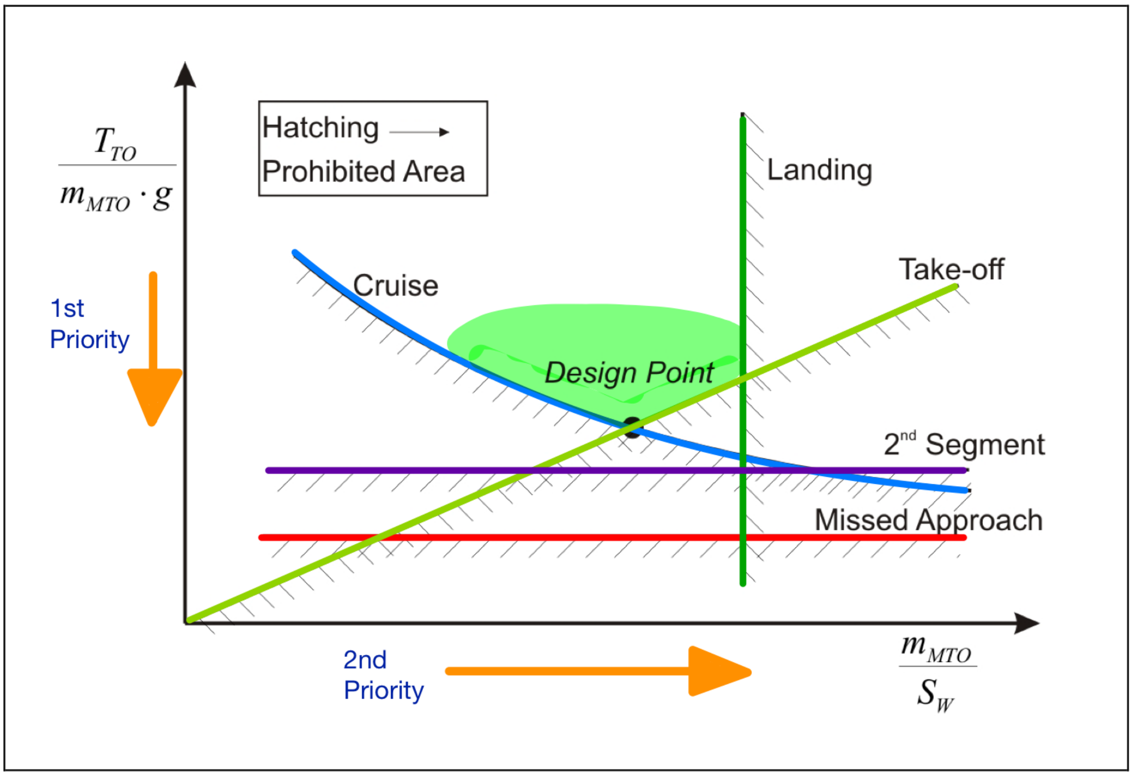

Figure 7.1: Hypothetical matching chart (Scholz 2015)

8 Aircraft Requirements

8.1 TLAR of a Conventional A320NEO

To properly substitute the current A320's market share in civil aviation, the liquid hydrogen variant proposed in this project must fulfil the same aspects by modifying as little as possible the traditional certified variants on Jet-A fuel so that the Type Certificate process must not act as a bottleneck in the development of the hydrogen aircraft. The specifications gathered from Airbus and Lufthansa's data related to the conventional A320NEO are expressed in Table 8.1. These values were used as the starting point to design the LH2-A320NEO.

Table 8.1: A320NEO Characteristics (Airbus 2020b)

Characteristics A320NEO	
S_{TOFL}	1925 m (@ m_{MTO})
V_{App}	135 kt
$C_{L,Max,L}$ *"Unswept"*	3.76
$C_{L,Max,TO}$ *"Unswept"*	2.85
m_{MLW}	67400 kg
m_{MTO}	79000 kg
m_{ML}/ m_{MTO}	0.8531
m_{ZF}	64300 kg
S_W	122.6 m^2
b	34.10 m (35.8 m with sharklets)
$A_{w,eff}$	10.5
n_E	2
nPAX	180
m_{cargo}	926.7 kg
ϕ_{25}	25°
λ_w	0.270
t/c	0.110
Engines	Pratt & Whitney PW1100G
T	120.6 kN
BPR	12.2
M_{CR}	0.78

8.2 Payload-Range Diagram Comparison

The Payload-Range Diagram must stay the same when moving from the conventional A320NEO aircraft to its LH2 counterpart. At least the Design Point "B" must be the same. However, making a hydrogen fueled A320NEO variant whose Payload-Range Diagram does match in every single point is not possible. By looking into a generic Payload-Range Diagram (Figure 8.1) of a conventional kerosene fueled aircraft we may see that Points B to C will present a variation derived from the fuel-density of hydrogen. The fuel consumption in terms of energy remains equal, but the mass reduction through the different flight phases does not have the same impact on the aircraft's overall weight. Thus, keeping the range at max payload (Point B) as a reference comparing both aircraft capabilities seems ideal.

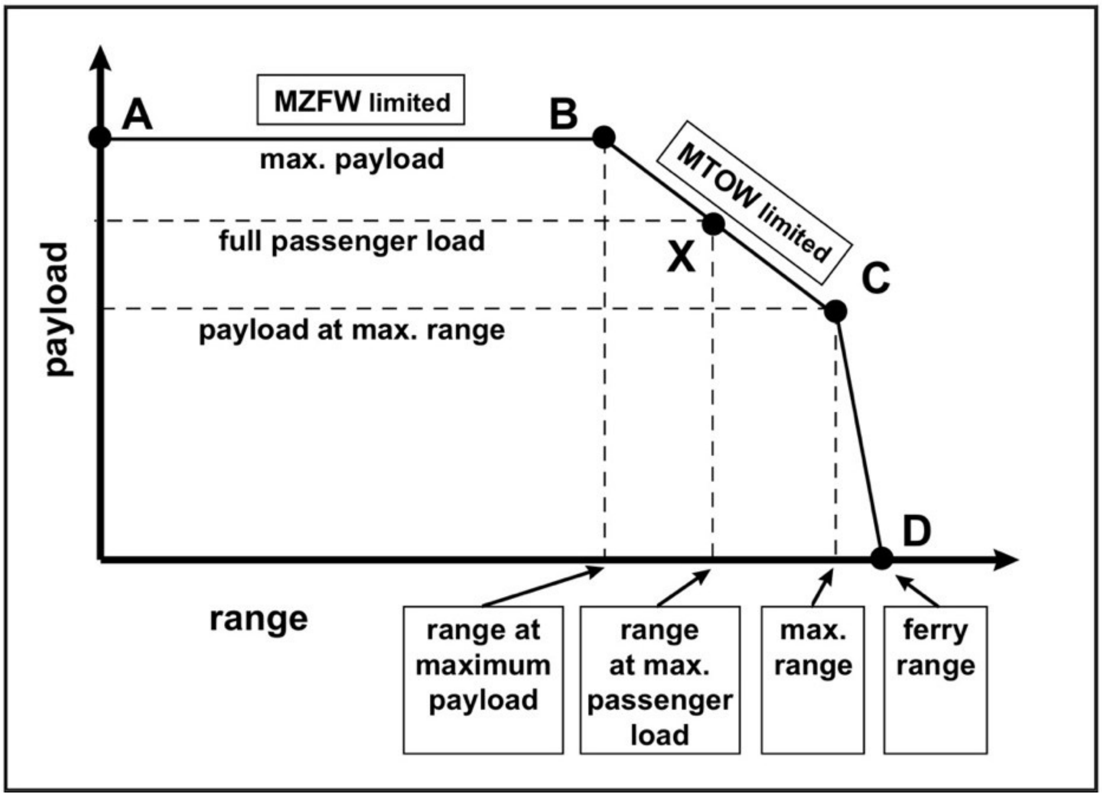

Figure 8.1: Generic payload-range diagram (Scholz 2015)

Otherwise, going through the diagram backwards we can see that the ferry range will not match. Besides both aircraft travelling without payload, the operating empty mass of the hydrogen variant must be higher than the kerosene aircraft. As the LH2 tanks and cryogenic systems must be included. Even at max payload, the fuel capacity will not be limited by m_{MTO}. The LH2 tanks integration was previously discussed in Chapter 6.3.1 but even if it was done the m_F of hydrogen would still be just 35.84% of the weight of Kerosene. (See Table 4.1)

Extracted from the gathered specifications of the conventional *A320NEO's Airport and Maintenance Planning December 2020*, the autonomy requirements for the LH2-A320NEO are based on the following payload-range diagram (Figure 8.2) of around 2433 NM at a m_{MTO} of 79000 kg from which 17666 kg correspond to the m_{MPL} on the ACT1. It is important to note on the range that the fuel reserve must be included to reach the divergence airport in 200 NM.

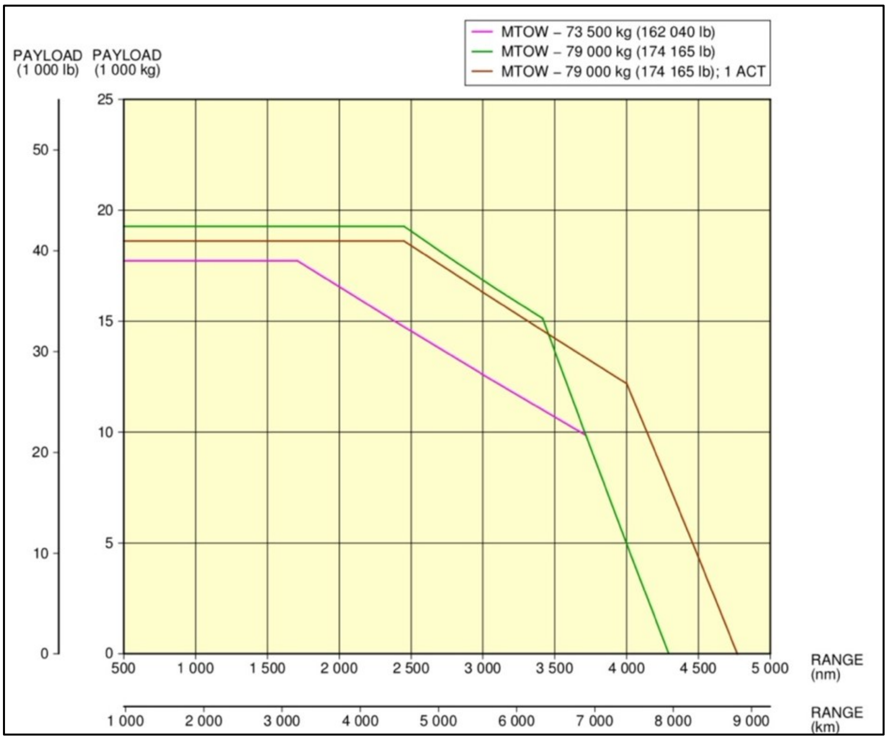

Figure 8.2: Payload-Range diagram A320NEO-ISA conditions (Airbus 2020)

From the m_{MTO} the take-off field length from Table 8.1 can be confirmed from the diagram extracted from *A320NEO's Airport and Maintenance Planning December 2020*. It is shown in Figure 8.3

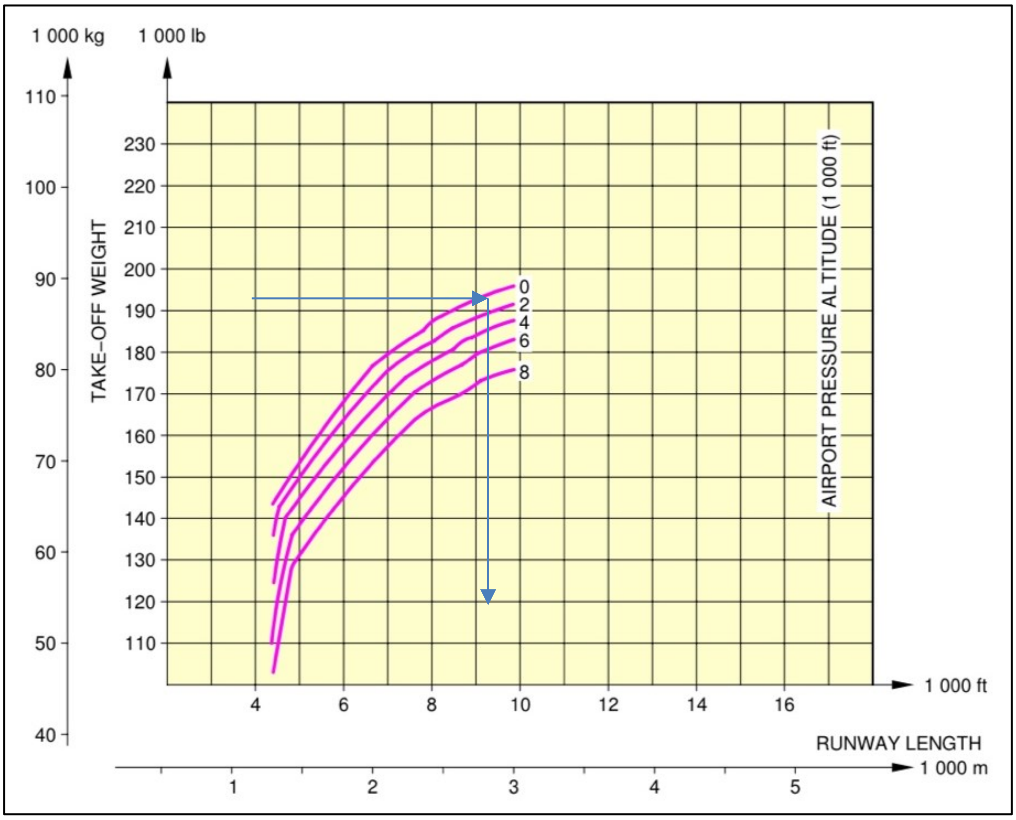

Figure 8.3: Take-off weight limitation A320NEO-ISA conditions (Airbus 2020)

In the same way the expected runway required at maximum take-off weight can be read from the diagram in Figure 8.3. By connecting both axis through the airport pressure at ISA conditions of *MLW* as the arrows show, the runway length is about 1925 m for take-off. This value will be later used in the SAS Tool to check if the LH2 variant still complies with the requirements of the conventional A320NEO-WV050.

The Cruise Mach number is not a TLAR but can be adjusted as an economic optimization of the aircraft. (Scholz 2015)

8.3 Payload, Fuel-Mass Interactions and Dimensions

If energy is required to make every gram of mass to be transported from point A to point B it is necessary to differentiate between masses on an aircraft. Right when a passenger aircraft's wheels leave the runway, is the heaviest the plane can be on its flight mission. A maximum take-off weight is set on every aircraft following the first law of aircraft design (Equation 8.1). If the total mass is below the given design limit and the CG deviation is within its limits, the plane should be capable of performing correctly within the basic Civil Aviation requirements of FAA and EASA for a safe take-off (CS25.113). Going through the different flight stages, the fuel mass fraction starts to decrease as the payload and aircraft's operating empty weight and payload remain unchanged. (Torenbeek 1982).

$$m_{MTOW} = m_{PL} + m_F + m_{OE} \tag{8.1}$$

With the given m_{MZF} from Table 8.1 combined with the m_{PL} from Figure 8.2, the value for m_{OE} can be calculated in Equation 8.2.

$$m_{MZF} = m_{OE} + m_{PL} \tag{8.2}$$

$$m_{OE} = 64300\text{ kg} - 17666\text{ kg}$$

$$m_{OE} = 45133\text{ kg}$$

The m_{cargo} can be calculated by using the n_{PAX}, the average m_{PAX} and $m_{baggage}$ from statistical data for middle range flights as shown in Equation 8.3

$$m_{PL} = \frac{m_{PAX}}{n_{PAX}} \cdot n_{Seat} + \frac{m_{baggage}}{n_{baggage}} \cdot n_{seat} + m_{Cargo} \tag{8.3}$$

$$m_{cargo} = 1766\text{ kg} - 79.4\text{ kg} \cdot 180 - 13.6\text{ kg} \cdot 180$$

$$m_{cargo} = 926 \text{ kg}$$

The missing m_F can be calculated with help of the m_{MTO}, m_{OE} and m_{PL} as follows in Equation 8.4.

$$m_{MTOW} = \frac{m_{PL}}{1 - \frac{m_f}{m_{MTOW}} - \frac{m_{OE}}{m_{MTOW}}} \tag{8.4}$$

$$m_f = m_{MTOW} - m_{PL} - m_{OE}$$

$$m_f = 16200 \text{ kg}$$

The lower part of Equation 8.4 saves some steps in which the fuel fraction and the relative operating empty mass are already given.

$$\frac{m_f}{m_{MTOW}} = 0.20506329$$

$$\frac{m_{OE}}{m_{MTOW}} = 0.5713081$$

For the fuel calculations is that Airbus used the density of kerosene at 785 g/l. An A320NEO-WV050 is equipped with four fuel tanks embedded in the wings and a central tank in the fuselage (Table 8.2) which add up to a capacity of 23858 l or 18728 kg (Airbus 2020b)

Table 8.2: Usable fuel tanks in A320NEO-WV050 1.28.10 (Airbus 2020b)

USABLE FUEL					
		OUTER TANKS	INNER TANKS	CENTER TANK	TOTAL
VOLUME	(liters)	880 x 2	6924 x 2	8250	23858
	(US gallons)	232 x 2	1829 x 2	2180	6302
WEIGHT *	(KG)	691 x 2	5435 x 2	6476	18728
	(LB)	1520 x 2	11982 x 2	14281	41285

* Fuel density : 0.785 kg/l or 6.551 lb/US Gal.

It is important to note that in the SAS calculations discussed in Chapter 9.1 the usage of the central tank is not accounted, thus the required volume is not met only by adjusting the taper ratio of the A320NEO sharklets.

The taper ratio of the wings set at λ = 0.27 with c_{root} = 6.07 m and c_{tip} =1.64 m. This slight change from the CEO increases the fuel capacity of the wings. Figure 8.4.

The fuselage diameter was also extracted from the aircraft clearance measurements shown in Figure 8.5.

The wetted area of the aircraft is a value indirectly given by Airbus on their maintenance data related to de-icing and external cleaning (Figure 8.6). For the wing surface reference area, the projected area across the fuselage still must be considered. This is done with the rectangle made by multiplying the fuselage diameter and the cord at the wing's root.

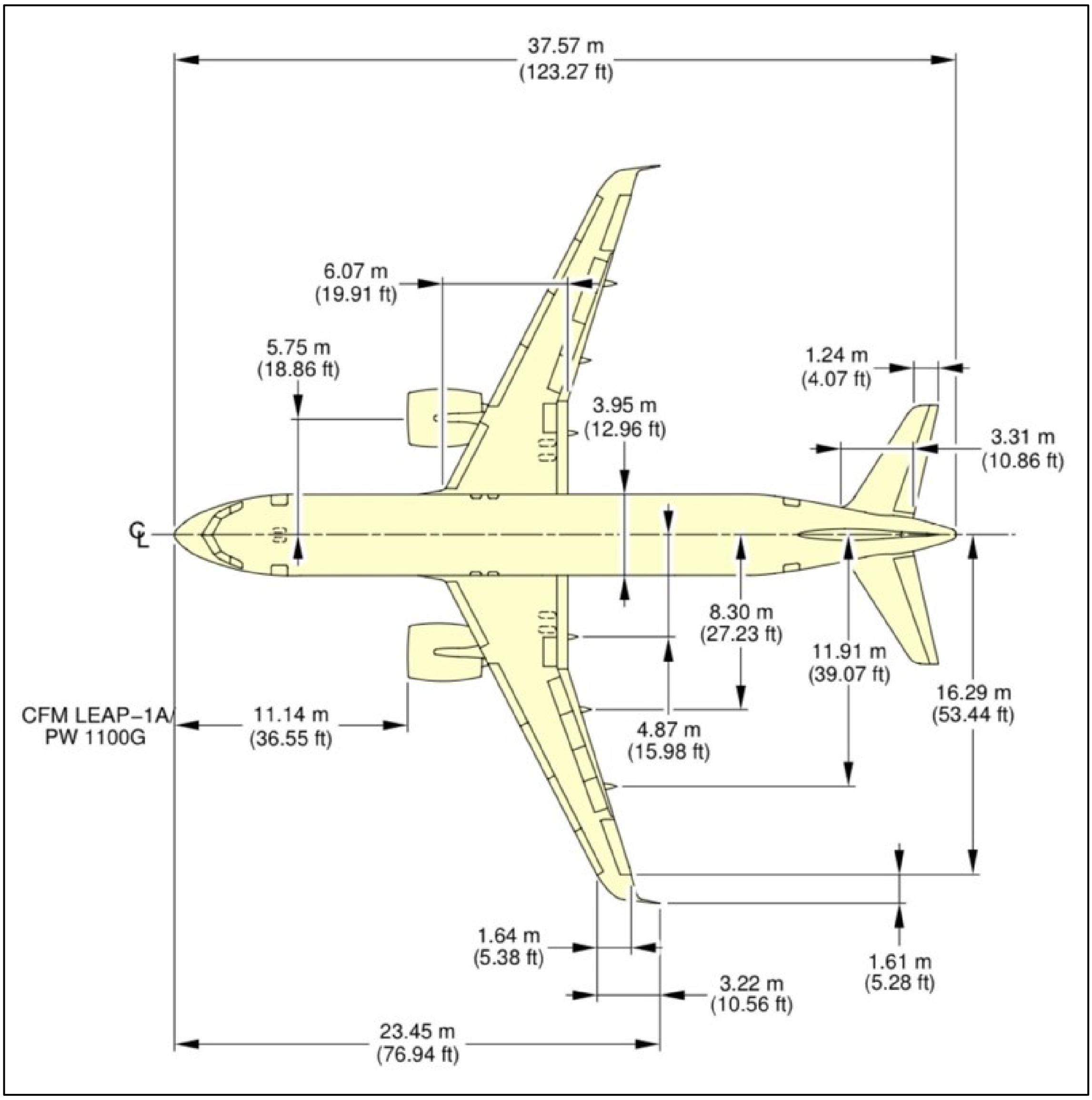

Figure 8.4: A320NEO general aircraft dimensions (Airbus 2020b)

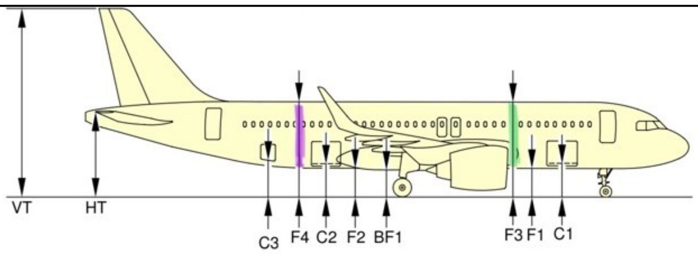

A/C CONFIGURATION		MRW FWD CG (17%) m	MRW FWD CG (17%) ft	MRW AFT CG (36.8%) m	MRW AFT CG (36.8%) ft	41 000 kg (90 389 lb) CG (26.5%) m	41 000 kg (90 389 lb) CG (26.5%) ft	A/C JACKED FDL = 4.60 m (15.09 ft) m	A/C JACKED FDL = 4.60 m (15.09 ft) ft
DOORS	D1	3.38	11.09	3.45	11.32	3.48	11.42	4.13	13.55
	D2	3.87	12.70	3.88	12.73	3.98	13.06	4.54	14.89
	D4	3.60	11.81	3.50	11.48	3.70	12.14	4.13	13.55
	C1	1.98	6.50	2.04	6.69	2.09	6.86	2.71	8.89
	C2	2.12	6.96	2.07	6.79	2.22	7.28	2.71	8.89
	C3	2.19	7.19	2.11	6.92	2.29	7.51	2.75	9.02
FUSELAGE	F1	1.72	5.64	1.76	5.77	1.82	5.97	2.43	7.97
	F2	1.84	6.04	1.79	5.87	1.95	6.40	2.43	7.97
	F3	5.86	19.23	5.90	19.36	5.97	19.59	6.58	21.59
	F4	5.99	19.65	5.93	19.46	6.09	19.98	6.58	21.59
	BF1	1.62	5.31	1.60	5.25	1.72	5.64	2.26	7.41
	CP1	4.17	13.68	4.27	14.01	4.28	14.04	4.96	16.27
WINGS	W1	6.70	21.98	6.65	21.82	6.80	22.31	7.25	23.79
	W2	4.05	13.29	4.01	13.16	4.16	13.65	4.65	15.26
TAILPLANE	HT	5.46	17.91	5.32	17.45	5.56	18.24	5.93	19.46
	AP	4.74	15.55	4.59	15.06	4.84	15.88	5.20	17.06
	VT	11.98	39.30	11.83	38.81	12.08	39.63	12.45	40.85
ENGINE/ NACELLE	N1 (CFM LEAP−1A)	0.46	1.51	0.47	1.54	0.56	1.84	1.13	3.71
	N1 (PW 1100G)	0.46	1.51	0.47	1.54	0.56	1.84	1.13	3.71

NOTE:
PASSENGER AND CARGO DOOR GROUND CLEARANCES ARE MEASURED FROM THE CENTER OF THE DOOR SILL AND FROM FLOOR LEVEL.

N_AC_020300_1_0320101_01_02

Figure 8.5: A320NEO fuselage diameter calculation (Airbus 2020b)

3. External Cleaning

AIRCRAFT TYPE	Wing Top Surface (Both Sides) m²	Wing Top Surface (Both Sides) ft²	Wing Lower Surface (Including Flap Track Fairing) (Both Sides) m²	Wing Lower Surface (Including Flap Track Fairing) (Both Sides) ft²	Wingtip Devices (Both Inside and Outside Surfaces) (Both Sides) m²	Wingtip Devices (Both Inside and Outside Surfaces) (Both Sides) ft²
A320	100	1 076	103	1 109	2	22
A320 Sharklet/neo	100	1 076	103	1 109	10	108

AIRCRAFT TYPE	HTP Top Surface (Both Sides) m²	HTP Top Surface (Both Sides) ft²	HTP Lower Surface (Both Sides) m²	HTP Lower Surface (Both Sides) ft²	VTP (Both Sides) m²	VTP (Both Sides) ft²
A320	27	291	27	291	43	463

AIRCRAFT TYPE	HTP Top Surface (Both Sides) m²	HTP Top Surface (Both Sides) ft²	HTP Lower Surface (Both Sides) m²	HTP Lower Surface (Both Sides) ft²	VTP (Both Sides) m²	VTP (Both Sides) ft²
A320 Sharklet/neo	27	291	27	291	43	463

AIRCRAFT TYPE	Fuselage and Belly Fairing m²	Fuselage and Belly Fairing ft²	Nacelle and Pylon (All Engines) m²	Nacelle and Pylon (All Engines) ft²	Total Cleaned Area m²	Total Cleaned Area ft²
A320	421	4 532	73	786	796	8 568
A320 Sharklet/neo	421	4 532	73	786	804	8 654

Figure 8.6: A320NEO external surface (Airbus 2020b)

Just as described in Chapter 7.5 ,the ratio from the overall exposed wetted area and the wing area for the maximum glide ratio at cruise calculated in the SAS tool remains between the statistical range of 6.1 and 6.2.

$$S_{wet}/_{S_w} = 6.105 \tag{8.5}$$

At the same time, if kerosene as energy carrier happens to be completely replaced by hydrogen, cryogenic systems, insulated tanks, or any other device which does not experience a considerable mass reduction during flight should be included as part of the airframe's operating empty weight as stated in Chapter 6.1.1.

9 Use of the Simple Aircraft Sizing Tool

For the preliminary sizing stage of the design of a LH2 passenger aircraft, the optimization spreadsheet-based tool *Simple Aircraft Sizing* developed at HAW Hamburg was used.

The SAS project arises as an extension of the previous OPerA – Optimization in Preliminary Aircraft Design following the contributions of Nita 2008, Heinemann 2012, Scholz 2012 and Krull 2022.

For its wide compatibility, SAS and OPerA were programed with Microsoft Excel taking advantage of the Solver and Visual Basic Macros functions. The SAS tool has been enhanced through the last decade in joint development of Prof. Dieter Scholz (Scholz 2012) with students at the Hamburg University of Applied Sciences based on the Preliminary Sizing chapter of his lecture notes (Scholz 2015). SAS provides optimized preliminary sizing by comparing through an iterative automated algorithm with roots in the OPerA tool. The ultimate output of this tool is the Design Point extracted out of the Matching Chart criteria lines previously described in Chapter 7.

9.1 Preliminary Sizing of a Conventional A320NEO

Firstly, the information gathered in Table 8.1 was written into the SAS Part 25 tool for turbofan passenger aircraft as user defined values in the *INPUT* sheet (Figure 9.1). By setting the take-off field length and range as values from the payload-range diagram in Figure 8.2, the following Matching Chart (Appendix A) and Design Point (Figure 9.20) and output parameters (Figure **9.2**) were obtained. The overall values calculated from the SAS tool do match the gathered information of the A320NEO (Figure 9.2 and Figure 9.3).

	A	B	C	D	E	F	G	H
1	Input Parameters	Values	Low	High	Remark	Input Value?	No of Inputs / Controls	
2	s_{LFL} [m]	1670	1400	1670		yes	1	
3	s_{TOFL} [m]	1925	1500	2000		no		
4	$C_{L,max,L}$ "unswept"	3.76	2.5	3.8		no	Stability 1	
5	$C_{L,max,TO}$ "unswept"	2.85	2.5	3.8		no		
6	m_{ML}/m_{MTO}	0.853	0.8	1		no		
7	$A_{W,eff}$	10.5	9	15		no		
8	n_E	2	2	4		no	Stability 2	
9	n_{PAX}	180	100	250		no		
10	m_{cargo} [kg]	926.66	0	3000		no		
11	φ_{25} [deg]	25	0	35		no		
12	λ_W	0.270	0.15	0.5		no	Find DESIGN POINT	
13	t/c	0.110	0.1	0.2		no		
14	BPR	12.20	6	14		no		
15	M_{CR}	0.780	0.55	0.85		no		
16	R at max. payload [NM]	2433	1000	2500		no		
17	Range type (for payload calculation)	1	1	2			Run DOE DIAGONAL Algorithm for a Single Input	
18	Reserve type (for calculating fuel reserves)	2	1	2				
19	**Design Objective** (in Matching Chart)	6	1	6				
20	Reference values (shown or not?)	1	0	1				

Figure 9.1: SAS-Part 25 for a conventional A320NEO-WV050

	A	B	C	D	E	F
48					DOE:	Output or
50	Output Parameters				DE:	Objective
51	m_F	16200	kg			no
52	m_{MTO}	79000	kg			yes
53	S_{wet} / S_W	6.1052239				no
54	m_{OE}	45134	kg			no
55	SFC	1.503E-05	kg/(Ns)			no
56	V / V_{md}	1.032				no
57	m_{MTO} / S_W	712				no
58	T_{TO} / (m_{MTO} · g)	0.324				no
59	h_{CR}	10257	m			no
60	V_{CR}	233	m/s			no
61	m_{ML}	67400	kg			no
62	S_W	110.9	m²			no
63	T_{TO}	125440	N			no
64	E_{CR}	18.7				no
65	$C_{L,CR}$	0.65				no
66	E_{max}	18.71				no
67	B_s	29466702	m			no
68	$C_{L,max,L,swept}$	3.41				no
69	Oswald Factor, e	0.783				no
70	λ_{opt}	0.18				no
71	$C_{L,max,TO,swept}$	2.58				no
72	b_{eff}	34.05	m			no
73	m_{MZF}	67196	kg			no
74	check_DP	1				no
75	check_fuel-tank-size	0				no
76	check_max-landing-mass	1				no
77						
78	Temperature above ISA, ΔT_L	0	K			
79	Temperature above ISA, ΔT_{TO}	0	K			
80						
81	*... pull more data from PS I and PS II to this INPUT tab, if you want to see more details here!*					
82						

Figure 9.2: SAS Output parameters for a conventional A320NEO-WV050

18				Play with di
19	**Design goal selected:**	**6**		
20				
21	Possible design goals for setting the cruise line (select on INPUT tab in B19)			
22	**1.)** Max. take-off mass	m_{MTO}	79000	kg
23	**2.)** Mission fuel mass	m_F	16200	kg
24	**3.)** Operating empty mass	m_{OE}	45134	kg
25	**4.)** Take-off thrust (one engine)	T_{TO}	250880	N
26	**5.)** Wing area	S_W	110.9	m²
27				

Figure 9.3: SAS Masses, thrust, and wing area conventional A320NEO-WV050

Although the wings taper was adjusted the fuel tanks volume as expressed in Chapter 8.3, the use of the central tank as it is included in the original Airbus maintenance manuals is still missing in the original SAS calculations. The corresponding matching chart can be found in Appendix A

As expressed at the end of the calculations in tab PSII shown in Figure 9.4, the required volume is 20,88 m^2. In Table 8.2 the volume of the center tank is 8250 l. Adding up outer-, inner- and central- tanks of a A320NEO the total volume is 23858 l. This means that instead of missing volume for kerosene, almost 3 m^3 of the tanks remain unused.

135						
136	Wing aspect ratio, effective	Aeff	10.45			
137	Wing taper ratio	λ	0.27		<<< from INPUT tab	
138	Fuel tank volume, geometric	V_{tank}	17.87	m³		
139	CS 25.979(b) fuel tank correction	k_{CS}	-2%		$V_{tank} = 0.54 \cdot S_W^{1.5} \cdot (t/c)_{av} \cdot \frac{1}{\sqrt{A}} \frac{1+\lambda+\lambda^2}{(1+\lambda)^2}$	
140	Correction accounting for unusable fuel	k_{UF}	-3%			
141	Sum of corrections	$k_{CS} + k_{UF}$	-5%			
142	Fuel tank volume, corrected	$V_{tank,corr}$	16.98	m³		
143						
144						
145						
146	Check, if wing fuel tank volume is sufficient on it own		$V_{tank,corr}$		>	$V_{F,erf}$?
147			16.98	m³	>	20.88 m³
148					no	
149	The wing geometry cannot accomodate the required fuel volume. Include ACT (Additional Center Tank) or ATT (Additional Tail Tank) or find other solutions to accomodate all fuel!					
150						

Figure 9.4: Fuel capacity conventional A320NEO-WV050 without center tank

9.2 Preliminary Sizing of a LH2-A320NEO

The same data computed for the conventional A320NEO was used as a foundation for the preliminary sizing using SAS for a modified A320 running exclusively on hydrogen. For this to be possible the LH2 parameter adjustment previously mentioned in Chapter 6.1, had to be added into the SAS-Part 25 tool as indicated in Figure 9.5. These three adjustments can easily be activated or deactivated on the INPUT sheet in cell E18 (Figure 9.6). By applying the parameter adjustments (Figure 9.7) , the data from Figure 9.8 and Figure 9.9 was gathered.

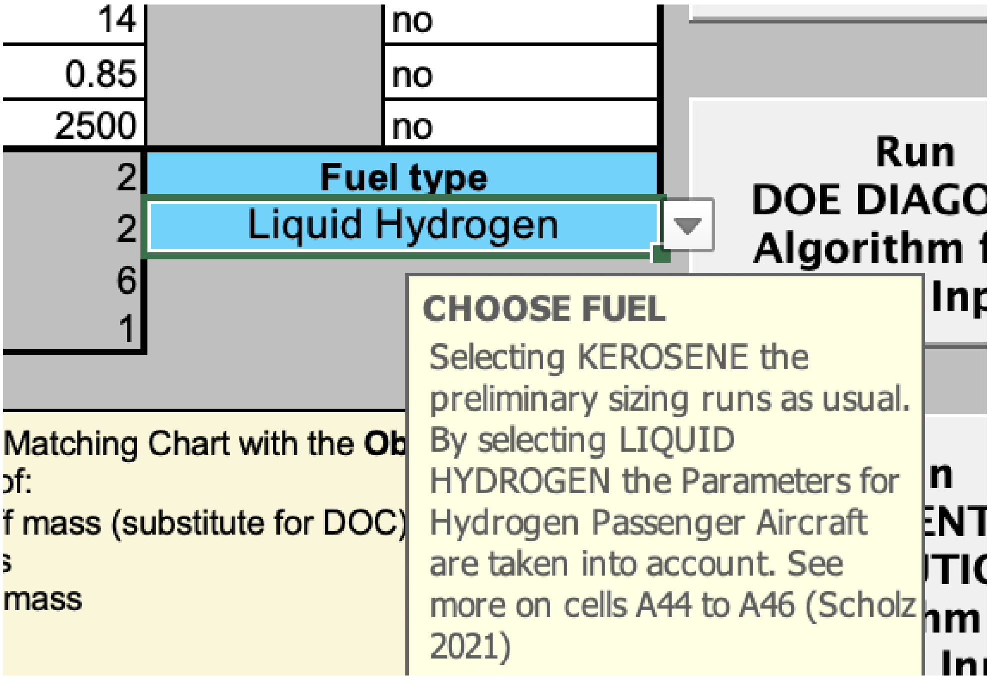

Figure 9.5: Fuel type switch integrated to SAS-Part25

41	$M_{ff,L}$	0.993
42	Relative operating empty mass, chosen	Own value
43	m_{OE}/m_{MTO} (own value)	0.571
44	Specific Fuel Consuption Adjustment	Active:LH2
45	mOE/mMTO (Adjustment LH2 fuel tanks structure)	Active:LH2
46	Emax (Adjustment Swet increase LH2 Plane)	Active:LH2
47		

Figure 9.6: Individual parameter switch indicators in SAS-Part25

	A	B	C	D	E	F	G	H
1	Input Parameters	Values	Low	High	Remark	Input Value?	No of Inputs / Controls	
2	s_{LFL} [m]	1670	1400	1670		yes	1	
3	s_{TOFL} [m]	1925	1500	2000		no		
4	$C_{L,max,L}$ "unswept"	3.76	2.5	3.8		no	Stability 1	
5	$C_{L,max,TO}$ "unswept"	2.85	2.5	3.8		no		
6	m_{ML}/m_{MTO}	0.923	0.8	1		no		
7	$A_{W,eff}$	10.5	9	15		no		
8	n_E	2	2	4		no	Stability 2	
9	n_{PAX}	180	100	250		no		
10	m_{cargo} [kg]	926.66	0	3000		no		
11	φ_{25} [deg]	25	0	35		no		
12	λ_W	0.270	0.15	0.5		no	Find DESIGN POINT	
13	t/c	0.110	0.1	0.2		no		
14	BPR	12.20	6	14		no		
15	M_{CR}	0.780	0.55	0.85		no		
16	R at max. payload [NM]	2433.00	1000	2500		no		
17	Range type (for payload calculation)	1	1	2	Fuel type		Run DOE DIAGONAL Algorithm for a Single Input	
18	Reserve type (for calculating fuel reserves)	2	1	2	Liquid Hydrogen			
19	**Design Objective** (in Matching Chart)	6	1	6				
20	Reference values (shown or not?)	1	0	1				

Figure 9.7: SAS Part 25 for a LH2-A320NEO

46	Emax (Adjustment Swet increase LH2 Plane)	Active:LH2		
47			Algorithm:	Define one:
48			DOE:	**Output** or
50	**Output Parameters**		DE:	**Objective**
51	m_F	7435 kg		no
52	m_{MTO}	71984 kg		yes
53	S_{wet} / S_W	6.1052239		no
54	m_{OE}	46882 kg		no
55	SFC	5.329E-06 kg/(Ns)		no
56	V / V_{md}	1.032		no
57	m_{MTO} / S_W	658		no
58	T_{TO} / (m_{MTO} · g)	0.349		no
59	h_{CR}	10764 m		no
60	V_{CR}	231 m/s		no
61	m_{ML}	66441 kg		no
62	S_W	109.3 m²		no
63	T_{TO}	123294 N		no
64	E_{CR}	18.7		no
65	$C_{L,CR}$	0.65		no
66	E_{max}	18.71		no
67	B_s	82511884 m		no
68	$C_{L,max,L,swept}$	3.41		no
69	Oswald Factor, e	0.783		no
70	λ_{opt}	0.18		no
71	$C_{L,max,TO,swept}$	2.58		no
72	b_{eff}	33.81 m		no
73	m_{MZF}	69067 kg		no
74	check_DP	1		no
75	check_fuel-tank-size	0		no
76	check_max-landing-mass	1		no
77				
78	Temperature above ISA, ΔT_L	0 K		
79	Temperature above ISA, ΔT_{TO}	0 K		
80				
81	*... pull more data from PS I and PS II to this INPUT tab, if you want to see more details here!*			
82				

Figure 9.8: SAS Output parameters for a LH2-A320NEO

18					Play with di
19	**Design goal selected:**	**6**			
20					
21	Possible design goals for setting the cruise line (select on INPUT tab in B19)				
22	1.) Max. take-off mass	m_{MTO}	71984	kg	
23	2.) Mission fuel mass	m_F	7435	kg	
24	3.) Operating empty mass	m_{OE}	46882	kg	
25	4.) Take-off thrust (one engine)	T_{TO}	246587	N	
26	5.) Wing area	S_W	109.3	m²	
27					

Figure 9.9: SAS Comparative masses, thrust and wing area LH2-A320NEO

135							
136	Wing aspect ratio, effective	Aeff	10.45				
137	Wing taper ratio	λ	0.27		<<< from INPUT tab		
138	Fuel tank volume, geometric	V_{tank}	17.49	m³			
139	CS 25.979(b) fuel tank correction	k_{CS}	-2%				
140	Correction accounting for unusable fuel	k_{UF}	-3%				
141	Sum of corrections	$k_{CS} + k_{UF}$	-5%				
142	Fuel tank volume, corrected	$V_{tank,corr}$	16.62	m³			
143							
144							
145							
146	Check, if wing fuel tank volume is sufficient on it own		$V_{tank,corr}$		>	$V_{F,erf}$	?
147			16.62	m³	>	107.67	m³
148					no		
149		The wing geometry cannot accomodate the required fuel volume. Include ACT (Additional Center Tank) or ATT (Additional Tail Tank) or find other solutions to accomodate all fuel!					
150							
151							

$$V_{tank} = 0.54 \cdot S_W^{1.5} \cdot (t/c)_{av} \cdot \frac{1}{\sqrt{A}} \frac{1+\lambda+\lambda^2}{(1+\lambda)^2}$$

Figure 9.10: Fuel volume required for a LH2-A320NEO

As expressed at the end of the calculations in tab PSII shown in Figure 9.10, the required volume is 107.67 m^2. Unfortunately, none of the available tanks from Table 8.2 could be utilized to store LH2.

The matching chart of the LH2-A320NEO shown in Appendix B compared to the one of the conventional A320NEO-WV050 seems to have the take-off diagonal and cruise curve displaced to the right, consequently increasing the potential wing loading only to be limited by the landing vertical line.

9.3 Preliminary Sizing of a Turboprop variant of a A320

The task of designing an aircraft meant to substitute the functions of a short medium range aircraft capable of handling around double the number of passengers than De Havilland Canada Dash 8, British Aerospace ATP or ATR72 while keeping the A320 base design will demand more changes than a simple integration of different engines. Despite trying to leave as many components as possible unmodified from the conventional A320, major changes on the wings must be conducted to adjust to the new cruise speed. These modifications must be made in such a way that the ICAO Aerodrome Reference code does not change. The A320 falls on the reference field length of 1800 m and above (code number 4). The wingspan falls on the wingspan between 24 m and 36 m (code letter C). (Skybrary 2024)

The main objective of executing these changes is to have an aircraft that fulfills the role of the short/medium range jet such as the A320 in passenger transport with a lower environmental impact than their jet's counterparts by flying more efficiently at lower speeds and reducing the fuel consumption per passenger per nautical mile drastically. This consequently would also reduce the DOCs for the operators without falling into the reliability issues of piston engines responding quickly to power changes and delivering high thrust at lower speeds. The main downside would be on the side of the passengers' flight times being extended due to the reduction on cruise speeds and noise of the propellers.

As a starting point the fuselage construction by using the same frames, nose and empennage sections are kept unchanged from the original as the A320 family. The calculations were also conducted on the SAS-Part25-Prop tool (Figure 9.11), keeping in mind the TLAR with its corresponding changes on cruise speed. On the preliminary sizing the cruise altitude for the turboprop was adjusted by setting a longer take-off length than the conventional A320NEO. The overall values calculated from the SAS tool are summarized in Figure 9.12 and Figure 9.13.

	A	B	C	D	E	F	G	H
1	**Input parameters**	**Value**	**Low**	**High**		**yes/no**	**No. of Inputs**	
2	S_LFL	1580	1200	2000		no	1	
3	S_TOFL	1925	900	2000		no	**Control buttons**	
4	CL_maxL	3.45	2.50	3.50		no		
5	CL_maxTO	3.10	2.50	3.50		no	STABILITY 1	
6	mML_to_mMTO	0.98	0.75	1.00		yes		
7	A	9.0	8	16		no		
8	n_E	4	2	4		no	STABILITY 2	
9	n_PAX	180	100	180		no		
10	m_cargo	927	0	3000		no	FIND DESIGN POINT	
11	Phi_25	10	0	25		no		
12	Lambda	0.430	0	1		no		
13	t/c	0.143	0.1	0.2		no		
14	M_CR	0.47	0.40	0.60		no		
15	Propeller_diameter	5.85	3	7		no	DOE Diagonal ALGORITHM FOR SINGLE INPUT	
16	Range	2433	500	3000		no		
17	Range_type	1	1	2		no		
18	Reserve_type	2	1	2		no		
19	Design_goal	6	1	6		no		
20	Reference_values	1	0	1			Differential Evolution	

Figure 9.11: SAS-Part 25 for a conventional A320NEO Turboprop

57			
58	**Output**		Define one:
59	m_F	29340	no
60	m_MTO	110604	yes
61	m_OE	63598	no
62	SFC	6.87E-08	no
63	V_to_Vmd	0.900	no
64	mMTO_to_SW	583	no
65	P_W	186	no
66	h_CR	6660	no
67	V_CR	147	no
68	m_ML	108761	no
69	S_W	190	no
70	P_TO	5132	no
71	L_D	15.3	no
72	C_L	0.86	no
73	E_max	15.7	no
74	CD_0	0.0222	no
75	Bs	20970361	no
76	CL_maxL_swept	3	no
77	Osw	0.77	no
78	CL_maxTO_swept	3	no
79	mML_Airbus	86953	no
80	eta	0.92	no
81	check_MLM	1	no
82	check_fuel-tank-size	1	no
83	check_DP	0	no
84	check_eta	1	no
85			

Figure 9.12: SAS Output parameters for a A320NEO Turboprop

18				
19	**Possible design goals:**			
20	Max. take-off mass	m_{MTO}	110604	kg
21	Mission fuel mass	m_F	29340	kg
22	Operating empty mass	m_{OE}	63598	kg
23	Take-off power (one engine)	P_{TO}	5132	kW
24	Wing area	S_W	189.7	m²
25				

Figure 9.13: SAS Comparative masses, thrust and wing area A320NEO Turboprop

As expressed at the end of the calculations in tab PSII shown in Figure 9.14, the required volume is 37 m^3. Since the wings found on the conventional A320NEO were modified in favor of lower cruise speeds and a turboprop drive, instead of missing volume for kerosene, plenty of the wing's capacity remains unused.

138	Check of fuel tank volume	V_F	144.45	m³				
139	CS 25.979(b) fuel tank correction	k_{CS}	-2%					
140	Correction accounting for unusable fuel	k_{UF}	-3%					
141	Sum of corrections	$k_{CS} + k_{UF}$	-5%					
142	Fuel tank volume, corrected	V_F	137.23	m³				
143								
144								
145	Check of mass assumptions	check:	m_{ML}		>	$m_{MZF} + m_{F,res}$	?	
146			108761	kg	>	88294	kg	
147					yes			
148					Aircraft sizing finished!			
149								
150	Check of assumptions		V_F		>	$V_{F,erf}$	?	
151			137.23	m³	>	37.0	m³	
152					yes			
153					The wing geometry can accomodate the required fuel volume!			
154								

$$V_{tank} = 0.54 \cdot S_W^{1.5} \cdot (t/c)_r \cdot \frac{1}{\sqrt{A}} \cdot \frac{1+\lambda \cdot \sqrt{\tau} + \lambda^2 \cdot \tau}{(1+\lambda)^2}$$

Figure 9.14: Fuel volume required for a A320NEO Turboprop

The corresponding matching chart can be found in Appendix C

9.4 Preliminary Sizing of a Turboprop variant of a LH2-A320

By incorporating the fuel type selector switch into the SAS-Part25-Prop program, the preliminary sizing calculations for a turboprop A320 powered by liquid hydrogen can be conducted. The fuel tanks integration into the fuselage would be similar to the one on the turbofan LH2 variant, the fuselage extension would need to be longer to accommodate the necessary fuel to match the range and payload from the A320NEO. The environmental impact from non-CO2 emissions would be reduced in a great manner by changing the cruise altitude to avoid contrail formation as mentioned in Chapter 10.5. This being a consequence of allowing the aircraft a longer distance to take-off and to land.

For the input parameters (Figure 9.15), following the LH2 parameter adjustment previously mentioned in Chapter 6.1, had to be added into the SAS-Part 25 as indicated in Figure 9.16. These three adjustments can easily be activated or deactivated on the INPUT sheet in cell D33. By applying the parameter adjustments for LH2 fuel, the data from Figure 9.17 and Figure 9.18 was gathered.

	A	B	C	D	E	F	G	H
1	Input parameters	Value	Low	High		yes/no	No. of Inputs	
2	S_LFL	1260	900	1800		no	1	
3	S_TOFL	1925	900	2000		no	Control buttons	
4	CL_maxL	3.25	2.50	3.50		no	STABILITY 1	
5	CL_maxTO	2.66	2.50	3.50		no		
6	mML_to_mMTO	0.98	0.75	1.00		yes		
7	A	11.00	9	16		no		
8	n_E	4	2	4		no	STABILITY 2	
9	n_PAX	180	100	180		no		
10	m_cargo	927	0	3000		no		
11	Phi_25	1.25	0	25		no	FIND DESIGN POINT	
12	Lambda	0.620	0	1		no		
13	t/c	0.14	0.1	0.2		no		
14	M_CR	0.40	0.40	0.60		no		
15	Propeller_diameter	3.5	3	7		no	DOE Diagonal ALGORITHM FOR SINGLE INPUT	
16	Range	2433	500	3000		no		
17	Range_type	1	1	2		no		
18	Reserve_type	2	1	2		no		
19	Design_goal	6	1	6		no		
20	Reference_values	1	0	1			Differential Evolution	

Figure 9.15: SAS-Part 25 for a LH2-A320NEO Turboprop

FUEL TYPE
Liquid Hydrogen

Specific Fuel Consuption Adjustment	Active:LH2
mOE/mMTO (Adjustment LH2 fuel tanks structure)	Active:LH2
Emax (Adjustment Swet increase LH2 Plane)	Active:LH2

Figure 9.16: Individual parameter switch indicators in SAS-Part25 Turboprop

57			
58	**Output**		Define one:
59	m_F	8117	no
60	m_MTO	60669	yes
61	m_OE	34885	no
62	SFC	2.69E-08	no
63	V_to_Vmd	0.900	no
64	mMTO_to_SW	445	no
65	P_W	181	no
66	h_CR	6904	no
67	V_CR	125	no
68	m_ML	59658	no
69	S_W	136	no
70	P_TO	2745	no
71	L_D	16.9	no
72	C_L	0.94	no
73	E_max	17.3	no
74	CD_0	0.0219	no
75	Bs	54399005	no
76	CL_maxL_swept	3	no
77	Osw	0.76	no
78	CL_maxTO_swept	3	no
79	mML_Airbus	56230	no
80	eta	0.85	no
81	check_MLM	1	no
82	check_fuel-tank-size	1	no
83	check_DP	0	no
84	check_eta	1	no
85			

Figure 9.17: SAS Output parameters for a LH2-A320NEO Turboprop

18				
19	**Possible design goals:**			
20	Max. take-off mass	m_{MTO}	60669	kg
21	Mission fuel mass	m_F	8117	kg
22	Operating empty mass	m_{OE}	34885	kg
23	Take-off power (one engine)	P_{TO}	2745	kW
24	Wing area	S_W	136.4	m²
25				

Figure 9.18: SAS masses, thrust and wing area LH2-A320NEO Turboprop

138	Check of fuel tank volume	V_F	76.19	m³			
139	CS 25.979(b) fuel tank correction	k_{CS}	-2%				
140	Correction accounting for unusable fuel	k_{UF}	-3%				
141	Sum of corrections	$k_{CS} + k_{UF}$	-5%				
142	Fuel tank volume, corrected	V_F	72.38	m³			
143							
144							
145	Check of mass assumptions	check:	m_{ML}		>	$m_{MZF} + m_{F,res}$	?
146			59658	kg	>	54526	kg
147					yes		
148					Aircraft sizing finished!		
149							
150	Check of assumptions		V_F		>	$V_{F,erf}$	?
151			72.38	m³	>	10.3	m³
152					yes		
153					The wing geometry can accomodate the required fuel volume!		
154							

$$V_{tank} = 0.54 \cdot S_W^{1.5} \cdot (t/c)_r \cdot \frac{1}{\sqrt{A}} \cdot \frac{1+\lambda \cdot \sqrt{\tau} + \lambda^2 \cdot \tau}{(1+\lambda)^2}$$

Figure 9.19: Fuel volume required for a LH2-A320NEO Turboprop

Just as expected, at the end of the calculations in tab PSII shown in Figure 9.19, the required volume of LH2 is 72,38m^2. Unfortunately, none of the available tanks from Table 8.2 could be utilized to store LH2.

The corresponding matching chart for the *LH2-A320NEO-TP* can be found in Appendix D Compared to the one of the *A320NEO-TP* seems to have the take-off diagonal and cruise curve displaced to the left, consequently decreasing the potential wing loading and lowering the power-to-mass ratio.

9.5 Design Point Priorities Comparison

Besides having significant mass adaptation from the conventional turbofan A320NEO-WV050 (Figure 9.20), the LH2 variant (Figure 9.21) in terms of wing loading, it decreased up to 7,567% which allows for more room for the cryogenic systems, fuel lines, heat exchangers and tank insulation. The thrust-to-weight ratio had an 7,867% increase.

A320-200	Reference value	Actual value
m_{MTO} / S_W	600.49	712.19
$T_{TO} / m_{MTO} \cdot g$	0.30845	0.32372

Figure 9.20: Design Point conventional A320NEO WV050

A320-200	Reference value	Actual value
m_{MTO} / S_W	600.49	658.30
$T_{TO} / m_{MTO} \cdot g$	0.30845	0.34919

Figure 9.21: Design Point LH2-A320NEO

The main difference between the two variants is found at the end of the PS II sheet, which states that the volume for the tanks available in the wings is not sufficient to accommodate the LH2, as expressed in Figure 9.10. Apart from not being capable of storing any pressurized LH2 into the wings in the same manner as Kerosene is, newer solutions must be thought about. A redesign of the fuel storage previously discussed in Chapter 6.3.1 could be implemented.

Between the turboprop variants the wing loading difference was more pronounced with a 23.671% decrease on the LH2 aircraft. The thrust-to-weight ratio remained around the same with a minimum variation of 2.688% lower than the kerosene aircraft. (Figure 9.22 and Figure **9.23**)

ATR 72	Reference value	Value
m_{MTO} / S_W	369	583
$P_{S,TO}/m_{MTO}$	191	186

Figure 9.22: Design Point A320NEO Turboprop

ATR 72	Reference value	Value
m_{MTO} / S_W	369	445
$P_{S,TO}/m_{MTO}$	191	181

Figure 9.23: Design Point LH2-A320NEO Turboprop

10 Environmental Impact of LH2 Combustion

10.1 Water Vapor and Its Effects

The ideal combustion of fossil fuels like Jet-A should follow the reaction as expressed in Equation (4.3).

$$2\ C_{12}H_{26} + 37\ O_2 \rightarrow 24\ CO_2 + 26\ H_2O \tag{10.1}$$

But air contains more than oxygen: 78% nitrogen, 21% oxygen, 0.04% CO2 and 0.96% other gases mostly argon. (UCAR 2024)

In an ideal hydrogen combustion, a similar reaction is expected with water as a by-product.

$$2\ H_2 + O_2 \rightarrow 2H_2O$$

As seen in Formulas 10.1 and 10.2, another potential by-product of the combustion process besides CO2 is water vapor. The effect of water vapor as an obstacle to reach zero emissions can be overcome by avoiding flying over areas with atmospheric conditions that predispose contrail formation. Commonly overseen by the majority or considered as a harmless emission, several studies have shown that cirrus clouds induced by contrails could contribute to global warming about 3 to 4 times the amount CO2 does by trapping heat in the Earth's atmosphere that otherwise would be released into space (Figure 10.1). Contrails form in air above 25.000 ft in moist conditions when temperatures below -40°C are present. If the air is not cool or moist enough, contrails may not form or may dissolve quickly. Otherwise, they remain as white lines in the sky gradually spreading to create thin layers of ice clouds. The time the contrails remain in the sky varies from a few seconds to many hours, causing what is known as Aviation Induced Cloudiness. (Pearce 2019)

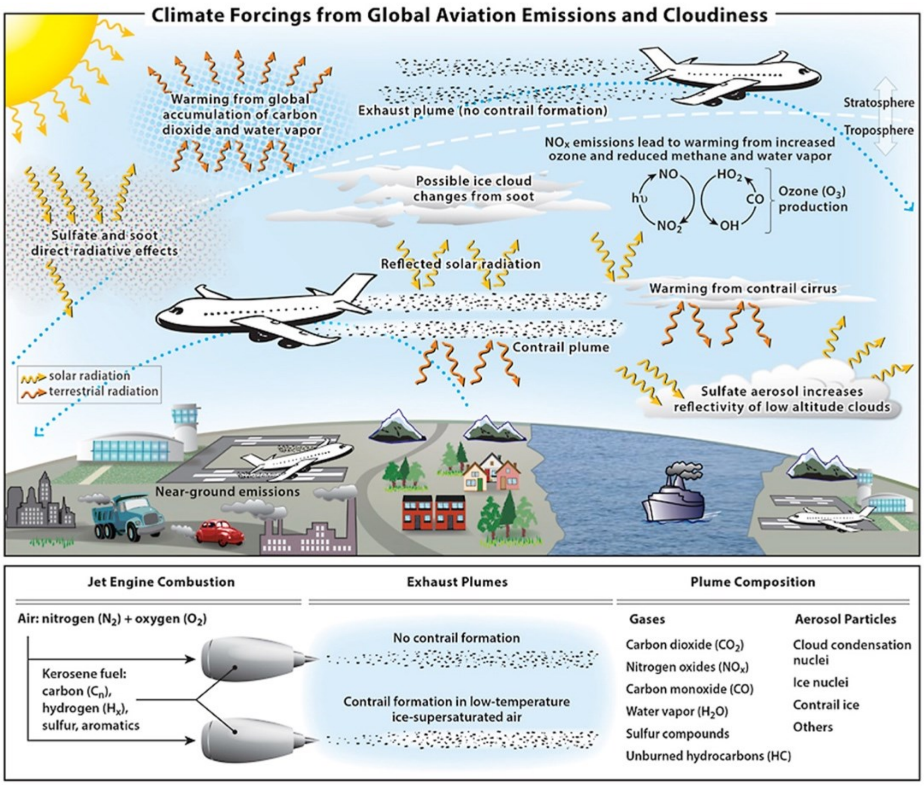

Figure 10.1: Aviation Emissions and AIC (Lee 2021)

10.2 Nitrogen Oxides as a By-Product

Burning hydrogen is not technically clean as when used inside fuel-cells, but it still represents a huge improvement over kerosene combustion. Hydrogen as a propellant is not free of Nitrogen Oxides emissions. Also known as NOx, which are a significant source of air pollution and greenhouse effects globally. Usually, NOx is part of the exhaust of diesel engines and other internal combustion vehicles. Tests have shown that by burning hydrogen fewer NOx emissions are produced compared to conventional jet fuel. This is because hydrogen is characterized by a much wider flammability limits than kerosene (Wang 2023). Hydrogen burns by a concentration ranging from 5% to 78%. A much leaner combustion can be achieved by adjusting the air-fuel mixture ratio throughout the flight's stages. These different air-fuel mixtures can produce a more controlled hydrogen combustion giving lower flame temperatures consequently reducing NOx emissions up to just 10% of the NOx emissions present on traditional Kerosene combustion. (Sethi 2021)

10.3 AIC from LH2 Combustion

Hydrogen combustion is free of CO_2 emissions, but it is known that it produces 2.58 times more water emissions than kerosene. Talking in CO_2 equivalent emissions, if this primary effect is applied to Aviation Induced Cloudiness the overall impact would be 50% higher than the one kerosene. The burning temperature of hydrogen is also higher, consequently the NOx emissions would boost as well. Assuming the technology in which hydrogen's lean combustion at lower temperatures can be achieved we start form the premise that the NOx emissions are the same as for kerosene. (Scholz 2020a)

A secondary effect is ice crystals formation. Hydrogen combustion has no particles to serve as seeds for the growth of such crystals. In contrast, kerosene has soot serving as nuclei for ice crystal growth. The radius of the crystals formed by H2 combustion are assumed to be about 1/0.3 = 3.33 times larger than the ones made from kerosene combustion. By that the volume is $3.33^3 = 37.037$ times larger than the one occupied by the kerosene ice crystals. The projected area of the ice crystals from hydrogen combustion is $3.33^2 = 11.11$ times larger than the area of kerosene ice crystals. If the substitution of the conventional aircraft by LH2 aircraft takes place, there would be an increase in contrails by a factor of 1.2 due to LH2 contrails forming already at lower altitudes. This gives a reduction of the equivalent CO_2 emissions down to the percentage

$$1.2 \cdot \frac{\left(\frac{1}{0.3}\right)^2}{\left(\frac{1}{0.3}\right)^3} = 36\% \quad . \tag{10.3}$$

The initial LH2 contrail has 2.58 times more water and as such the reduction is only down to 92.9%. The size of the older contrail, however, is dominated by water drawn from the surroundings. For the NOx equivalent CO_2 emissions by a leaner combustion at lower temperatures a reduction up to 35% could be assumed. (Scholz 2020c)

In the long run water vapor effects on the environment do not last as long as CO_2 which has a half-life of about 120 years. Because of this, water vapor besides having a much higher greenhouse effect at the beginning it is not equivalent but still must be mitigated. (ISU 2024)

One way in which the AIC can be drastically reduced is if LH2 planes fly at lower altitudes than the traditional kerosene powered aircraft. The Primary and Secondary Effects of LH2 combustion shown on the following express the way in which AIC and NOx are present the most depending on flight altitudes. It is assumed that with hydrogen combustion, due to various effects, NOx only has 35% and AIC only 92.9% of their usual effect. (Scholz 2020a)

Through the graphical representation on formation of Figure 10.2, flying at around 24000 ft seems to be a reasonable altitude to reduce greenhouse effects of AIC and NOx caused by LH2 combustion.

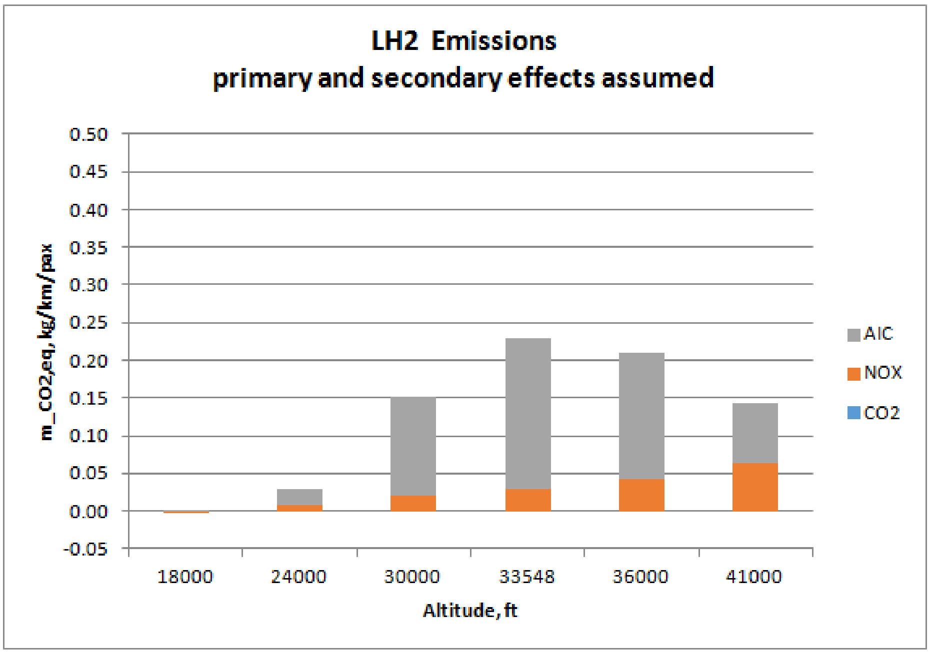

Figure 10.2: Environmental impact of CO2 equivalent emissions. Secondary effects are calculated with the "Sphere Model" (0.3). Taking also care of more contrails forming (factor 1.2) yields 0.36. Accounting for a factor 2.58 (more water) we arrive at 0.36 · 2.58 = 0.929 to be taken as the overall effect. (Scholz 2020c)

The cruise altitude was adjusted accordingly to achieve this emission reduction on Chapter 9.4 the preliminary sizing of the LH2 variants.

10.4 Google's AI Approach to Contrail Formation

In 2023 a Research division from Google's Climate and Energy team headed by Carl Elkin, attempting to reduce carbon footprint, started a test phase of a contrail avoidance program in conjunction with the biggest airline in the world: American Airlines. By making use of Google's satellite imagery capabilities, combined with their huge meteorological, flight database centers and newly developed Artificial Intelligence, a program which actively helps detect persistent contrail formation areas in the atmosphere. As seen on the work of Scholz form 2020c (seen in Figure 10.32), the flight areas below 24000 ft and above 41000 ft do not provide the conditions in which contrails can be formed. By avoiding ice supersaturated regions of the atmosphere, the CO2 equivalent effect of aviation can drastically be reduced.

Figure 10.3: Example of contrail formation region recognition (Google 2023a)

Another important aspect of this program has been training the reconnaissance capability of the AI so that it can accurately differentiate naturally produced cirrus cloud formations form persistent contrails spreading out after several hours. It cannot be distinguished with full certainty by this system if the overall beneficial effect of contrails in which they do reflect sunrays back into space during the daytime, and only trap the heat at noon (Figure 10.4). Ground weather forecasts do not seem to provide reliable data at such flight altitudes, making it difficult to know the actual relative humidity of a specific atmospheric region. That is why the research has been mostly based on image recognition collected via satellite. Just as we as humans have cluelessly been helping on the ReCAPTCHA, inc. machine learning process of self-driven cars by selecting the stoplight or motorcycles in *"Are you a robot?"* tests, the same had to be done to teach Google's AI to get a set of labelled imagery.

The demo software was handed to some American Airlines' pilots themselves to make the decision of changing flight altitudes. Capt. Deborah Hecker, director of flight operations described its use as pretty intuitive, similar to the way in which turbulence regions are avoided. During the test runs it was discovered that the heat trapped by a night-time contrail can be magnitudes greater than a daytime contrail. (Google 2023b)

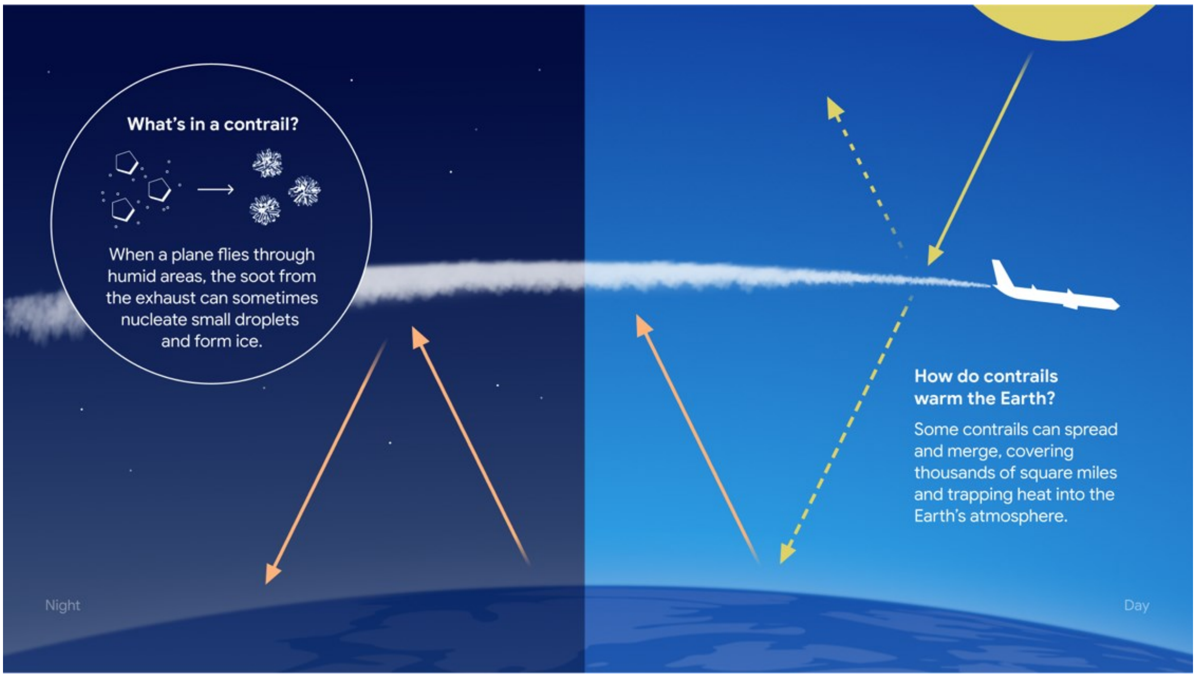

Figure 10.4: Contrail effects during nighttime (Google 2023a)

According to the tests results, American Airlines detected that a 54% Contrail reduction with this prediction was achieved. By performing the required altitude changes around 2% more kerosene was burned by the airplanes to avoid the ice supersaturated regions. Since not every airplane of its fleet had to be diverged to avoid the height region the kerosene consumption ends up evening out to just a 0.3% increase. Together the contrail avoidance costs could be in the range of $5 to $25 per ton of CO2 equivalent. One of the challenges for the future of the Contrail Avoidance Program from Google is going to be implementing it at scale and integrating it to ATC systems. (Google 2023a)

10.5 Latitude Influence on the AIC Formation

Cold conditions lead to lower tropopause since convection is rare at the polar regions. The height of the tropopause depends on the latitude and season with drastic drops in the area of subtropical and polar fronts (Geerts 1997) as shown in Figure 10.5 and Figure 10.6. The approach to reducing the impact of persistent contrails will not be the same all around the world. It will be needed to fly lower in equatorial regions and higher near the polar regions. (Barton 2023). The design of the lower flying hydrogen aircraft variant dependent on the earth regions are described in Chapter 9.4.

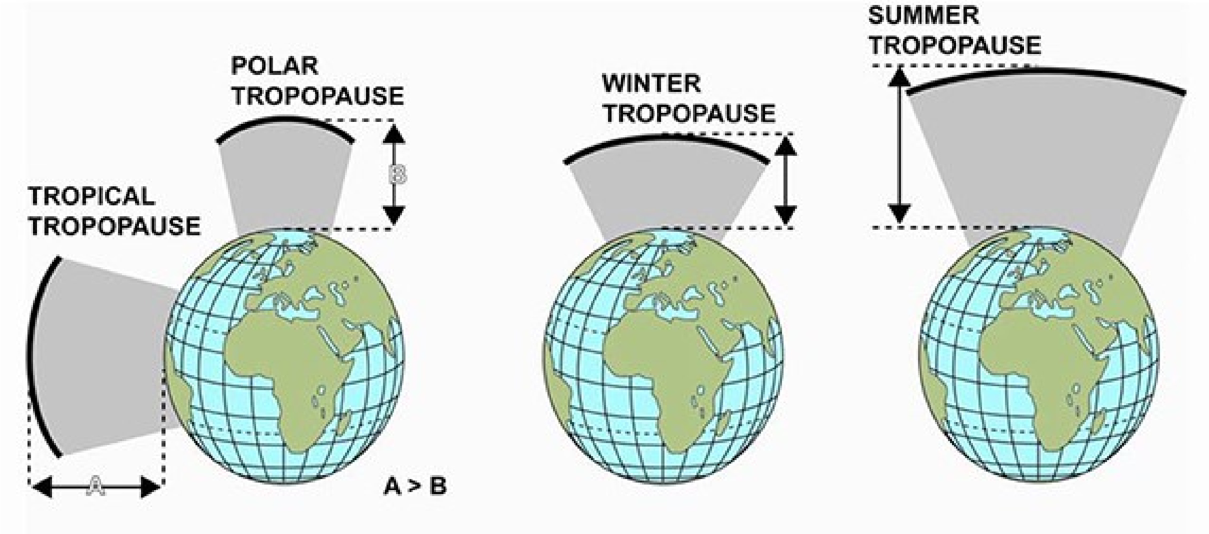

Figure 10.5: Annual tropopause variations at different latitudes (Jeppesen 2004)

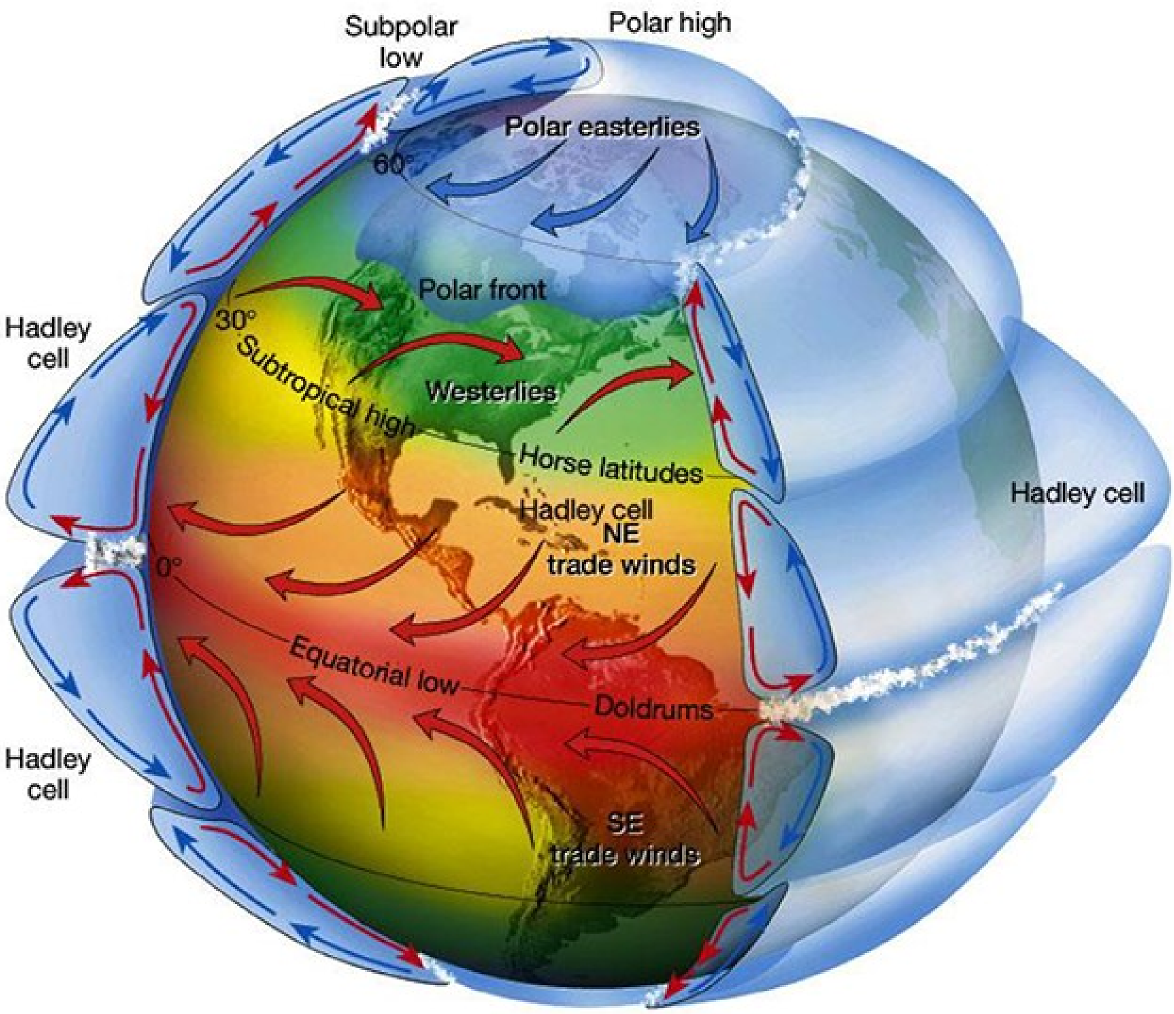

Figure 10.6: Tropopause at different latitudes (U.S Air Force 1997)

10.6 Altitude Dependent Equivalent CO2 Emissions

Aviation has other environmental concerns besides CO2 emissions. The repercussions on a time scale by the impact they exert on the atmosphere fluctuate from one another. With the intent of primarily reducing the greenhouse effects contributing to global warming and its consequences, a conversion to measure these derived effects on a comparable proportional scale was essential. Specifically, to point out the main compounds and elements that contribute to climate change in civil aviation.

To find the overall equivalent CO2 mass emitted by an aircraft per km a passenger is flown due to the atmospheric conditions the proportional effects variate depending on the cruise altitude. These variations are condensed on the *Forcing Factors S(h)* (Table 10.1) for each compound and element. The values for this calculation were extracted from the atmospheric calculations conducted by Schwartz in 2009 and 2011. (Scholz 2022c)

Table 10.1: Forcing Factors (Schwartz 2009)

O_3 (S)		CH_4 and O_3 (L)		AIC	
forcing factor s	altitude (ft)	forcing factor s	altitude (ft)	forcing factor s	altitude (ft)
0.46942	17502	0.86771	17470	0.02845	17470
0.55761	19484	0.92461	19484	0.00000	19548
0.62020	21498	0.95590	21498	0.00000	21530
0.71124	23480	0.96159	23543	0.17354	23511
0.71124	25525	0.94452	25525	0.39545	25525
0.81366	27507	0.92745	27539	0.79943	27507
0.93030	29521	0.92745	29521	1.25178	29457
1.00996	31502	0.94168	31534	1.70982	31598
1.13229	33484	0.97582	33516	2.10526	33548
1.42816	35562	1.14083	35562	1.82077	35530
1.62447	37575	1.21479	37543	1.53343	37543
1.80370	39589	1.20341	39589	0.96728	39557
1.93172	41539	1.20341	41571	0.79374	41539

Knowing the cruise altitude and the *Sustained Global Temperature Potential (SGTP)* (Table 10.2) of each compound or element present on the exhaust of the aircraft's engines a *Characterization Factor (CF)* can be calculated (Equation 10.4 & 10.5) (Scholz 2022).

Table 10.2: Sustained Global Temperature Potential (Scholz 2020c)

Species	$SGTP_{i,100}$	rel. to CO2
CO2 (K/kg CO_2)	3.58E-14	1.0000
Short O3 (K/kg NOx)	7.97E-12	222.6257
Long O3 (K/NOx)	-9.14E-13	-25.5307
CH4 (K/kg NO_x)	-3.90E-12	-108.9385
Contrails (K/km)	1.37E-13	3.8268
Cirrus (K/km)	4.12E-13	11.5084

$$CF_{midpoint,NOx}(h) = \frac{SGTP_{O_{3S},100}}{SGTP_{CO_2,100}} \cdot S_{O_3,S}(h) + \frac{SGTP_{O_{3L},100}}{SGTP_{CO_2,100}} \cdot S_{O_3,L}(h) + \frac{SGTP_{CH_4,100}}{SGTP_{CO_2,100}} \cdot S_{CH_4}(h) \tag{10.4}$$

$$CF_{midpoint,AIC}(h) = \frac{SGTP_{Contrails,100}}{SGTP_{CO_2,100}} \cdot S_{Contrails}(h) + \frac{SGTP_{Cirrus,100}}{SGTP_{CO_2,100}} \cdot S_{Cirrus}(h) \tag{10.5}$$

The Characterization Factors are used to adjust the fuel type dependent *Emission Index (EI)* seen on Table 10.3 . The EI_{NOx} is deeply related to the efficiency of each engine and increases in proportion to higher combustion temperatures. With LH2 this can be regulated, as mentioned in Chapter 10.2 to increase its efficiency. Knowing the aircraft's fuel consumption, passengers flown and range, an overall equivalent CO2 mass emitted by an aircraft per km a passenger is flown can be determined on Equation 10.6. Providing a comprehensive evaluation of an aircraft's environmental backlash. (Scholz 2020c)

Table 10.3: Emission index by fuel type (Scholz 2020c)

KEROSENE Jet-A	Emission Index, EI (kg, kg fuel)		Liquid Hydrogen LH2	Emission Index, EI (kg, kg fuel)
EI_{CO2}	3.15		EI_{CO2}	0
EI_{NOx}	0.0238		EI_{NOx}	0.0664
EI_{H2O}	1.24		EI_{H2O}	8.94
Q(MJ/kg)	43		Q(MJ/kg)	120
$EI_{Nox}/Q_{Kerosene}$	0.000553		EI_{NOx}/Q_{LH2}	0.000553
$EI_{H2O}/Q_{Kerosene}$	0.0288		EI_{H2O}/Q_{LH2}	0.0745

The AIC calculated based on the average fuel consumption of the World Airliner Census of 2020 comes around $f_{NMref} = 4{,}74$ kg/km (Scholz 2022)

$$\begin{aligned} m_{CO_2,eq} = {} & \frac{EI_{CO2} \cdot f_{NM}}{n_{Seat}} \cdot CF_{midpoint,CO2}(h) + \frac{EI_{NOx} \cdot f_{NM}}{n_{Seat}} \cdot CF_{midpoint,NOx}(h) \\ & + \frac{R_{NM} \cdot f_{NM}}{R_{NM} \cdot f_{NM,ref} \cdot n_{Seat}} \cdot CF_{midpoint,AIC}(h) \end{aligned} \tag{10.6}$$

10.7 Variants Emission Comparison to Conventional A320NEO

As a means of comparing the ecological impact each of the aircraft variant of Chapter 9 and to serve as a tool for future designs, the exhaust altitude dependent equivalent CO2 emissions was automatized into each SAS spreadsheet. Figure 10.7 serve as an example of this calculations. For a more detailed calculation the three different *Forcing Factors S* (Figure 10.8) are extracted from the work of Schwartz (2009) by performing an interpolation. The fuel dependent *Emission Index EI* are selected accordingly by being connected to the same fuel selector switch (see Figure 9.5) in the INPUT sheet.

	A	B	C	D	E	F	G	H	I	J	K	L
1	**Altitude-Dependent Equivalent CO2 Mass**											
2					*Numbers by van Endert (HAW Hamburg, 2017) based on Schwartz 2009*							
3					https://doi.org/10.7910/DVN/DLJUUK							
4			Cruise altitude	22651	ft			Forcing Factors S(h)				
5												
6					O_3 (S)			CH_4 and O_3 (L)			AIC	
7	**Species**	$SGTP_{i,100}$	rel. to CO2		forcing factor s	altitude (ft)		forcing factor s	altitude (ft)		forcing factor s	altitude (ft)
8	CO2 (K/kg CO_2)	3.58E-14	1.0000		0.46942	17502		0.86771	17470		0.02845	17470
9	Short O3 (K/kg NOx)	7.97E-12	222.6257		0.55761	19484		0.92461	19484		0.00000	19548
10	Long O3 (K/NOx)	-9.14E-13	-25.5307		0.62020	21498		0.95590	21498		0.00000	21530
11	CH4 (K/kg NO_x)	-3.90E-12	-108.9385		0.71124	23480		0.96159	23543		0.17354	23511
12	Contrails (K/km)	1.37E-13	3.8268		0.71124	25525		0.94452	25525		0.39545	25525
13	Cirrus (K/km)	4.12E-13	11.5084		0.81366	27507		0.92745	27539		0.79943	27507
14					0.93030	29521		0.92745	29521		1.25178	29457
15					1.00996	31502		0.94168	31534		1.70982	31598
16	$CF_{midpoint\ ,NOx}(h) = \frac{SGTP_{O_{3S},100}}{SGTP_{CO_2,100}} \cdot s_{O_3,S}(h) + \frac{SGTP_{O_{3L},100}}{SGTP_{CO_2,100}} \cdot s_{O_3,L}(h) + \frac{SGTP_{CH_4,100}}{SGTP_{CO_2,100}} \cdot s_{CH_4}(h)$				1.13229	33484		0.97582	33516		2.10526	33548
17					1.42816	35562		1.14083	35562		1.82077	35530
18					1.62447	37575		1.21479	37543		1.53343	37543
19	$CF_{midpoint\ ,cloudiness}(h) = \frac{SGTP_{contrails\ ,100}}{SGTP_{CO_2,100}} \cdot s_{contrails}(h) + \frac{SGTP_{cirrus\ ,100}}{SGTP_{CO_2,100}} \cdot s_{cirrus}(h)$				1.80370	39589		1.20341	39589		0.96728	39557
20					1.93172	41539		1.20341	41571		0.79374	41539
21												
22	Range	2433.0	km	Interpolation min	0.620199	21498		0.95590	21498		0	21530
23				Interpolation max	0.711238	23480		0.961593	23543		0.173542	23511
24												
25	**KEROSENE**	**Emission Index, EI (kg, kg fuel)**			S_O3_Short	0.67318981		S_O3_Long	0.95911151		S_AIC	0.09821588
26	EI_CO2	3.15						S_CH4	0.95911151			
27	EI_NOx	0.0238	Caers 2019									
28	EI_H2O	1.24										
29	Q(MJ/Kg)	43										
30	EI_Nox/Q	0.000553			CF_mid_CO2(h)	0						
31	EI_H2O/Q	0.0288										
32					CF_mid_NOX(h)	20.898						
33	**Liquid Hydrogen LH2**	**Emission Index, EI (kg, kg fuel)**	rel. to Kerosene									
34	EI_CO2	0			CF_mid_AIC(h)	1.506						
35	EI_NOx	0.0664										
36	EI_H2O	8.94										
37	Q(MJ/Kg)	120	2.79	Factor	Caers 2019 (HAW Hamburg):							
38	EI_NOx/Q_LH2	0.000553	2.58	Factor	https://nbn-resolving.org/urn:nbn:de:gbv:18302-aero2019-07-28.013							
39	EI_H2O/Q_LH2	0.0745	1.00	Assumption								
40												

Figure 10.7: Altitude Dependent Equivalent CO2 mass calculations example

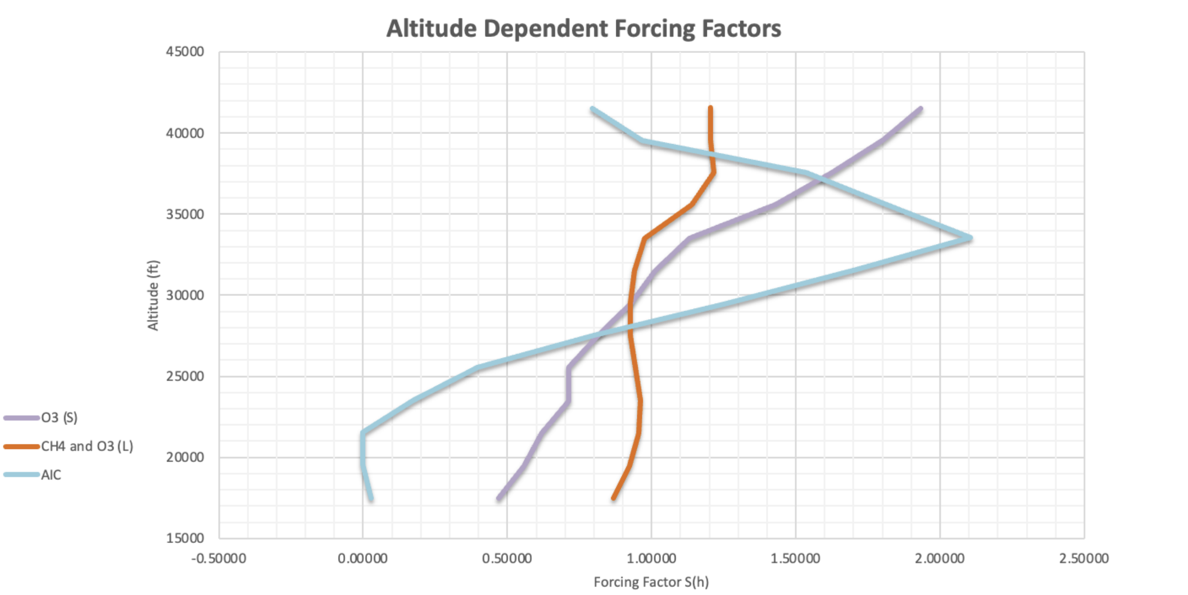

Figure 10.8: Forcing factors (Schwartz 2009)

Setting the conventional A320NEO as a reference point, the results of the calculated equivalent CO2 masses outlined in Table 10.4 by just considering hydrogen combustion primary effects (see Chapter 10.3) and Table 10.5 for the overall effects. More details regarding the equivalent emissions proportions and its comparison is available in Appendix A, Appendix B, Appendix C and Appendix D and the "*CO2_eq*" tab in each spreadsheet calculation.

Table 10.4: Primary effects equivalent emissions compared to conventional A320NEO

Engine type	Turbofan		Turboprop	
Variant	*A320NEO [kg/(km*Seat)]*	LH2-A320NEO (primary effects)	A320NEO-TP	LH2-A320NEO-TP (primary effects)
m_CO2	0.06292	∅	+235.41%	∅
m NOx eq	0.05929	+110.70%	-65.04%	-58.41%
m AIC eq	0.13507	-22.34%	-95.50%	-95.82%
Σ m_CO2eq	**100%**	**-10.67%**	**-7.56%**	**-88.22%**

Even if the turbofan LH2 did not undergo a major change of cruise altitude or speed, a very optimistic 68.33% reduction was achieved. By considering the secondary factors over the primary factors of LH2 combustion the benefits can be

Table 10.5: Overall equivalent emissions compared to conventional A320NEO

Engine type	Turbofan		Turboprop	
Variant	*A320NEO [kg/(km*Seat)]*	LH2-A320NEO (primary & secondary effects)	A320NEO-TP	LH2-A320NEO-TP (primary & secondary effects)
m_CO2	0.06292	∅	+235.41%	∅
m NOx eq	0.05929	-26.25%	-65.04%	-85.44%
m AIC eq	0.13507	-72.04%	-95.50%	-98.50%
Σ m_CO2eq	**100%**	**-68.33%**	**-7.56%**	**-95.86%**

The mass reduction expressed as their CO2 equivalent on both LH2 propelled variants is notable. Generally speaking, the best performance was achieved by the low and slow LH2 turboprop variant. Eradicating the CO2 out of the equation and a substantial cutback of the AIC by the secondary effects of the hydrogen. Nonetheless, an absolute reduction to achieve a zero-emission aircraft was not possible. A remaining 4.14% up to 11,78% of the CO2 equivalent mass of the conventional A320NEO will still be present.

10.8 Evaluation: Zero Emission Achievability

Hydrogen aircraft could represent a promising step towards the EU 2050 goals discussed in Chapter 1.4 by eliminating the actual CO2 emissions. A congruent CO2 emission reduction in aviation would only be true if the supply chain of liquid hydrogen is using Green-, Pink-, Turquoise-Hydrogen production methods. Nonetheless an eye must still be kept on the CO2-equivalent greenhouse effects, since the AIC and NOx emissions are diminished but do not disappear only by using LH2 propulsion systems.

Lowering the cruise altitude, substituting kerosene by LH2 and flying turboprop aircraft instead, based on the CO2 equivalent emissions of the LH2-A320NEO-TP (Appendix D); extrapolated to the civil aviation the best-case scenario would still represent the remaining the 14,56% of the NOx and 1,5% of the AIC effects in equivalent CO2 scale only if the truth of the secondary effects of the water on AIC crystals can be demonstrated.

Considering the 5% forecast as a projected growth of civil aviation for the following years means adding to the CO2 equivalent greenhouse effects by water vapor and nitrogen oxides. The lack of globally unified goals and the impossibility to trace all emissions means that rather than stopping, most probably global warming from aviation will keep on rising in the following years.

11 Summary and Conclusions

The argument about hydrogen being less convenient or more expensive than fossil fuels cannot be denied. Fossil fuels are a storage of highly concentrated amounts of energy dating back hundreds of millions of years, being also relatively easy to process and transport. Any solution that comes out to compete in terms of price and convenience will be more expensive and less convenient than their fossil counterparts. Knowing the pollution impact of greenhouse gases on the environment, consequent of the practicality of the continuous use of fossil fuels, drastically measures should have been applied decades ago. CO2 being just a fraction of the emissions, having the possibility to reduce the other aspects of the same issue, all we might still have left in the near future as a feasible quick action is reducing AIC. As a society there is no other option but to abandon fossil fuels for something more expensive and less convenient as soon as possible. A change must be made before the food and water crisis caused by global warming worsen. These series of changes should also take place in other industries that unfortunately do not get the same media attention. Around 20% of the world's electricity is used every year in bauxite to aluminum refinement with electrolysis. There are very few incentives for aluminum recycling worldwide. To make things worse, due to the construction methods involving several layers of aluminum glued together, retired aircraft's aluminum parts cannot be used to build new aircraft either. (De Berker 2022)

12 Recommendations

On this project some of the possibilities for the future of aviation have been explored. Overall, as a western society we have condensed the whole environmental crisis mostly into CO2 emissions. Although it might be easier to communicate to the masses than going deeper into the several contributions and repercussions of humans in global warming and our planet's pollution. On an economic driven basis, people's ability to make decisions about their own implementation of conscious environmental repercussions in their daily lives and how they also impact on other organisms comes down to their own pocket. It would be naive for the airline industry to think that passengers are willing to pay for the flight that has the least environmental impact if it happens to be more expensive. And that is pretty much what the environmental compensations offered by airlines to passengers buying tickets represent. Letting the final user have a sense of accomplishment by just experiencing the cleanliness of a non-contaminant solution and kicking under the rug all the polluted steps should not be something to be proud about as a company. On the other hand, by using the term "Carbon Footprint" passengers get the illusion that the climate change problems rely only on the individuals when the industry behind really does not provide tangible cleaner solutions besides artificially reducing remorseful feelings without transmitting the biased perspective of the businessman behind. To communicate this an impartial frame of reference such as the Ecolabels (Haß 2015) proposal is needed.

Even the smallest improvements in terms of environmental sustainability in aviation come with a large price tag which has not been correctly addressed if it always lands on the passengers. Through the years of commercial aviation, government authorities have enjoyed the benefits of flying its population around without needing to worry about the infrastructure between both ends of the trip. That is a phenomenon that cannot be found in any other means of transportation besides maritime. Train tracks and highways must be built and well maintained to keep them safe and useful for the public.

The civil aviation industry continues its long effort for more efficient air travel and better transportation options for the public. The hard truth is that it will be neither perfect nor cheap. Every decision comes with a cost, and how we, as human race manage that is in our hands.

List of References

ABSOLUT HYDROGEN, 2021. *Liquid hydrogen & Liquefaction*. Grenoble, France: Absolut Hydrogen.
Available from: https://bit.ly/3UIqzuX
Archived at: https://perma.cc/T3GE-43BB

ACI EUROPE, 2024. *Airport Industry Manifesto: For the Next EU Political Cycle 2024-2029*. Brussels, Belgium: ACI Europe
Available from: https://bit.ly/4ai0sAP
Archived at: https://perma.cc/7E7E-DFEK

AIRBUS, 2020a. *ZEROe- Low Carbon Aviation*. Toulouse, France: Airbus S.A.S.
Available from: https://bit.ly/3WrCMa1
Archived at: https://perma.cc/G4NP-D7R6

AIRBUS, 2020b. *Aircraft Characteristics Airport and Maintenance Planning: A320*. Toulouse, France: Airbus S.A.S.
Available from: https://bit.ly/3VUK0CE
Archived at: https://perma.cc/ZB98-A2LW

AIRBUS, 2021. *How to Store Liquid Hydrogen for Zero-Emission Flight*. Toulouse, France: Airbus S.A.S.
Available from: https://bit.ly/3xr6Fgx
Archived at: https://perma.cc/3WC6-5JMC

ALCOCK, Charles, 2023. *Rolls-Royce Achieves Max Takeoff Thrust with Hydrogen-powered Pearl Engine*. Aviation International News.
Available from: https://bit.ly/3wpc877
Archived at: https://perma.cc/J6F5-K2E7

BARTON, David ; Hall, Cesare; OLDFIELD, Matthew. 2023. *Design of a Hydrogen Aircraft for Zero Persistent Contrails.* University of Cambridge.
Available from: https://doi.org/10.3390/aerospace10080688
Archived at. https://perma.cc/L587-DDWC

BERESNEVICIUS 2023: *EASA's Fuel Tank Safety Requirements Could Compromise a321xlr Range.* Vilnius, Lithuania: Aerotime Hub.
Available from: https://bit.ly/4bblHVz
Archived at: https://perma.cc/Y34F-GLEJ

BEVILL, Kris, 2010. *GE Powers Turbines with Ethanol in Brazil.* North Dakota ,USA: Ethanol Producer Magazine.
Available from: https://bit.ly/4bCaGx5
Archived at: https://perma.cc/9VBG-2WQZ

BLOOMBERG, 2022a. *Why Hydrogen-Powered Planes Might Be Inevitable.* Film, New York, USA.
Available from: https://youtu.be/f-4if26F_RA

BLOOMBERG, 2022b. *How Cheap Hydrogen Could Become the Next Clean Fuel*. Film, New York, USA.
Available from: https://youtu.be/JGe8R0N20ps

BOCK, Lisa; BURKHARDT, Ulrike, 2019. *Contrail Cirrus Radiative Forcing for Future Air Traffic.* Article DLR Oberpfaffenhofen, Germany: European Geosciences Union
Available from: https://acp.copernicus.org/articles/19/8163/2019/
Archived at: https://perma.cc/XT5Q-JAVU

BOEING-747.COM, 2017. *KLM's The Flying Dutchman:747-400M (Combi)*
Available from: https://bit.ly/3VDLe3K
Archived at: https://perma.cc/S6LF-HSF4

BRITANNICA, 2024a. *Contrail*. Definition
Available from: https://www.britannica.com/science/vapor-trail

BRITANNICA, 2024b. *Electrolysis*. Definition
Available from: https://www.britannica.com/science/electrolysis

CFM RISE, 2021. *RISE Program: Revolutionary Innovation for Sustainable Engines*. Ohio, USA: CFM International
Available from: https://www.cfmaeroengines.com/rise/
Archived at: https://perma.cc/CG7G-XP3Z

CHEVRON, 2007. *Aviation Fuels-Technical Review*. California, USA: Chevron Products Company.
Available from: https://bit.ly/3V4GkOs
Archived at: https://perma.cc/S864-QNZA

CLEAN SKY 2, 2020. *Hydrogen-powered aviation: A fact-based study of hydrogen technology, economics, and climate impact by 2050*. First Edition, Brussels, Belgium: Clean Aviation Joint Undertaking

Available from: https://www.clean-aviation.eu/media/publications
Archived at: https://perma.cc/4DEP-2AH5

COLLINS DICTIONARY, 2024. Definition: *Hydrogen*

Available from: https://www.collinsdictionary.com/

CONCEPT GROUP, 2024. *Glossary- What does cryogenic mean?*

Available from: https://conceptgroupllc.com/glossary/what-does-cryogenic-mean/

C-ZERO, 2023. *Decarbonizing Natural Gas*: *Methane Pyrolysis.* USA

Available from: https://www.czero.energy/technology
Archived at: https://perma.cc/W9GE-958B

DE BERKER, Archy 2022. *Understand your Aluminum Emissions*. London, UK: Carbon Chain

Available from: https://bit.ly/4euahz3
Archived at: https://perma.cc/RKQ9-WTMU

DELTA CARGO, 2024. *Delta Air Lines: Cargo Aircraft Specifications A320.* Delta Air Lines.

Available from: https://bit.ly/45CPMMu
Archived at: https://perma.cc/JB9G-ETZV

DIB, Leon, 2015. The Aviation Fuel and the Passenger Aircraft for the Future – Hydrogen. Master Thesis, Hamburg University of Applied Sciences.

Available from: http://library.profscholz.de/

EASA, 2023. *Certification Specifications and Acceptable Means of Compliance for Large Aeroplanes (CS-25).* Amendment 28. Cologne, Germany

Available from: https://bit.ly/3VUyEOX
Archived at: https://perma.cc/6S6P-JYZ4

EERE 2016. *New Software Will Enable Chemical Manufacturers to Optimize Distillation Column Configuration and Save Energy*. Washington DC, USA: US Department of Energy-Office of Energy Efficiency & Renewable Energy.

Available from: https://bit.ly/3V2IfBV
Archived at: https://perma.cc/WF2B-LCYB

ENERGY TRANSITIONS COMISSION, 2022: *Aviation Transition Strategy-Making Net-Zero Aviation Possible*. Washington DC, USA: Mission Impossible Partnership
Available from: https://bit.ly/4bj9DSI
Archived at: https://perma.cc/2EV2-467U

ENERVENUE, 2023a. *Energy Storage Vessel.* California, USA.
Available from: https://enervenue.com/product/
Archived at: https://perma.cc/Y52B-4STS

ENERVENUE, 2023b. *Energy Storage Vessel: Data Sheet.* California, USA.
Available from: https://bit.ly/4akZNif
Archived at: https://perma.cc/J8KD-579S

ENERVENUE, 2023c. *EnerVenue Opening Gigafactory in Shelby County*, *Kentucky to Scale Production of its Differentiated Energy Storage Solutions.* California, USA.
Available from: https://bit.ly/4byIBXq
Archived at: https://perma.cc/75SF-C6EN

EPA, 2023. *Greenhouse Gases.* Definition. Washington D.C., USA: Environmental Protection Agency
Available from: https://bit.ly/4blwFHZ
Archived at: https://perma.cc/3SV6-YU25

EUROPEAN COMMISSION, 2019. *Going climate-neutral by 2050: A strategic long-term vision for a prosperous, modern, competitive and climate-neutral EU economy*. Brussels, Belgium: Directorate-General for Climate Action Publications Office.
Available from: https://data.europa.eu/doi/10.2834/02074
Archived at: https://perma.cc/C69U-386V

FINANCIAL TIMES, 2023. *Can hydrogen help the world reach net zero?* Film. London, England
Available from: https://youtu.be/v7UwbJ8n9L0

FLUX POWER, 2020. *What is the Energy Density of a Lithium-Ion Battery?* California, USA
Available from: https://bit.ly/3V5mRgA
Archived at: https://perma.cc/G6PA-MTKF

FRANKOTERM, 2024. *Multi-Layer Insulation (MLI)*. Otłoczyn, Poland
Available from: https://frakoterm.com/cryogenics/multi-layer-insulation-mli/
Archived at: https://perma.cc/JNY3-UJ8F

GAO, Qi; BLECK, Wolfgang; ZANDER, Brita Daniela, 2017. *Investigations on Hydrogen Embrittlement of Advanced High Strength Steels for Automotive Applications.* Aachen, Germany: RWTH Aachen
Available from: https://bit.ly/3XGDgK2
Archived at: https://doi.org/10.18154/RWTH-2017-08357

GEERTS, Bart; LINACRE, Edward, 1997. *The Height of the Tropopause.* Wyoming, USA: University of Wyoming
Available from: http://www-das.uwyo.edu/~geerts/cwx/notes/chap01/tropo.html
Archived at: https://perma.cc/KD48-4DLR

GOOGLE, 2023a. *Project Contrails: A Cost Effective and Scalable Way AI is Helping to Mitigate Aviation's Climate Impact*. California, USA: Google Research
Available from: https://sites.research.google/contrails/
Archived at: https://perma.cc/26WV-GE4K

GOOGLE, 2023b. *Google Interview: The future of flight: Can AI make flying sustainable?* California, USA: Google Research
Available from: https://youtu.be/xBkK7olwjx0

HEINEMANN, Joeri. 2012: *Preliminary Sizing of FAR Part 23 and Part 25 Aircraft*. Master Thesis, Hamburg University of Applied Sciences.
Available From: http://SAS.ProfScholz.de

HAß, Tim, 2015. *Developing an Ecolabel for Aircraft.* Bachelor Thesis, Hamburg University of Applied Sciences.
Available from: http://Ecolabel.ProfScholz.de

HIIROC, 2024. *Thermal Plasma Electrolysis.*
Available from: https://hiiroc.com/our-technology/
Archived at: https://perma.cc/XD65-J97G

HYDROGEN NEWSLETTER, 2022.*What is Steam Methane Reforming(SMR)?*
Available from: https://bit.ly/45C8yn4
Archived at: https://perma.cc/34NR-YDC3

H2PRO, 2023. *Electrochemical-Thermically Activated Chemical (E-TAC): Revolutionary Method for Splitting Water*. Caesarea ,Israel:H2 Pro, Ltd.
Available from: https://www.h2pro.co/technology
Archived at: https://perma.cc/77Y5-TBGZ

IBERDROLA, 2022. *Iberdrola instala la mayor planta de hidrógeno verde para uso industrial en Europa*. Bilbao, Spain: Iberdrola S.A.
Available from: https://bit.ly/4eGFj6G
Archived at: https://perma.cc/Y68B-86YV

ISU, 2024. *Greenhouse Gas Lifetime in the Atmosphere.* Iowa, USA: Iowa State University
Available from: https://bit.ly/4exDAAF
Archived at: https://perma.cc/5YRD-YZQF

JEPPESEN, 2004. *Meteorology: JAA ATPL Training*. Colorado, USA: Jeppesen Sanderson Inc.
Available from: https://code7700.com/tropopause.htm#ref
Archived at: https://perma.cc/FW2T-BEND

JORDAN, Thomas, 2007. *Safety of Hydrogen as an Energy Carrier: Chapter 1-Fundamentals.* Karlsruhe, Germany: HySafe-International Association for Hydrogen Safety
Available from: http://www.hysafe.org/index.php?ID=40&kwd=Presentation
Archived at: https://perma.cc/BT2R-HSK5

KEEN, 2020. *Hydrogen Conversion Data.* Delaware, USA: Keen Compressed Gas Co.
Available from: https://keengas.com/gases/hydrogen/
Archived at: https://perma.cc/F5JV-GHVC

KRULL, Marlis, 2022. *Preliminary Sizing of Propeller Aircraft (Part 25)*. Project, HAW Hamburg.
Available from: https://nbn-resolving.org/urn:nbn:de:gbv:18302-aero2022-04-29.012

KURAL, Saim; AYVAZ, Mehmet, 2018. The Ballistic Behavior of Type 1 Metallic Pressurized Hydrogen Storage Tanks Against Ballistic Threats. International Journal of Hydrogen Energy PDF
Available from: http://dx.doi.org/10.1016/j.ijhydene.2018.06.126
Archived at: https://perma.cc/3LUH-Q5VG

LAW INSIDER, 2014. Definition: *Near Zero-Emission*
Available from: https://www.lawinsider.com/dictionary/near-zero-emission-vehicle
Archived at: https://perma.cc/KX5M-ZT9F

LEE, D, 2021. *The contribution of global aviation to anthropogenic climate forcing for 2000 to 2018.* Manchester, UK: ELSEVIER
Available from: https://bit.ly/4bk7o0O
Archived at: https://perma.cc/R84C-QVMM

LIU Junnan; MAYNARD-CASELY, Helen E., et al 2021. *$Sc_{1.5}Al_{0.5}W_3O_{12}$ Zero Thermal Expansion between 4 and 1400 K*. ACS Publications
Available from: https://pubs.acs.org/doi/10.1021/acs.chemmater.1c01007
Archived at: https://perma.cc/C8CZ-FAAX

LOFTIN, Laurence, 1980. *Subsonic Aircraft: Evolution and the Matching of Size to Performance*. Virginia, USA: NASA.
Available from: https://ntrs.nasa.gov/citations/19800020744

MCCOY, Michael, 2021. *C-Zero: Developing a Liquid Catalyst That Could Usher in an Era of Turquoise Hydrogen*. Washington DC, USA: American Chemical Society.
Available from: https://pubs.acs.org/doi/10.1021/cen-09942-cover4
Archived at: https://perma.cc/A95K-5XHZ

MC LACHAN, Robert, 2023. *Hydrogen Aircraft: Fool me once?*. Auckland, New Zealand: Carbon News NZ
Available from: https://www.carbonnews.co.nz/story.asp?storyID=27206
Archived at: https://perma.cc/8N2A-BAZ4

MERRIAM-WEBSTER DICTIONARY, 2023a. Definition: *Passenger*
Available from: https://www.merriam-webster.com/dictionary/passenger
Archived at: https://perma.cc/VK28-HFE5

MERRIAM-WEBSTER DICTIONARY, 2023b. Definition: *Aircraft*
Available from: https://www.merriam-webster.com/dictionary/aircraft
Archived at: https://perma.cc/QY5T-DNXC

MILLER, Joshua, et al. 2017. Failure Mechanisms of Ni-H2 and Li-Ion Batteries under hypervelocity impacts. Conference Paper: Texas, USA: NASA
Available from: https://ntrs.nasa.gov/citations/20170003810
Archived at: https://perma.cc/82E4-P68X

NEUTRIUM, 2014. Fuel Properties: *Specific Energy and Energy Density of Fuels.* Sydney, Australia: Native Dynamics
Available from: https://bit.ly/3K1HIe3
Archived at: https://perma.cc/34DL-P7HB

NIȚĂ, Mihaela Florentina, 2013. *Contributions to Aircraft Preliminary Design and Optimization*. Munich, Germany: Verlag Dr. Hut. - ISBN 978-3-8439-1163-4,
Available from: http://OPerA.ProfScholz.de

NIȚĂ, Mihaela Florentina, 2008. *Aircraft Design Studies Based on the ATR 72*. Hamburg University of Applied Sciences.
Available from: http://Library.ProfScholz.de

NW FUEL CANADA, 2017. *What's the Deal with Winter Diesel Fuel?* British Columbia, Canada: New Westminster Newsletter Archives
Available from: https://nwfuel.ca/whats-deal-winter-diesel/
Archived at: https://perma.cc/RN7L-KKEB

PADDISON, Laura, 2023. *Wind energy has a massive waste problem.*, Georgia, USA: CNN World
Available from: https://bit.ly/45z2Lih
Archived at: https://perma.cc/B557-Q9M6

PEARCE, Fred, 2019. *How Airplane Contrails are Helping Make the Planet Warmer.* USA: Yale E360
Available from: https://bit.ly/3KVRW0a
Archived at: https://perma.cc/2DTX-X64C

RAYMER, P. Daniel, 1989. *Aircraft Design: A Conceptual Approach*. Second Edition, Washington DC,USA: AIAA Education Series.
Available from: https://amzn.eu/d/00RIjZYX
Archived at: https://perma.cc/3LDL-JMMM

ROSEN, Eli, 2023. *Discarded wind turbine blades fill thirty acres on the west side of Sweetwater*
Available from: https://youtu.be/aNVBP48ziXw
Archived at: https://perma.cc/Z375-8VCE

ROSKAM, Jan, 1989. *Preliminary Sizing of Airplanes.* Kansas, USA: DAR Corporation
Available from: https://amzn.eu/d/0eEeOvfO
Archived at: https://bit.ly/3zem58l

ROLLS-ROYCE , 2022. *Rolls-Royce and EasyJet set New World First.* London, UK: Rolls-Royce Holdings plc.
Available from: https://bit.ly/3QHOUzX
Archived at: https://perma.cc/6D7H-V8Y7

SCHOLZ, Dieter, 2012: *Aircraft Preliminary Sizing Tools @ Aero : SAS → OPerA → PreSTo → further Tool Chain*. Hamburg, Germany: Deutsches Zentrum für Luft- und Raumfahrt.
Available from: http://SAS.ProfScholz.de

SCHOLZ, Dieter, 2015. *Aircraft Design*. Lecture Notes. Hamburg University of Applied Sciences.
Available from: http://LectureNotes.AircraftDesign.org

SCHOLZ, Dieter, 2020a. *Design of Hydrogen Passenger Aircraft - How much "Zero-Emission" is Possible?* .AeroLectures Presentation. Hamburg University of Applied Sciences.
Available from: https://www.fzt.haw-hamburg.de/pers/Scholz/Seminar.html

SCHOLZ, Dieter, 2020b. *Aircraft Design - Design of Hydrogen Aircraft.* Lecture Notes. Hamburg University of Applied Sciences.
Available from: https://bit.ly/3xxIGwf

SCHOLZ, Dieter, 2020c . *Calculation of the Emission Characteristics of Aircraft Kerosene and Hydrogen Propulsion*. Hamburg, Germany: Harvard Dataverse, V4
Available from: https://doi.org/10.7910/DVN/DLJUUK

SCHOLZ, Dieter, 2021. *Parameter Selection for Hydrogen Passenger Aircraft Preliminary Sizing.* Hamburg University of Applied Sciences.
Available from: https://bit.ly/3xxIGwf

SCHOLZ, Dieter, 2022. *Updated CO2_eq equation: contrail effect is a function of fuel burn.* Lecture Notes. Hamburg University of Applied Sciences.
Available from: https://www.fzt.haw-hamburg.de/pers/Scholz/MaterialFM1.html

SCHWARTZ, Emily; KROO, Ilan M., 2009. *Aircraft Design: Trading Cost and Climate Impact.* Exposition. California, USA: Stanford University
Available from: https://doi.org/10.2514/6.2009-1261

SCHWARTZ, Emily; KROO, Ilan M., 2011. *Aircraft Design for Reduced Climate Impact.* PhD. California, USA: Stanford University
Available from: https://doi.org/10.2514/6.2011-265
Archived at: https://perma.cc/AB7V-PWH7

SEECKT, Kolja, 2010a. *Conceptual Design and Investigation of Hydrogen-Fueled Regional Freighter Aircraft. Stockholm*, Kungliga Tekniska Högskolan, School of Engineering Sciences, Aeronautical and Vehicle Engineering, Licentiate Thesis.
Available from: http://GF.ProfScholz.de.
Archived at: https://nbn-resolving.org/urn:nbn:se:kth:diva-26348.

SEECKT, Kolja, HEINZE, Wolfgang, SCHOLZ, Dieter, 2010b. *Hydrogen Powered Freighter Aircraft* – The Final Results of the *Green Freighter* Project.
Available from: http://GF.ProfScholz.de.

SETHI, Bobby; SUN, Xiaoxiao; ABBOTT, David, et al. 2021. *Numerical Investigation of Potential Cause of Instabilities in a Hydrogen Micromix Injector Array.* UK: Cranfield University

Available from: https://doi.org/10.1115/GT2021-59842
Archived at: https://perma.cc/4P5G-PZH8

SIDELNIKOV, Andrei, 2023. *TU-155, The First Hydrogen-Powered Plane Created in the USSR.* Moscow, Russia: Russkiy Mir Foundation

Available from: https://russkiymir.ru/en/publications/311196/
Archived at: https://perma.cc/737B-J9EF

SILVERSTEIN, Abe; HALL, Eldon,1955. *Liquid Hydrogen as a Jet Fuel for High Altitude Aircraft*. Cleveland, USA: NACA-Unclassified 1962

Available from: https://go.nasa.gov/3JTMLNP
Archived at: https://perma.cc/B85E-DCJD

SKYBRARY, 2024. *ICAO Aerodrome Reference Code.*

Available from: https://skybrary.aero/articles/icao-aerodrome-reference-code
Archived at: https://perma.cc/67UW-BD5D

SOONE, Jaan, 2023. ReFuelEU Aviation - Sustainable Aviation Fuels:Q4 2020. In: Legislative Train Schedule-European Green Deal .Strasbourg, France: European Parliament

Available from: http://bit.ly/4a6rOtz
Archived at: https://perma.cc/QKX4-8SJE

TECNAM, 2023. *Tecnam to Postpone the P-Volt Programme*. Capua, Italy: Costruzioni Aeronautiche TECNAM S.p.A

Available from: https://tecnam.com/tecnam-to-postpone-the-p-volt-programme/
Archived at: https://perma.cc/W48G-LM3E

TIME MAGAZINE, 2022. *When Checking a Bag at the Airport Is Worth It and When It Isn't*: *Business Aviation*. USA: New York

Available from: https://time.com/6201071/checked-bag-or-carry-on/
Archived at: https://perma.cc/6GPZ-EPE4

TORENBEEK, Egbert, 1982. *Synthesis of Subsonic Airplane Design*. Delft, Netherlands: Delft University Press.

Available from: https://amzn.eu/d/0aZEjxbi
Archived at: https://archive.org/details/SynthesisOfSubsonicAirplaneDesign

UCAR, 2024. *Air Quality: What's in the Air?* Colorado, USA: University Corporation for Atmospheric Research
Available from: https://scied.ucar.edu/learning-zone/air-quality/whats-in-the-air
Archived at: https://perma.cc/2BPD-B8BX

U.S. AIR FORCE, 1997. *Weather For Aircrews: Volume 1*. Washington, USA: Department of the Air Force
Available from: https://code7700.com/tropopause.htm#ref
Archived at: https://perma.cc/FW2T-BEND

U.S. DEPT. OF ENERGY, 2023. *Hydrogen Production: Natural Gas Reforming*. Washington, USA: Office of Energy Efficiency & Renewable Energy
Available from: https://bit.ly/4cfpQcg
Archived at: https://perma.cc/5EMF-UE64

US-NHHC, 2021. *Gasoline Related Fires in WW2: Section 3-32; 4-30*. USS Franklin Damage Report No. 56. Naval History and Heritage Command
Available from: https://bit.ly/44Lb8qt
Archived at: https://perma.cc/8R34-RUMJ

VILKAS, Gediminas, 2023. *Fit for 55: Parliament and Council reach deal on greener aviation fuels*. Strasbourg, France: European Parliament Press Room
Available from: https://bit.ly/3QBKASS
Archived at: https://perma.cc/5R4Q-U65Y

WANG, Xinyan, 2023. *Thinking Differently in Hydrogen.* London, UK: Brunel University-Centre for Advanced Powertrain and Fuels.
Available from: https://youtu.be/VIzQCRg_HWE

WEIGELT, Steffen; WINAND, Michel 2023. *Milestone for hydrogen combustion in aircraft turbines*. Cologne, Germany: DLR News
Available from: https://bit.ly/4dS4kf5
Archived at: https://perma.cc/ALK4-3HET

WIKIPEDIA, 2024a. *Pratt & Whitney/Allison 578-DX.*
Available from: https://en.wikipedia.org/wiki/Pratt_%26_Whitney/Allison_578-DX
Archived at: https://perma.cc/R3LF-TWND

WIKIPEDIA, 2024b . *Multi-layer Insulation: Properties.*
Available from: https://en.wikipedia.org/wiki/Multi-layer_insulation
Archived at: https://perma.cc/TE88-Y2S6

WIKIPEDIA, 2024c. *Radiative Forcing*. Definition
Available from: https://en.wikipedia.org/wiki/Radiative_forcing
Archived at: https://perma.cc/FZ6E-FR88

Appendix A – Conventional A320NEO

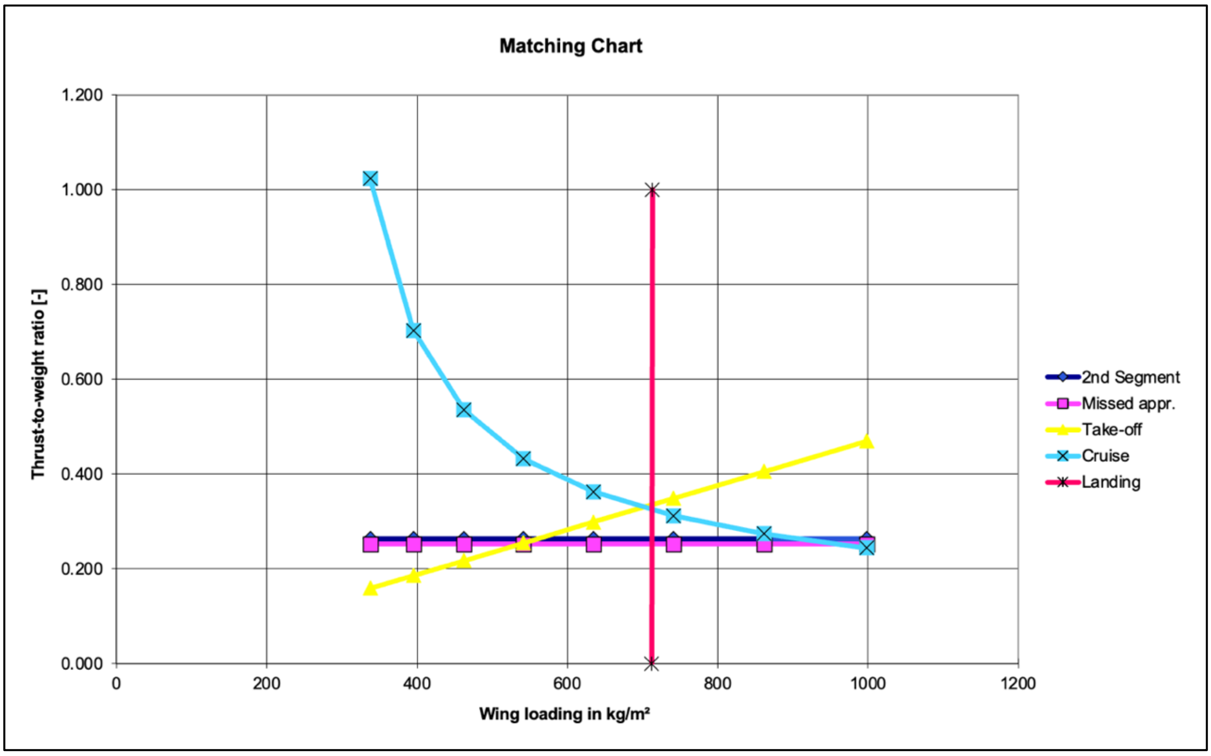

Figure A.1: Matching chart conventional A320NEO

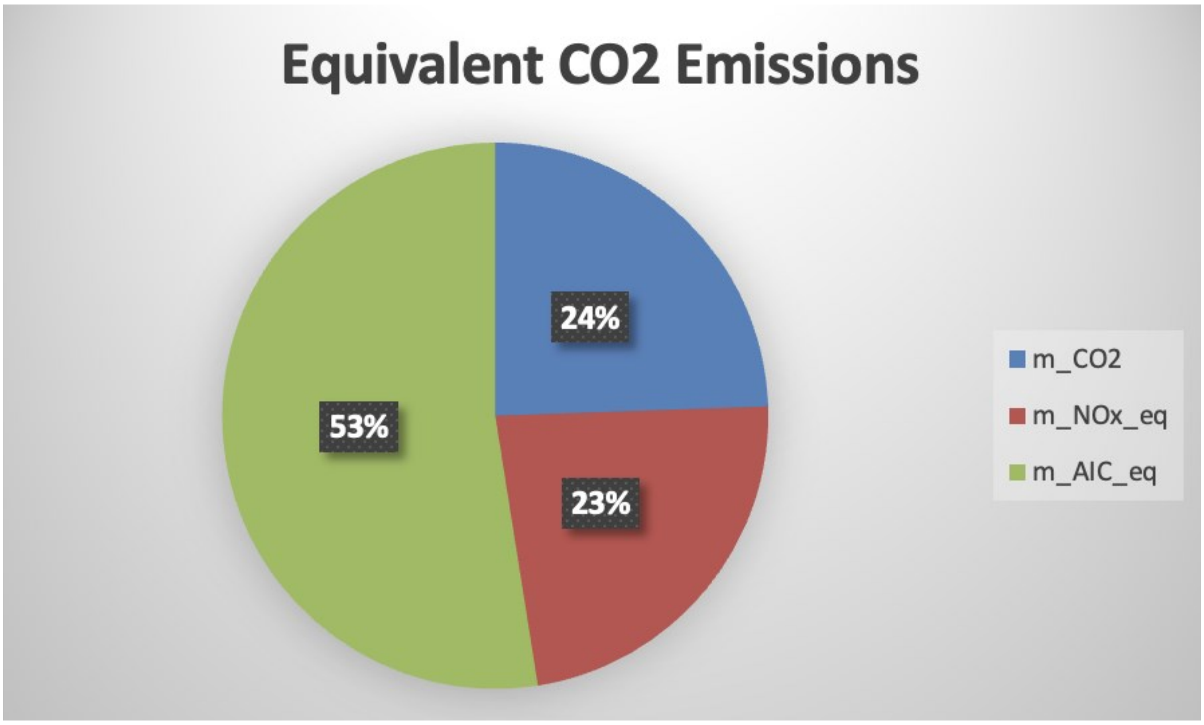

Figure A.2: CO2 equivalent percentual share conventional A320NEO- Pie chart

Equivalent CO2 Emissions [kg/(km*Seat)]		
m_CO2	0.06291788	24.45%
m_NOx_eq	0.05929198	23.05%
m_AIC_eq	0.13507182	52.50%
m_CO2_eq	**0.25728168**	**100.00%**
	25.7281679	**[kg/(100km*Seat)]**

Figure A.3: Conventional A320NEO - CO2 equivalent mass per km per passenger

Appendix B – LH2-A320NEO

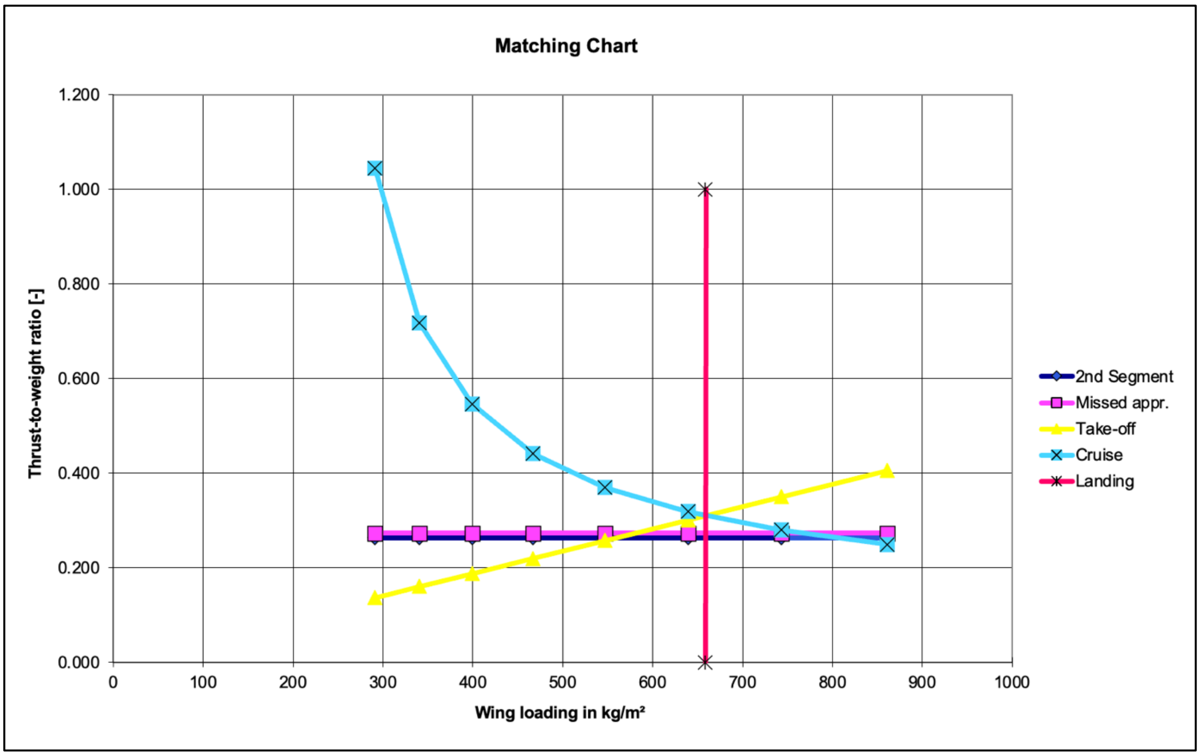

Figure B.1: Matching chart turbofan LH2-A320NEO

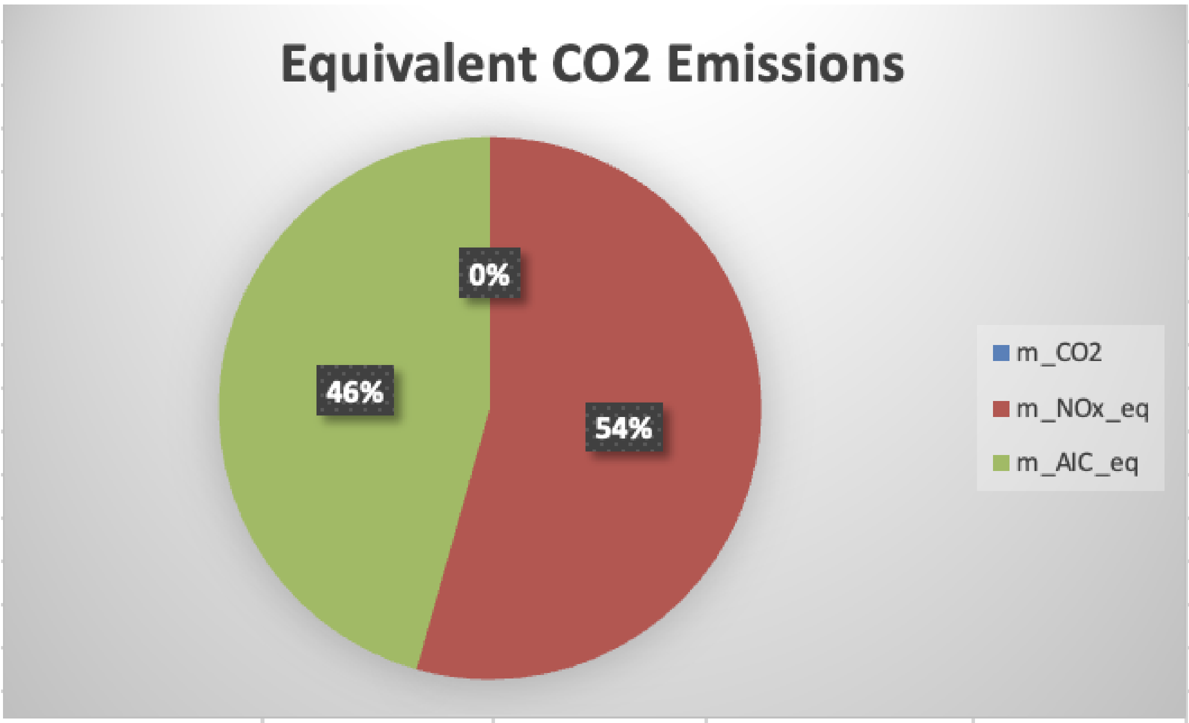

Figure B.2: LH2-A320NEO CO2 equivalent percentual share -Primary effects pie chart

LH2:Equivalent CO2 Emissions [kg/(km*Seat)]			Ref. Aircraft: A320NEO [kg/(km*Seat)]		Deviation
m_CO2	0	0.00%	0.062917877	24.45%	-100.00%
m_NOx_eq	0.12493071	54.36%	0.059291978	23.05%	110.70%
m_AIC_eq	0.10489683	45.64%	0.135071824	52.50%	-22.34%
m_CO2_eq	**0.22982754**	**100.00%**	0.257281679	100.00%	**-10.67%**
	22.9827541	**[kg/(100km*Seat)]**	**25.72816793**	**[kg/(100km*Seat)]**	

Figure B.3: LH2-A320NEO's CO2 equivalent mass compared to A320NEO- Primary effects

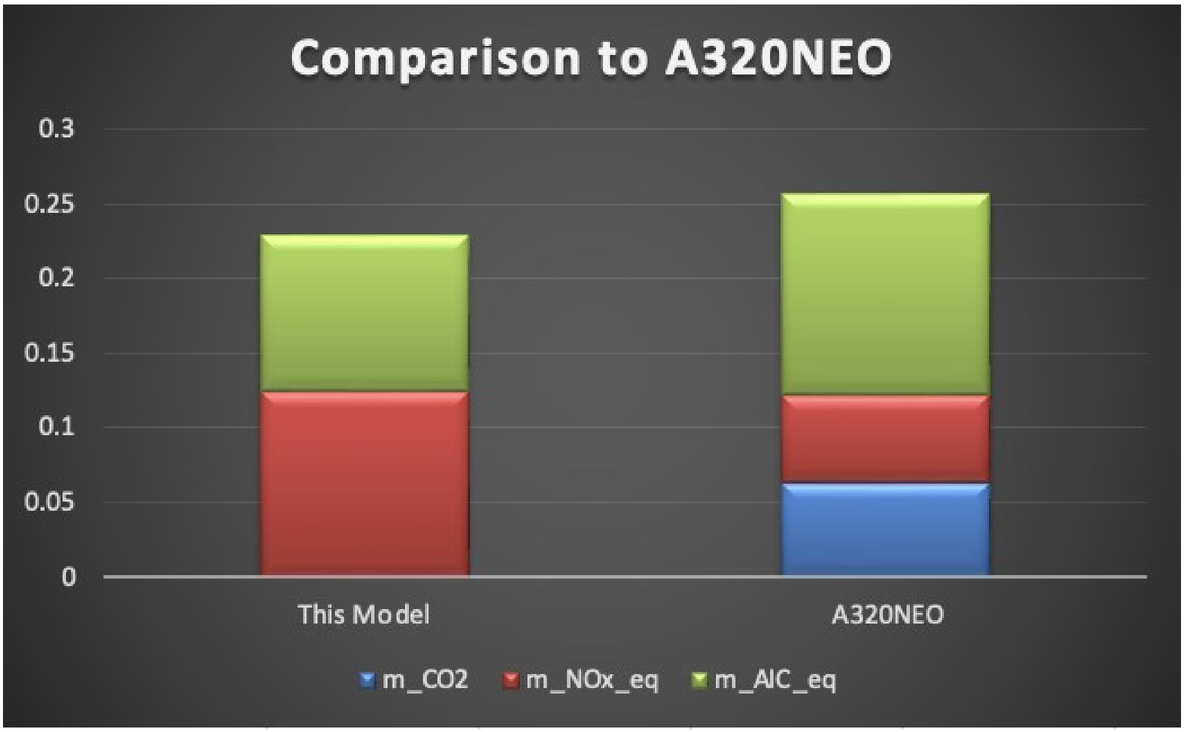

Figure B.4: LH2-A320NEO vs A320NEO - CO2 equivalent- Primary effects column chart

Hydrogen ONLY: Secondary Effects

		LH2:Secondary Equivalent CO2 Emissions [kg/(km*Seat)]			Ref. Aircraft: A320NEO [kg/(km*Seat)]		Deviation
		m_CO2	0	0.00%	0.062917877	24.45%	-100.00%
Nox Reduction Assumption	0.35	m_NOx_eq	0.04372575	53.66%	0.059291978	23.05%	-26.25%
AIC Reduction Factor	0.360	m_AIC_eq	0.03776286	46.34%	0.135071824	52.50%	-72.04%
		m_CO2_eq	0.08148861	100.00%	0.257281679	100.00%	-68.33%

Figure B.5: LH2-A320NEO's CO2 equivalent mass compared to A320NEO- Secondary effects

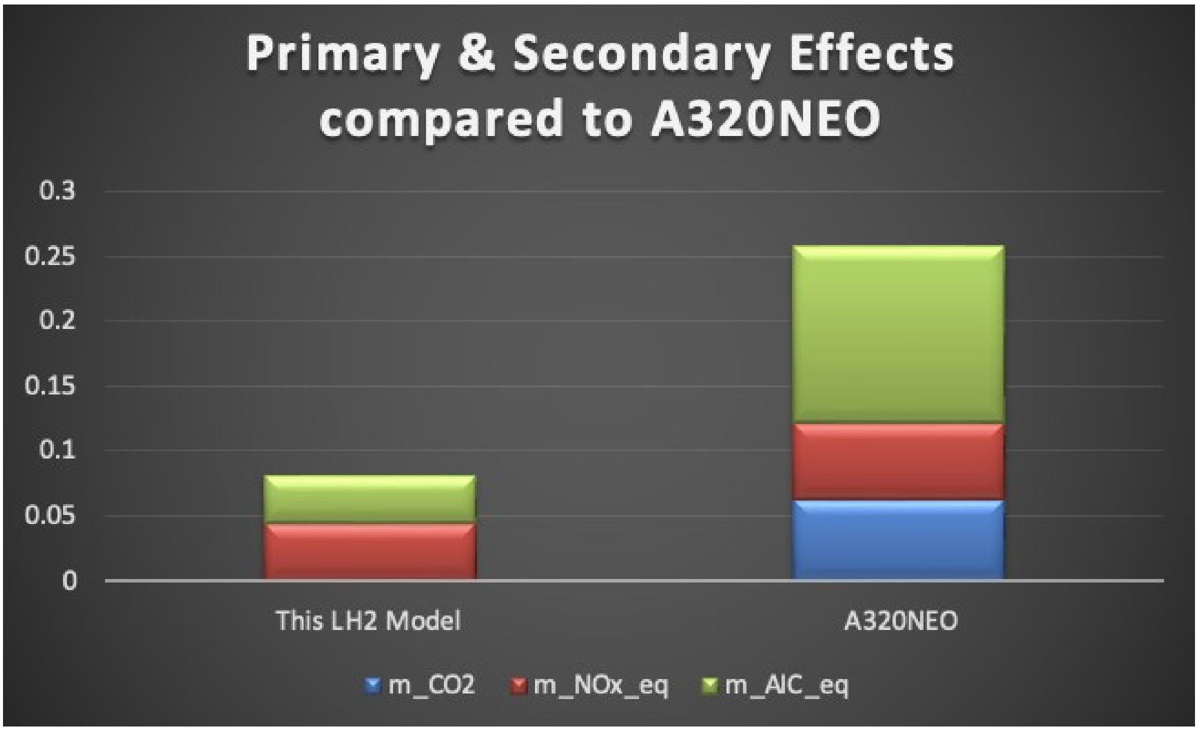

Figure B.6: LH2-A320NEO vs A320NEO - CO2 equivalent- Secondary effects column chart

Appendix C – A320NEO-Turboprop

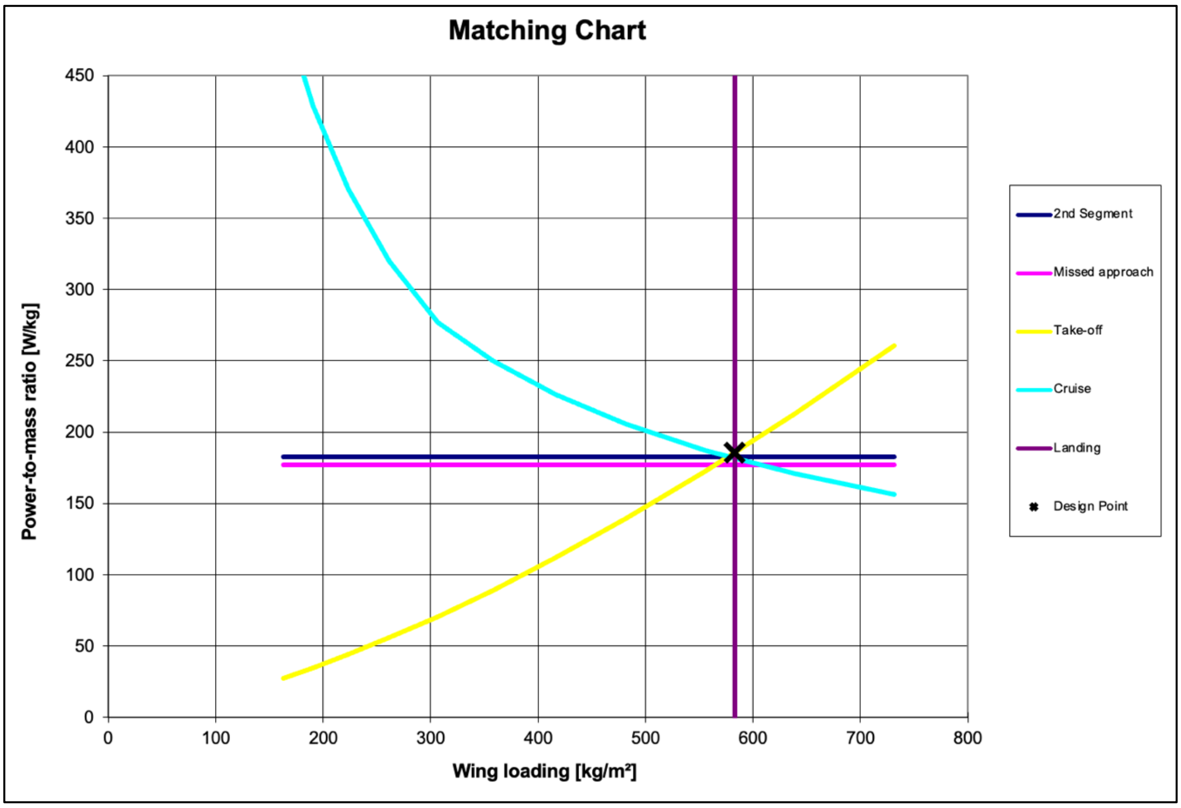

Figure C.1: Matching chart of A320NEO-TP

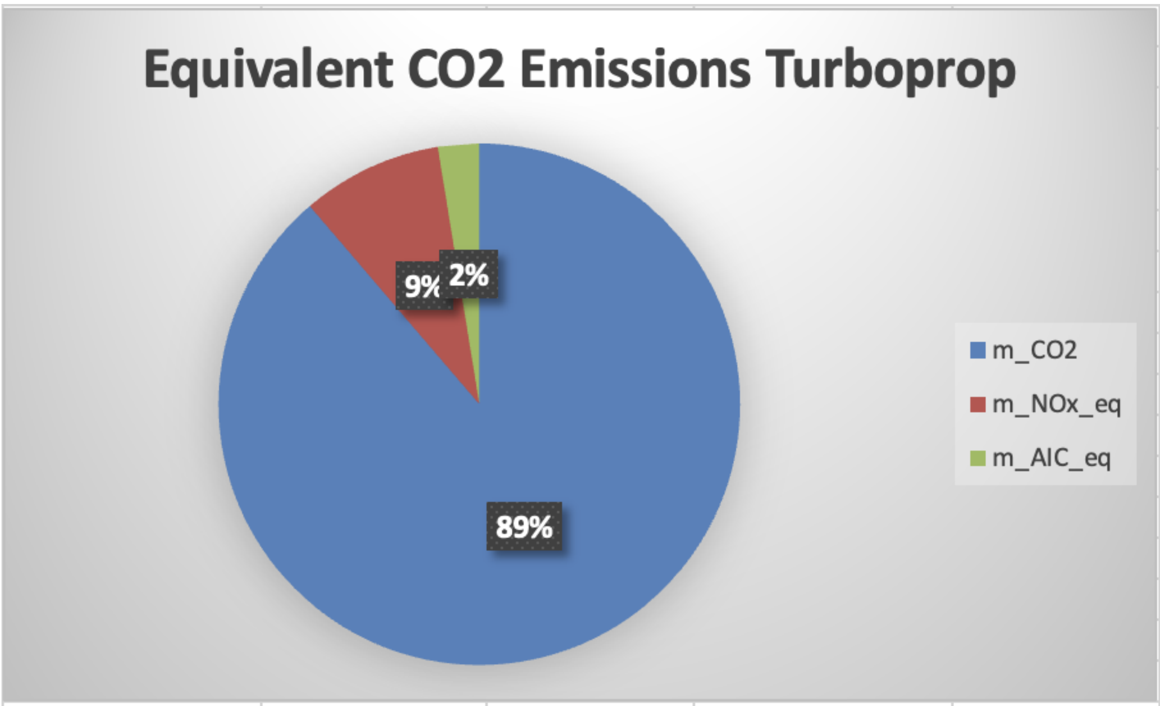

Figure C.2: CO2 equivalent percentual share A320NEO-TP- Pie chart

Equivalent CO2 Emissions [kg/(km*Seat)]				Ref. Aircraft: A320NEO [kg/(km*Seat)]		Deviation
m_CO2	0.21103490	88.73%		0.062917877	24.45%	235.41%
m_NOx_eq	0.02072764	8.72%		0.059291978	23.05%	-65.04%
m_AIC_eq	0.00607148	2.55%		0.135071824	52.50%	-95.50%
m_CO2_eq	**0.23783403**	**100.00%**		0.257281679	100.00%	**-7.56%**
	23.7834026	**[kg/(100km*Seat)]**		**25.72816793**	**[kg/(100km*Seat)]**	

Figure C.3: A320NEO-TP's CO2 equivalent mass compared to A320NEO

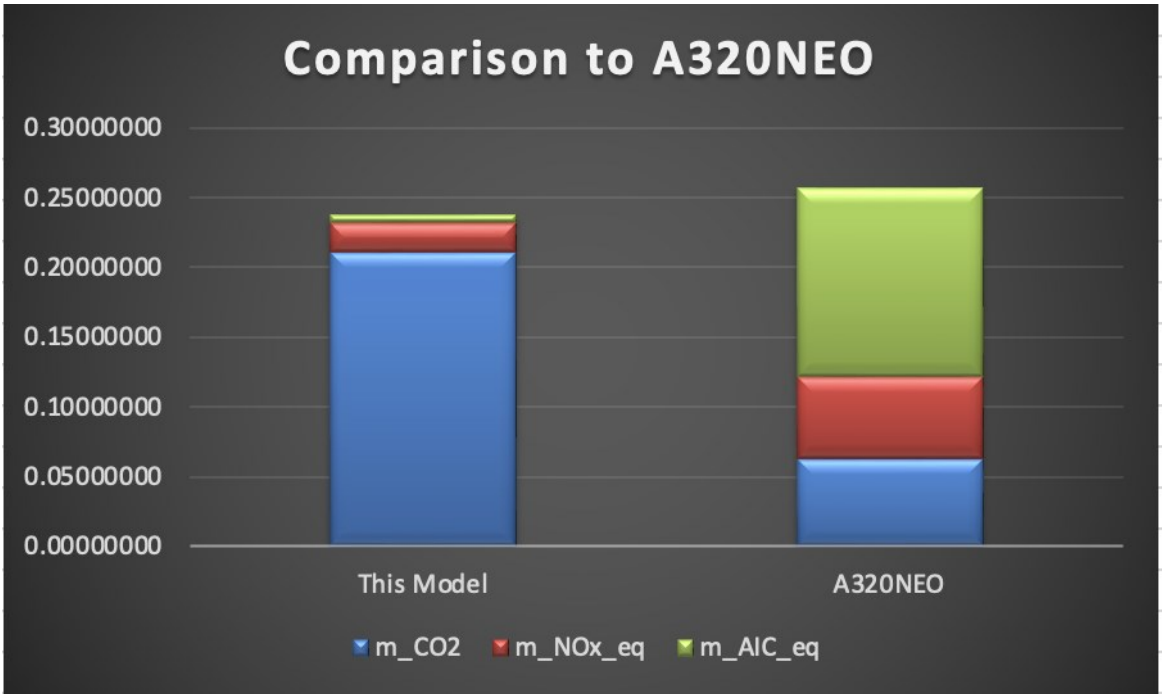

Figure C.4: A320NEO-TP vs A320NEO - CO2 equivalent- Column chart

Appendix D – LH2-A320NEO-Turboprop

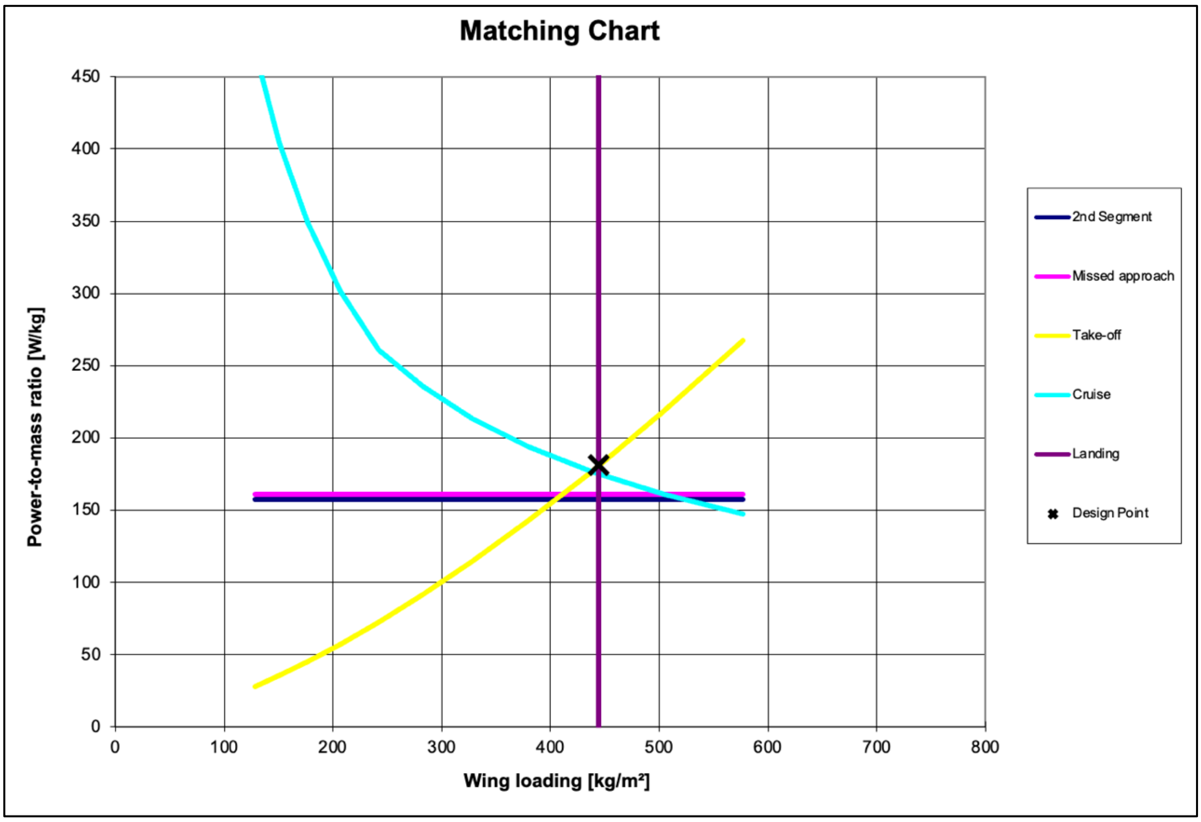

Figure D.1: Matching chart turbofan LH2-A320NEO-TP

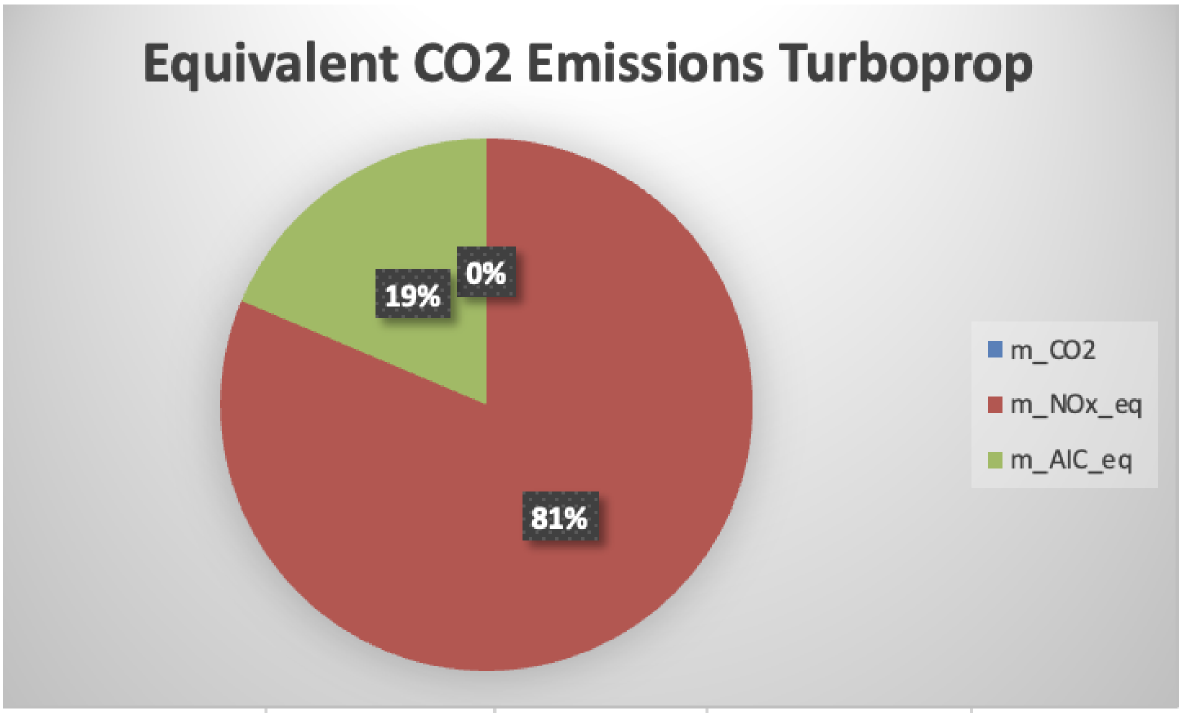

Figure D.2: LH2-A320NEO-TP CO2 equivalent percentual share -Primary effects pie chart

LH2:EquivalentCO2 Emissions [kg/(km*Seat)]			Ref. Aircraft: A320NEO [kg/(km*Seat)]		Deviation
m_CO2	0	0.00%	0.062917877	24.45%	-100.00%
m_NOx_eq	0.0246575	81.37%	0.059291978	23.05%	-58.41%
m_AIC_eq	0.0056447	18.63%	0.135071824	52.50%	-95.82%
m_CO2_eq	**0.0303022**	**100.00%**	0.257281679	100.00%	**-88.22%**
	3.03021987	**[kg/(100km*Seat)]**	**25.72816793**	**[kg/(100km*Seat)]**	

Figure B.3: LH2-A320NEO-TP's CO2 equivalent mass compared to A320NEO- Primary effects

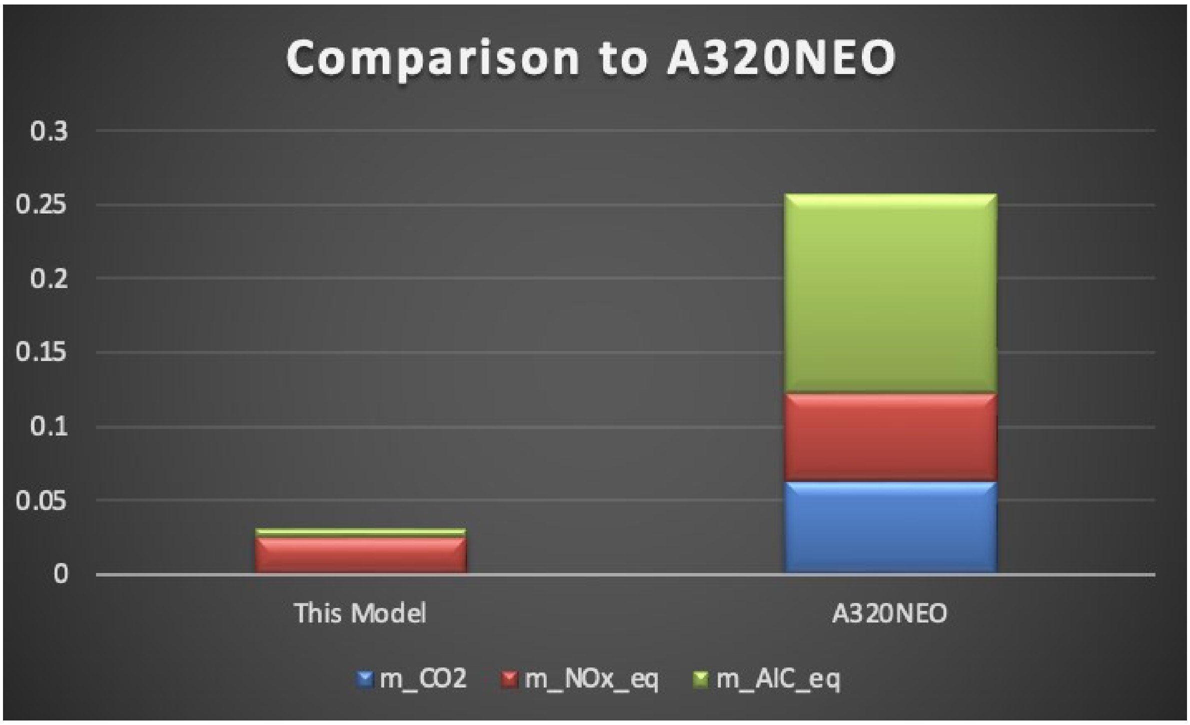

Figure B.4: LH2-A320NEO-TP vs A320NEO - CO2 equivalent- Primary effects column chart

Hydrogen ONLY: Secondary Effects

		LH2:Secondary Equivalent CO2 Emissions [kg/(km*Seat)]			Ref. Aircraft: A320NEO [kg/(km*Seat)]		Deviation
		m_CO2	0	0.00%	0.062917877	24.45%	-100.00%
Nox Reduction Assumption	**0.35**	m_NOx_eq	0.00863013	80.94%	0.059291978	23.05%	-85.44%
AIC Reduction Factor	**0.360**	m_AIC_eq	0.00203209	19.06%	0.135071824	52.50%	-98.50%
		m_CO2_eq	0.01066222	100.00%	0.257281679	100.00%	**-95.86%**

Figure B.5: LH2-A320NEO-TP's CO2 equivalent mass compared to A320NEO- Sec. effects

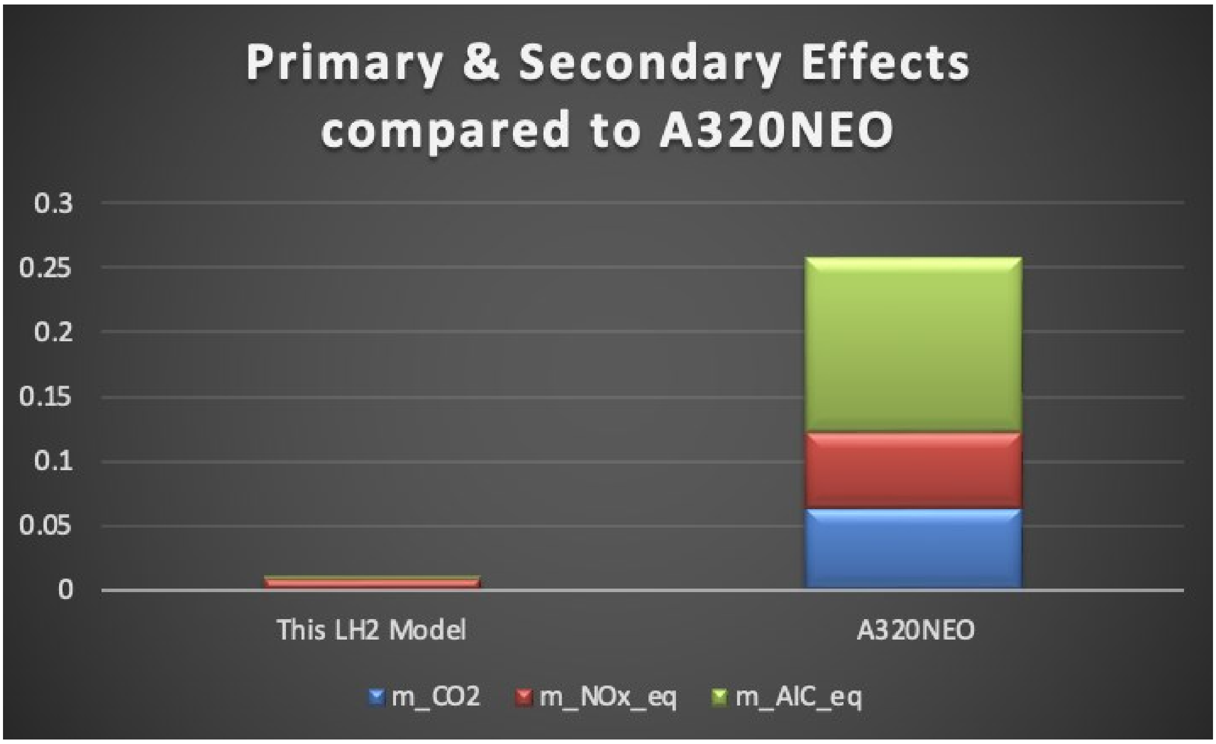

Figure D.6: LH2-A320NEO-TP vs A320NEO - CO2 equivalent- Secondary effects column chart.